SOME METHODS OF FAST-WAVE AMPLIFICATION IN PARAMETRIC ELECTRON-BEAM DEVICES

By
Jacques Spalter

Scientific Report No. 29
Contract AF 19(604)-1930

The research reported in this document has been
sponsored by the
Electronics Research Directorate
Air Force Cambridge Research Laboratories
Office of Aerospace Research
UNITED STATES AIR FORCE
BEDFORD, MASSACHUSETTS

M. L. Report No. 810
April 1961

Microwave Laboratory
W. W. Hansen Laboratories of Physics
Stanford University
Stanford, California

AFCRL 325

SOME METHODS OF FAST-WAVE AMPLIFICATION IN PARAMETRIC ELECTRON-BEAM DEVICES

By

Jacques Spalter

Scientific Report No. 29
Contract AF 19(604)-1930

M. L. Report No. 810

April 1961

The research reported in this document has been
sponsored by the
Electronics Research Directorate
Air Force Cambridge Research Laboratories
Office of Aerospace Research
UNITED STATES AIR FORCE
BEDFORD, MASSACHUSETTS

Microwave Laboratory
W. W. Hansen Laboratories of Physics
Stanford University
Stanford, California

AFCRL 325

SCIENTIFIC REPORT NO. 29

SOME METHODS OF FAST-WAVE AMPLIFICATION IN PARAMETRIC ELECTRON-BEAM DEVICES

By

Jacques Spalter

Electronics Research Directorate
Air Force Cambridge Research Laboratories
Office of Aerospace Research (USAF)

CONTRACT AF 19(604)-1930

M. L. Report No. 810

April 1961

The research reported in this document has been sponsored by The Electronics Research Directorate of the Air Force Cambridge Research Laboratories, Office of Aerospace Research, UNITED STATES AIR FORCE, BEDFORD, MASSACHUSETTS. The publication of this report does not necessarily constitute approval by the Air Force of the findings or conclusions contained herein.

Microwave Laboratory
W. W. Hansen Laboratories of Physics
Stanford University
Stanford, California

Requests for additional copies by Agencies of the Department of Defense, their contractors, and other Government agencies should be directed to the:

ARMED SERVICES TECHNICAL INFORMATION AGENCY
ARLINGTON HALL STATION
ARLINGTON 12, VIRGINIA

Department of Defense contractors must be established for ASTIA services or have their "need-to-know" certified by the cognizant military agency of their project or contract.

All other persons and organizations should apply to:

U.S. DEPARTMENT OF COMMERCE
OFFICE OF TECHNICAL SERVICES
WASHINGTON 25, D. C.

ABSTRACT

The amplification mechanism of two types of electron-beam parametric amplifiers is investigated. The first type is an electrostatically-focused amplifier; the second one is a space-charge wave amplifier which uses resonant cavities for fast-wave coupling. In both cases a small-signal approximation is made and the only effects considered are those of the signal, idler and pump frequencies.

ELECTROSTATICALLY FOCUSED PARAMETRIC AMPLIFIER

It has been shown that the transverse motion of the electrons in an electrostatically-focused helicoidal electron beam can be expressed as a fast and a slow wave. As is the case for ordinary fast and slow space-charge waves (or fast and slow cyclotron waves), the fast electrostatic wave carries positive power, and the slow electrostatic wave carries negative power. The electrostatic parametric amplifier consists of input and output couplers separated by an amplifying section. Although this device is similar to the Adler-type amplifier, it has the particular advantage that no magnetic field is required.

It is shown in this report that the pump frequency is given by $\omega_p = (2 + p/\sqrt{2})\ \omega_s$ where ω_p is the pump frequency, ω_s the signal frequency, and p the number of azimuthal variations of the pump electric field. The rf pumping of the electron beam gives rise to an exponential growth of the radial motion, at the signal frequency, of an electron. And it is shown that when all the electrons are taken into account gain is obtained.

Thus an electrostatic parametric amplifier was designed and built for the case where the pump frequency is twice the signal frequency.

SPACE-CHARGE WAVE PARAMETRIC AMPLIFIER

It can be shown that when the transit time through particular types of resonant cavities is properly chosen, interaction, between the cavity and the beam, will be only with the fast space-charge wave. Hence, with proper loading, all the energy can be transferred from the fast space-charge wave to the cavity and its load.

It has been shown that if the electron beam is pumped with an rf field an exponential growth of the signal can be obtained; this, however, introduces unwanted coupling to higher frequencies. An alternative approach, which can lead to amplification without growing waves, is utilized in this report. The pump is used to vary the electronic reactance of a cavity which couples only to the fast space-charge wave.

The beam-loading admittance in the presence of the pump is calculated for two specific cases:

(1) A "floating drift tube" klystron cavity, where it is shown that the presence of the pump destroys the 90° phase relationship between the modulating voltage and the current. This creates a negative conductance for conditions which would otherwise give only a reactance and no amplification (or oscillations).

(2) A resonant cavity supporting a longitudinal sinusoidal electric field, where the presence of the pump creates a negative conductance leading to amplification (or oscillations) of the signal.

In both cases the negative beam-loading conductance is obtained for conditions where there are no growing waves on the beam. However, in order to obtain a useful amount of negative conductance for a practical device, it is necessary to choose the parameters in such a way that growing waves are present in the electron beam.

ACKNOWLEDGEMENT

The author wishes to thank Professors M. Chodorow and R. H. Pantell for their help and guidance throughout this work. The author is indebted to Dr. G. S. Kino for helpful discussions and suggestions and to Mr. F. J. Willms of the Stanford Computation Center for his help in the numerical calculations. The author also wishes to express his appreciation to Mrs. B. Leichter, and Messrs. L. Nigro, W. J. Feazell, and D. L. Masterson.

TABLE OF CONTENTS

LIST OF FIGURES

PART I

STUDY OF AN ELECTROSTATIC PARAMETRIC AMPLIFIER

PART II

STUDY OF A FAST SPACE-CHARGE WAVE PARAMETRIC AMPLIFIER

PART I

LIST OF SYMBOLS

c	Radius of the inner conductor.
C	Constant proportional to the rf pump potential V_p. ($C = pr_0^2 B$ where B is defined in equation I.32).
E_ϕ	Azimuthal component of the rf electric field.
E_r	Radial component of the rf electric field.
I_0	DC current.
p	Number of azimuthal variations of the pump electric field.
Q_L	Loaded Q of a cavity.
r_0	DC equilibrium radius of the electrons.
r_1	RF radial displacement of the electrons, from its dc equilibrium position, at the signal frequency.
r_p	RF radial displacement of the electrons, from its dc equilibrium position at the pump frequency.
s	Radius of the outer conductor.
t_0	Entrance time of an electron in the amplifying section.
u_0	DC longitudinal velocity of the electrons.
v_f	Phase velocity of the fast wave.
v_s	Phase velocity of the slow wave.
V_0	Defined by $(V_c - V_s)/\ell n(s/c)$.
V_c	DC potential of the center conductor.
V_p	RF pump potential.
V_s	DC potential of the outer conductor.
β_i	Propagation constant at the idler frequency.

β_p Propagation constant at the pump frequency.

β_s Propagation constant at the signal frequency.

ϵ Small positive quantity.

η Absolute value of the ratio of the charge to the mass of an electron.

$\dot{\phi}_0$ DC angular velocity of the electrons.

$\dot{\phi}_1$ RF angular velocity of the electrons at the signal frequency.

$\dot{\phi}_p$ RF angular velocity of the electrons at the pump frequency.

ω_1 Idler frequency (rad/s).

ω_p Pump frequency (rad/s).

ω_s Signal frequency (rad/s).

PART II

LIST OF SYMBOLS

a	Radius of the helix.
a_1	Constant defined by $a_1 = \alpha_3/\alpha_1 = (\omega_{q3}/\omega_{q1})(\omega_1/\omega_3)$.
a_2	Constant defined by $a_2 = \alpha_3/\alpha_2 = (\omega_{q3}/\omega_{q2})(\omega_2/\omega_3)$.
A	Complex normalizing constant of the longitudinal electric field.
b	Beam radius.
c	Velocity of light.
$E'(z,t)$	Total external electric field.
$E_\ell(z)$	Space dependent external electric field at the frequency ω_ℓ .
$E_s'(z,t)$	Total space-charge field.
$E_{s\ell}(z)$	Space dependent space-charge field at the frequency ω_ℓ .
$E_T'(z,t)$	Total longitudinal electric field.
$E(z)$	Longitudinal electric field.
$F(z)$	Normalized longitudinal electric field.
$i_\ell(z)$	Modified current density at the frequency ω_ℓ .
$i_\ell^{(n)}$	n th space-charge wave $[(n) = 1,2,3,4]$ corresponding to the modified current density at the frequency ω_ℓ .
I_0	Defined by $I_0 = \rho_o u_0$.
I_0'	Total dc current density.
$I_1(z)$	Space dependent current density at the signal frequency.
$I_2(z)$	Space dependent current density at the idler frequency.
$I_3(z)$	Space dependent current density at the pump frequency.
$I(z,t)$	Time and z dependent total current density.
k_1	Defined by $k_1 = \omega_1/u_0$.
k_2	Defined by $k_2 = \omega_2/u_0$.

k_3 Propagation constant at the pump frequency $k_3 = \omega_3/u_0$.

k_ℓ Propagation constant of the ℓ th space-charge wave.

k_{q1} Reduced plasma propagation constant at the signal frequency.

k_{q2} Reduced plasma propagation constant at the idler frequency.

k_{q3} Reduced plasma propagation constant at the pump frequency.

K Perveance of the electron gun.

L Length of the cavity.

m The complex number used to define the strength of the current wave at the pump frequency.

n Length of the cavity in half-circuit wave length.

N Number of turns of the helix.

Q_L Loaded Q of the cavity.

R_1 Plasma reduction factor at the signal frequency.

R_2 Plasma reduction factor at the idler frequency.

R_3 Plasma reduction factor at the pump frequency.

R_{sh} Shunt resistance of the cavity.

u_f Phase velocity of the fast space-charge wave.

u_s Phase velocity of the slow space-charge wave.

$u_1(z)$ RF longitudinal velocity at the signal frequency.

$u_2(z)$ RF longitudinal velocity at the idler frequency.

$u_3(z)$ RF longitudinal velocity at the pump frequency.

v Phase velocity of a beam wave.

v_{ph} Phase velocity of the forward circuit wave.

V_0 Beam voltage.

V_f Kinetic voltage associated with the fast space-charge wave.

y Ratio of the dc velocity of the electrons to the phase velocity of the circuit $y = u_0/v_{ph}$.

α_ℓ	Constant defined by $\alpha_\ell = \omega_{q\ell}/\omega_\ell$.
β	Coupling coefficient.
$\beta_{0\ell}$	Absolute value of the coupling coefficient to a beam wave of propagation constant k_ℓ .
ϵ	Parameter defined by $\epsilon = 1 - v_{ph}/u_0$.
ν	Ratio of the signal frequency to the idler frequency.
ρ_0	DC charge density.
$\rho_1(z)$	RF charge density at the signal frequency.
$\rho_2(z)$	RF charge density at the idler frequency.
$\rho_3(z)$	RF charge density at the pump frequency.
ψ	Pitch angle of the helix.
$\omega_{q\ell}$	Reduced plasma at the frequency ω_ℓ .

INTRODUCTION

The use of beam-type parametric amplifiers is one possible approach to low-noise amplification at microwave frequencies. Parametric amplification has been known for more than one hundred years, but its application to electron tubes is very recent. This thesis is concerned with some aspects of electron-beam parametric amplification.

If a disturbance is impressed on an electron beam in dc equilibrium, the disturbance propagates along the beam in the form of two waves. The phase velocity of one of the waves is smaller than the dc velocity of the electrons; the phase velocity of the other is larger than the dc electron velocity. For these reasons the waves are called slow wave and fast wave respectively. Haus and Robinson[1] have shown that nonparametric amplifiers using a slow space-charge wave have a theoretical minimum noise figure. More recently Beam[2] has shown that the same conclusions can be attained for slow transverse waves. However, when fast waves are used, such a limitation does not exist. The noise can be removed from fast waves because they carry positive power,[3] and until recently[4] it was thought that the noise could not be extracted from the slow waves because they carry negative power.

For these reasons there has been a wide interest in the interaction between a fast wave and a circuit wave; this led to the development of the low-noise beam-type parametric amplifier in the same fashion that interaction between a slow wave and a circuit wave led to the development of the conventional traveling-wave tube. There is however another major difference between fast and slow wave interaction: fast waves do not give rise to amplification. An independent gain mechanism must be provided in the form of an amplifying section.

A typical beam-type parametric amplifier is schematically represented by Fig. 1.1. The fast-wave couplers extract the noise and couple the signal in and out. The rf-pumped middle section provides the energy which is necessary for signal amplification.

The beam-type parametric amplifiers can be classified into three main categories:

(1) Space-charge wave amplifiers.

In these tubes the electron beam is immersed in a longitudinal mag-

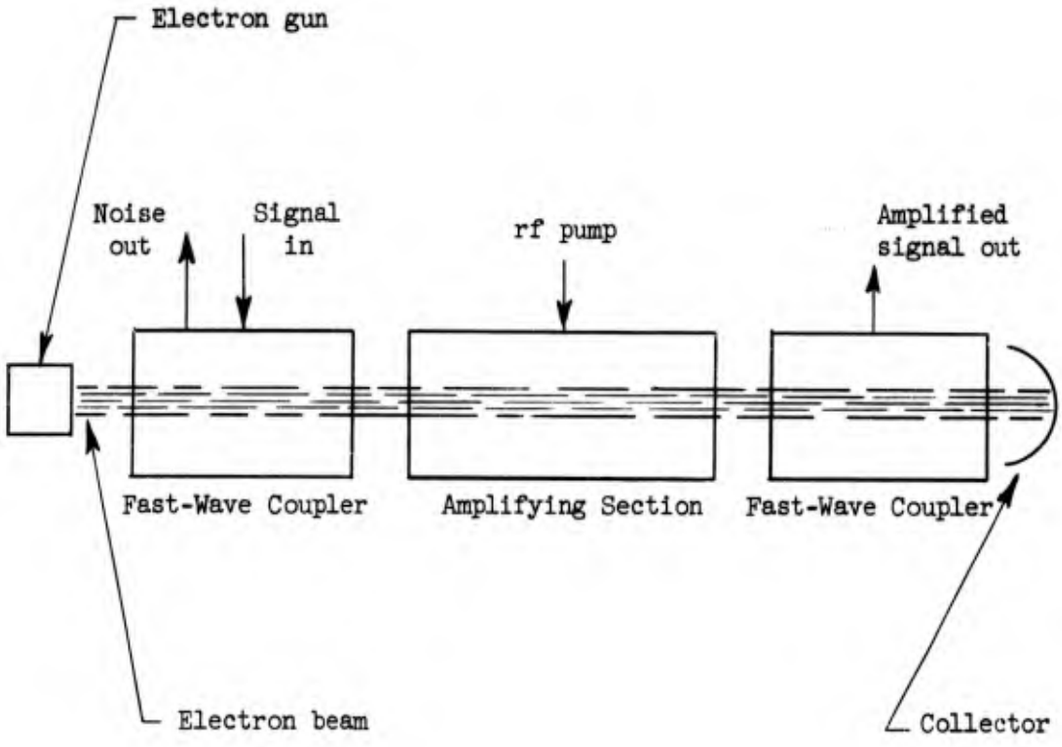

FIG. I.1--Schematic of a beam-type parametric amplifier.

netic field which is large enough to prevent any transverse motion of the electrons. A longitudinal disturbance impressed on the beam propagates as a fast and a slow space-charge wave. Amplifiers using fast space-charge waves have been studied by Bridges,[5] Louisell,[6,7] Quate,[6] Heffner and Wade,[8] and Ashkin,[9,10] among others.

(2) Cyclotron-wave amplifiers.

In this type of amplifier the longtiudinal magnetic field is such that the cyclotron frequency is equal to the signal frequency.[11,12] A transverse disturbance at the signal frequency propagates as a slow and a fast cyclotron wave. The most well known cyclotron-wave amplifier is the quadrupole amplifier.[13]

(3) Electrostatic-wave amplifiers.

Here the electron beam is electrostatically focused. The electrons trace the path of a helix between two concentric conductors, and the dc potential difference between the conductors maintains the beam in dc equilibrium. If a transverse disturbance is impressed on the beam, the disturbance propagates as a fast and a slow electrostatic wave. Pantell[14] proposed an electrostatic parametric amplifier using the fast electrostatic wave.

It is interesting to compare the phase velocities of these three different types of waves:

(1) Space-charge waves

$$v_s = \frac{u_0}{1 + (\omega_q/\omega_s)} \quad \text{(slow wave)}$$

$$v_f = \frac{u_0}{1 - (\omega_q/\omega_s)} \quad \text{(fast wave)}$$

where ω_s is the signal frequency in rad/sec
ω_q is the reduced plasma frequency in rad/sec
u_0 is the dc longitudinal velocity of the electrons.

(b) Cyclotron waves

$$v_s = \frac{u_0}{1 + (\omega_c/\omega_s)} \qquad \text{(slow wave)}$$

$$v_f = \frac{u_0}{1 - (\omega_c/\omega_s)} \qquad \text{(fast wave)}$$

where $\omega_c = (|e|/m)B$ (cyclotron frequency)

B is the magnetic induction

$|e|/m$ is the ratio of the charge to the mass of an electron.

(c) Electrostatic waves

$$v_s = \frac{u_0}{1 + (\sqrt{2}\,\dot{\phi}_0/\omega_s)} \qquad \text{(slow wave)}$$

$$v_f = \frac{u_0}{1 - (\sqrt{2}\,\dot{\phi}_0/\omega_s)} \qquad \text{(fast wave)}$$

where $\dot{\phi}_0$ is the dc angular velocity of the electrons.

In practice the ratio ω_q/ω_s is, at the most, equal to a few tenths. The phase velocities of the fast and slow space-charge waves are not very different, and it may become difficult to have good coupling to the fast wave without any coupling to the slow wave.

On the other hand, by choosing $\omega_s = \omega_c$ (cyclotron waves) or $\omega_s = \sqrt{2}\,\dot{\phi}_0$ (electrostatic waves), the phase velocity of the fast waves becomes infinite, and the phase velocity of the slow waves becomes one-half of the dc longitudinal velocity of the electrons. This large velocity spread insures excellent coupling to the fast wave only.

The first two types of amplifiers require large magnetic fields which add weight and bulk to the tubes. The electrostatic amplifier has the main advantage, inherent to any electrostatic system, in that it requires no magnetic field.

The work presented here consists of two parts. The amplifying properties of two particular kinds of electron beam parametric amplifiers are investigated: one uses electrostatic waves, and the other uses space-charge waves.

PART 1. STUDY OF AN ELECTROSTATIC PARAMETRIC AMPLIFIER

The theory of the amplifying section of the electrostatic parametric amplifier was derived. The trajectory of an electron was calculated from the ballistic equations of motion and it is shown that if all the electrons are taken into account, amplification can occur. Using this result, the gain of the amplifying section was derived. Using Pantell's fast wave couplers, an electrostatically focused parametric amplifier operating at L-band was designed and built.

PART 2. STUDY OF A SPACE-CHARGE WAVE PARAMETRIC AMPLIFIER

It is shown that long interaction klystron cavities,[15] supporting a sinusoidal resonant longitudinal electric field, can be used as fast-wave couplers. The beam loading admittance in an extended interaction klystron cavity, due to a parametrically-pumped electron beam,[6,7] is calculated. Under certain conditions, the real part of this admittance can become negative; this can lead to the amplification of an injected signal. These results are applied to two specific cases:

(a) "Floating drift tube" klystron cavity, leading to a better understanding of Bridges' tube.[5]

(b) "Long-interaction" klystron cavity, leading to a low-noise parametric amplifier.

It is shown in both cases that amplification can occur, at least in theory, without having any growing space-charge waves. A low-noise amplifier using space-charge waves was designed. The fast-wave coupler consists of long interaction cavities and the amplification arises from the negative beam-loading conductance across the output cavity.

PART I

STUDY OF AN ELECTROSTATIC PARAMETRIC AMPLIFIER

PART I: STUDY OF AN ELECTROSTATIC PARAMETRIC AMPLIFIER

CHAPTER I

INTRODUCTION

There has been wide interest in electrostatic focusing, instead of magnetic focusing, of the electron beams used in microwave tubes because this type of focusing does not require any magnet. The electrostatic tubes are lighter and less bulky; this makes them more suitable for all the applications where weight is an important factor. It should be noted, however, that the focusing becomes extremely difficult when the beam current becomes large, thus restricting electrostatic focusing to low-power tubes. It would be very useful, also, if these tubes could exhibit low-noise properties. This could be achieved, for example, with a low-noise electron gun or with parametric pumping.

The existence of fast electrostatic waves led Pantell to the conception of an electrostatically focused parametric amplifier which would combine the advantages of an electrostatic system with the low-noise characteristics of a parametric amplifier.

A beam-type parametric amplifier consists of three parts (Fig. I.1) which will be briefly discussed here.

(1) Electron beam.

The electron-beam is a cylindrical beam which has both a longitudinal and an azimuthal dc motion combined in such a way that the electrons trace the path of a helix between two concentric conductors (Fig. I.2). The dc potential which exists between the conductors creates an inward force which balances the outward centrifugal force due to the azimuthal motion.

(2) Fast-wave couplers.

The purpose of a fast-wave coupler is twofold: At the frequency for which the coupler is designed it extracts the noise (or signal) which existed in the fast electrostatic wave and it impresses on the beam, as a fast electrostatic wave, an externally applied signal (Fig. I.3). The signal frequency ω_s is chosen to be

$$\omega_s = \sqrt{2}\,\dot{\phi}_0$$

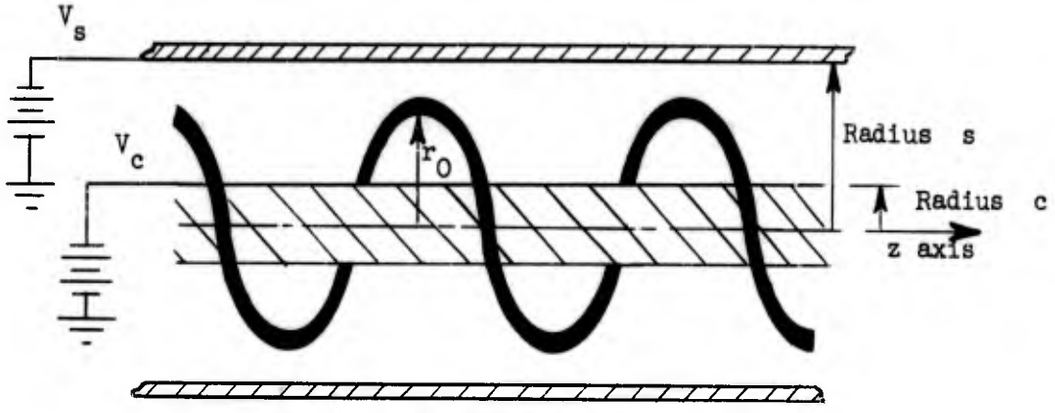

r_0 dc equilibrium radius of the electrons

FIG. I.2--DC electron trajectory in the electrostatic amplifier.

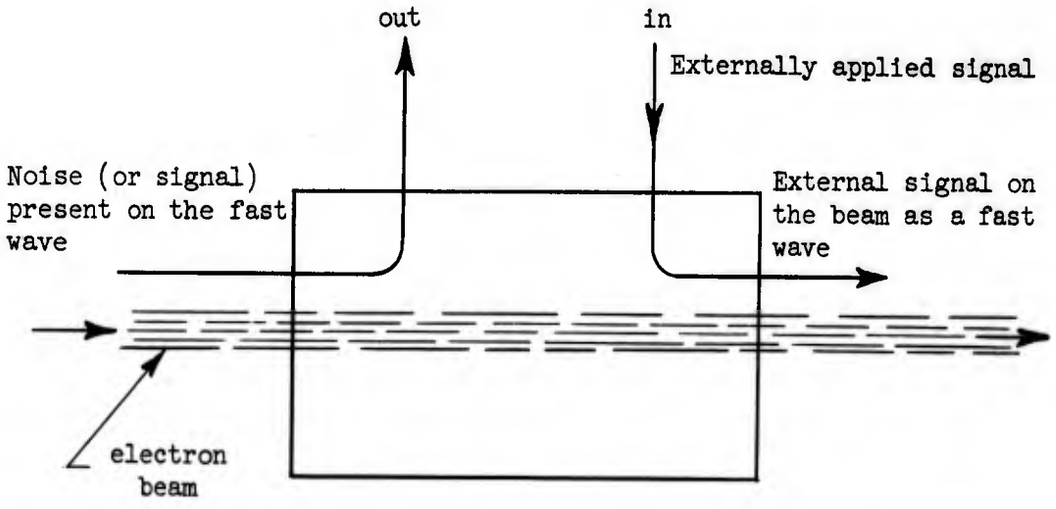

FIG. I.3--Diagram of the fast-wave coupler.

where $\dot{\phi}_0$ is the dc angular velocity of the electrons, and the phase velocity of the fast electrostatic wave is infinite.

Pantell[14] has studied two types of couplers for which the circuit wave interacts only with the fast wave:

(a) Traveling-wave coupler. The traveling-wave coupler consists of a proper length of coaxial transmission line (Fig. I.4). The signal is injected (or extracted) at one end, the other end being matched. This type of coupler is relatively long, is very narrow band, but is voltage tunable.

(b) Lumped resonant coupler. This coupler is made of a short length of coaxial line (Fig. I.4). The line is externally tuned to resonate at the signal frequency. No impedance matching is required but the loaded Q , Q_L , must have a critical value. This coupler is short, relatively broad band, but is not voltage tunable.

(3) Amplifying section.

The interaction between a fast wave and a circuit does not give rise to growing waves; that is, no amplification of the signal is achieved. An rf pumped amplifying section, inserted between the input and output couplers, provides a nonlinear interaction mechanism between a pump circuit wave and the fast electrostatic wave. This new interaction process creates growing waves at the signal frequency and amplification is achieved.

The rf pump frequency is found to be

$$\omega_p = \left(2 + \frac{p}{\sqrt{2}}\right)\omega_s$$

where ω_p is the pump frequency in rad/sec and
p is the number of azimuthal variations of the pump electric field in the amplifying section.

Two different cases will be studied:

(1) For $p = 0$, the electric field has cylindrical symmetry. The amplifying section consists of a given length of coaxial transmission line (Fig. I.5). The parametric amplifier is degenerate: the pump frequency is twice the signal frequency.

(2) For $p \neq 0$, the circuit consists of a $2p$ wire transmission line surrounding a central conductor (Fig. I.5). The central conductor provides the electrostatic focusing force and exerts no rf action.

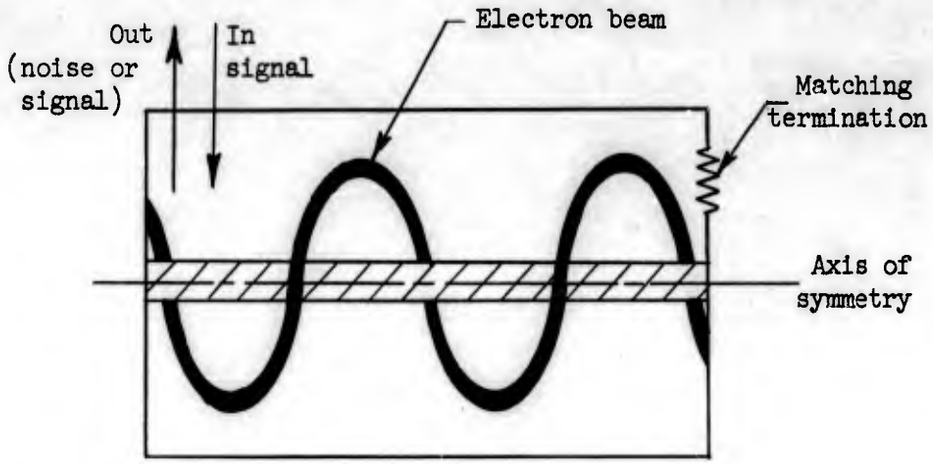

(a) Traveling-Wave Coupler

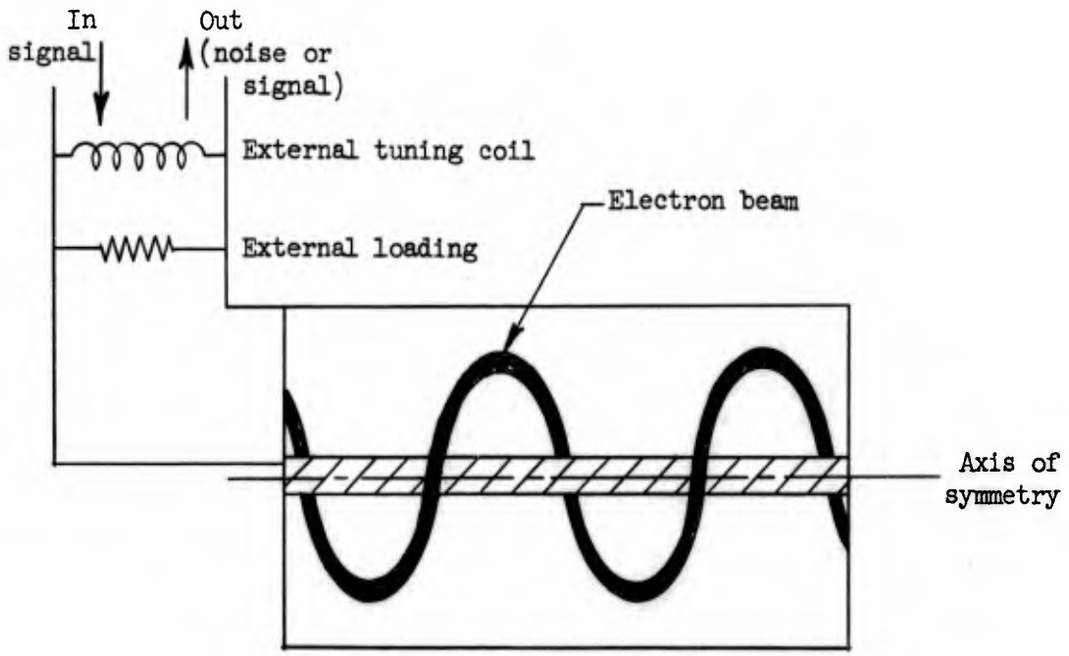

(b) Lumped Resonant Coupler

FIG. I.4--Fast-wave couplers.

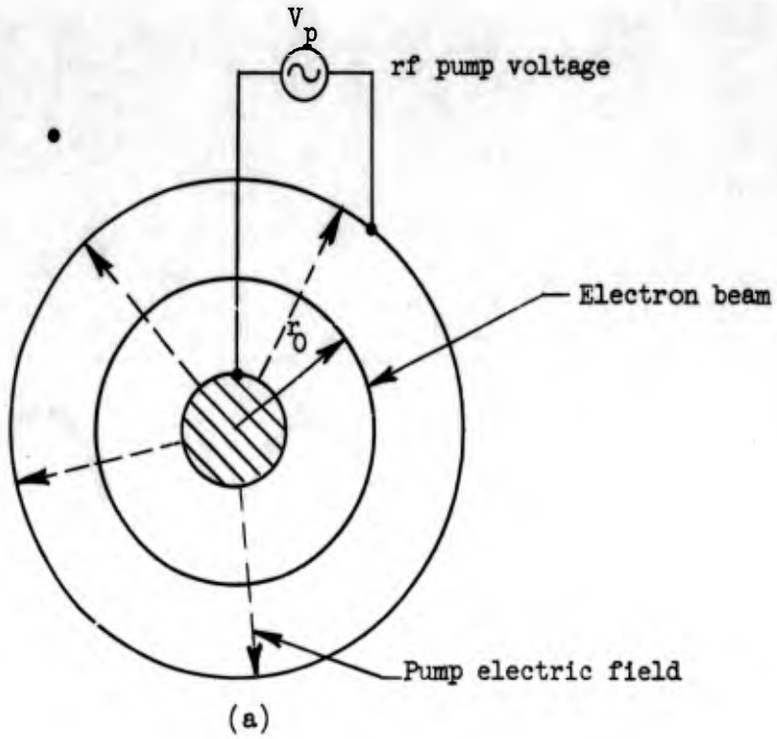

(a)

p = 0

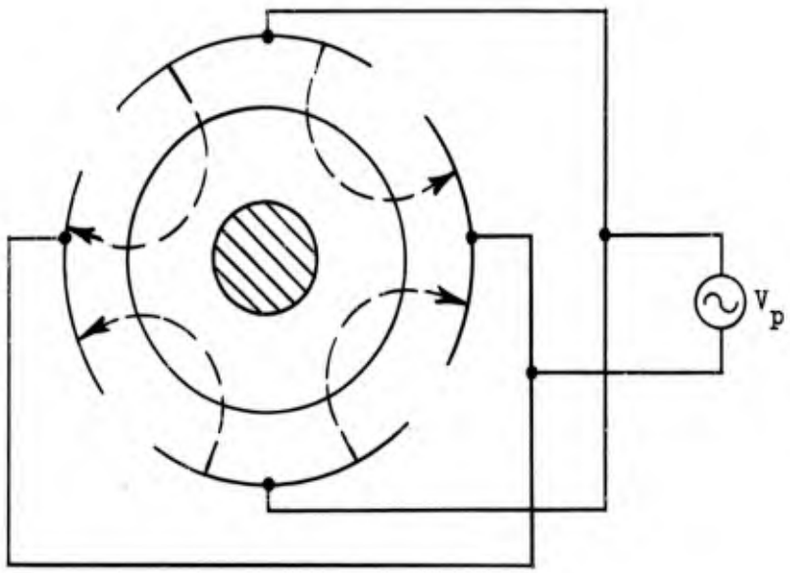

(b)

p = 2

FIG. I.5--Cross section of the amplifying section.

(a) Cylindrical Symmetry p = 0

(b) Two azimuthal variations of the pump electric field

CHAPTER II

FAST-WAVE COUPLERS

A detailed summary of Pantell's work will be presented here for the purpose of completeness. The theory is a small-signal theory.

The propagation of a transverse disturbance impressed on the beam will be established. The phase velocities of the fast and the slow electrostatic waves will be calculated. Finally, the theory of the fast-wave couplers will be outlined.

A. PROPAGATION OF A TRANSVERSE DISTURBANCE ON THE ELECTRON BEAM

The motion of the electrons in a beam, electrostatically focused as in Fig. I.2, is governed by the following equations in a cylindrical system of coordinates r , ϕ , z :

$$\ddot{r} - r\dot{\phi}^2 = -\left(\eta \frac{V_0}{r}\right) \tag{I.1}$$

$$r\ddot{\phi} + 2\dot{r}\dot{\phi} = 0 \ . \tag{I.2}$$

The term V_0 is defined as

$$V_0 = \frac{V_c - V_s}{\ln(s/c)} \tag{I.3}$$

where V_c is the dc potential of the center conductor
c is the radius of the center conductor
V_s is the dc potential of the outer conductor
s is the radius of the outer conductor,
and $\eta = |e|/m$ ratio of the charge to the mass of an electron.

As is customary in a small-signal analysis, the different quantities will be separated in their dc and rf components. Only first order rf terms will be retained, resulting in

$$\left.\begin{aligned} r &= r_0 + r_1 \\ \phi &= \phi_0 + \phi_1 \end{aligned}\right\} \tag{I.4}$$

where r_0 is the dc equilibrium radius of the electrons
$\dot{\phi}_0$ is the dc angular velocity of the electrons
r_1 is the rf radial displacement of the electrons
$\dot{\phi}_1$ is the rf angular velocity of the electrons.

The rf quantities vary as

$$e^{j\omega_s t} \quad e^{-\Gamma z} \tag{I.5}$$

Equations (I.1) through (I.5) yield the value of Γ as

$$\Gamma = j\beta_e \pm j(\sqrt{2}\,\dot{\phi}_0/u_0) \tag{I.6}$$

where $\beta_e = \omega_s/u_0$ and u_0 is the dc longitudinal velocity of the electrons along the z axis. The two values of Γ correspond to the two electrostatic waves. The corresponding phase velocities are

$$\left.\begin{aligned} v_s &= \frac{u_0}{1 + \sqrt{2}\,\dot{\phi}_0/\omega_s} \quad \text{(slow electrostatic wave)} \\ \text{and} \\ v_f &= \frac{u_0}{1 - \sqrt{2}\,\dot{\phi}_0/\omega_s} \quad \text{(fast electrostatic wave).} \end{aligned}\right\} \tag{I.7}$$

If $\omega_s = \sqrt{2}\,\dot{\phi}_0$ rad/sec, the phase velocity of the fast wave becomes infinite and the phase velocity of the slow wave is equal to half the dc velocity u_0. If a circuit has an infinite phase velocity at the frequency $\omega_s = \sqrt{2}\,\dot{\phi}_0$, it will couple only to the fast electrostatic wave.

The trajectory of an electron in a transverse plane, obtained from Eqs. (I.4) through (I.6), is shown in Fig. I.6. The angle corresponding to an rf period is $2\pi/\sqrt{2} = 254^\circ$.

A better picture of the electron trajectory can be obtained by changing the frame of reference. Consider a Cartesian system of coordinates rotating with the beam with a constant angular velocity $\dot{\phi}_0$. The origin O' describes the circle of radius r_0 and the y axis is in the radial

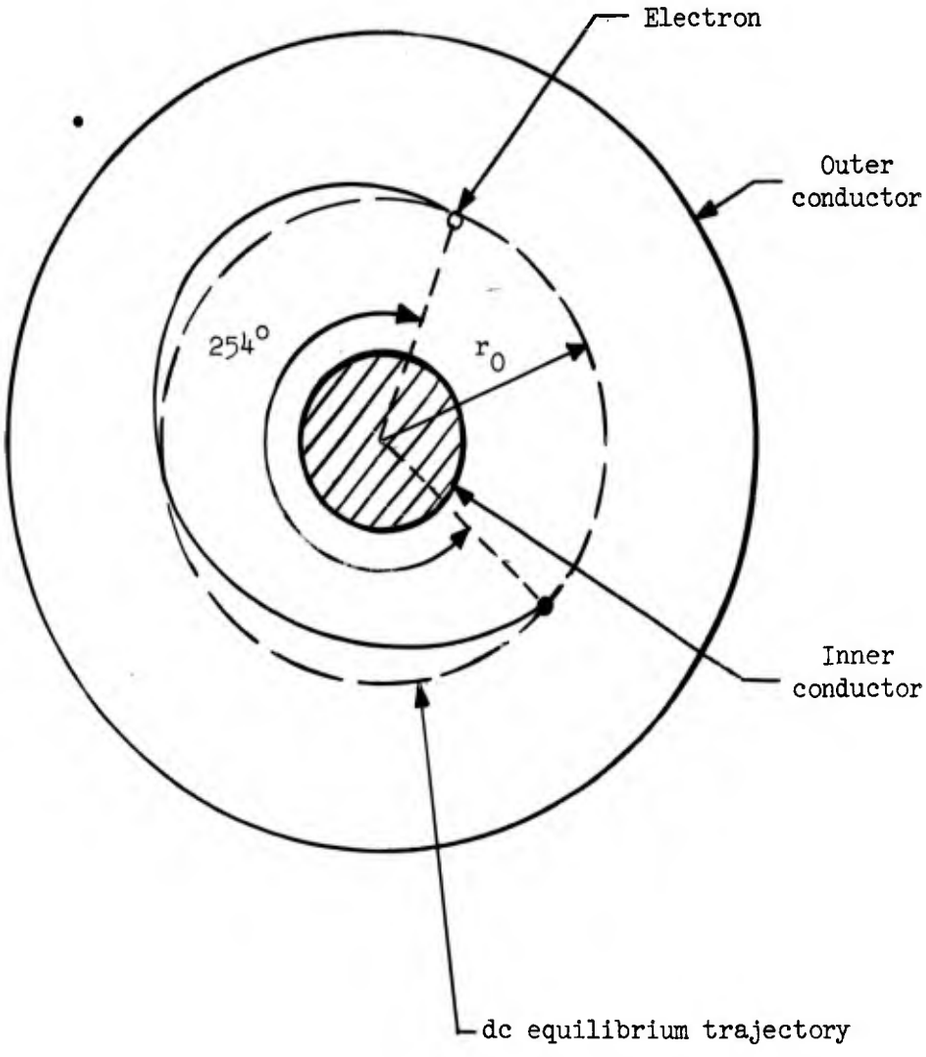

FIG. I.6--Trajectory of an electron.

$(\vec{r})$ direction, as in Fig. I.7, if

$$r_1 = A \cos \sqrt{2}\,\dot{\phi}_0 t \ .$$

Then, from Eq. (I.2), the result is

$$\dot{\phi}_1 = -\frac{\sqrt{2}}{r_0} A \sin \sqrt{2}\,\dot{\phi}_0 t \ .$$

In the Cartesian coordinate system the position of the electron in a transverse plane is given by

$$\left.\begin{aligned} x &= \sqrt{2}\, A \sin \sqrt{2}\,\dot{\phi}_0 t \\ y &= A \cos \sqrt{2}\,\dot{\phi}_0 t \ . \end{aligned}\right\} \qquad (I.8)$$

The trajectory is an ellipse centered on $0'$ with its major axis along the x axis. An electron describes the complete ellipse in one period $T = 2\pi/\omega_s$.

A cumulative interaction between an electron and a radial electric field of frequency $\omega_s = \sqrt{2}\,\dot{\phi}_0$ is possible. If the field is zero at the instant t_1 and has the direction shown in Figs. I.7b and I.7c, the field delivers energy to the electron during the full cycle, since the rf field reverses when the direction of the radial motion of the electron changes.

B. TRAVELING-WAVE COUPLER

A fast-wave coupler is a microwave circuit which couples only to the fast wave. The circuit must support a wave at the signal frequency $\omega_s = \sqrt{2}\,\dot{\phi}_0$ with the proper phase velocity in order to obtain the cumulative interaction described above. The traveling-wave coupler is one of the two fast-wave couplers studied by Pantell.[14]

With an rf radial electric field E_r present, and for the same geometrical structure (Fig. I.4a), the equations of motion, Eqs. (I.1) and (I.2), become

$$\left.\begin{aligned} \ddot{r} - r\dot{\phi}^2 &= -\eta E_r - \frac{\eta V_0}{r} \\ \text{and} \qquad r\ddot{\phi} + 2\dot{r}\dot{\phi} &= 0 \ . \end{aligned}\right\} \qquad (I.9)$$

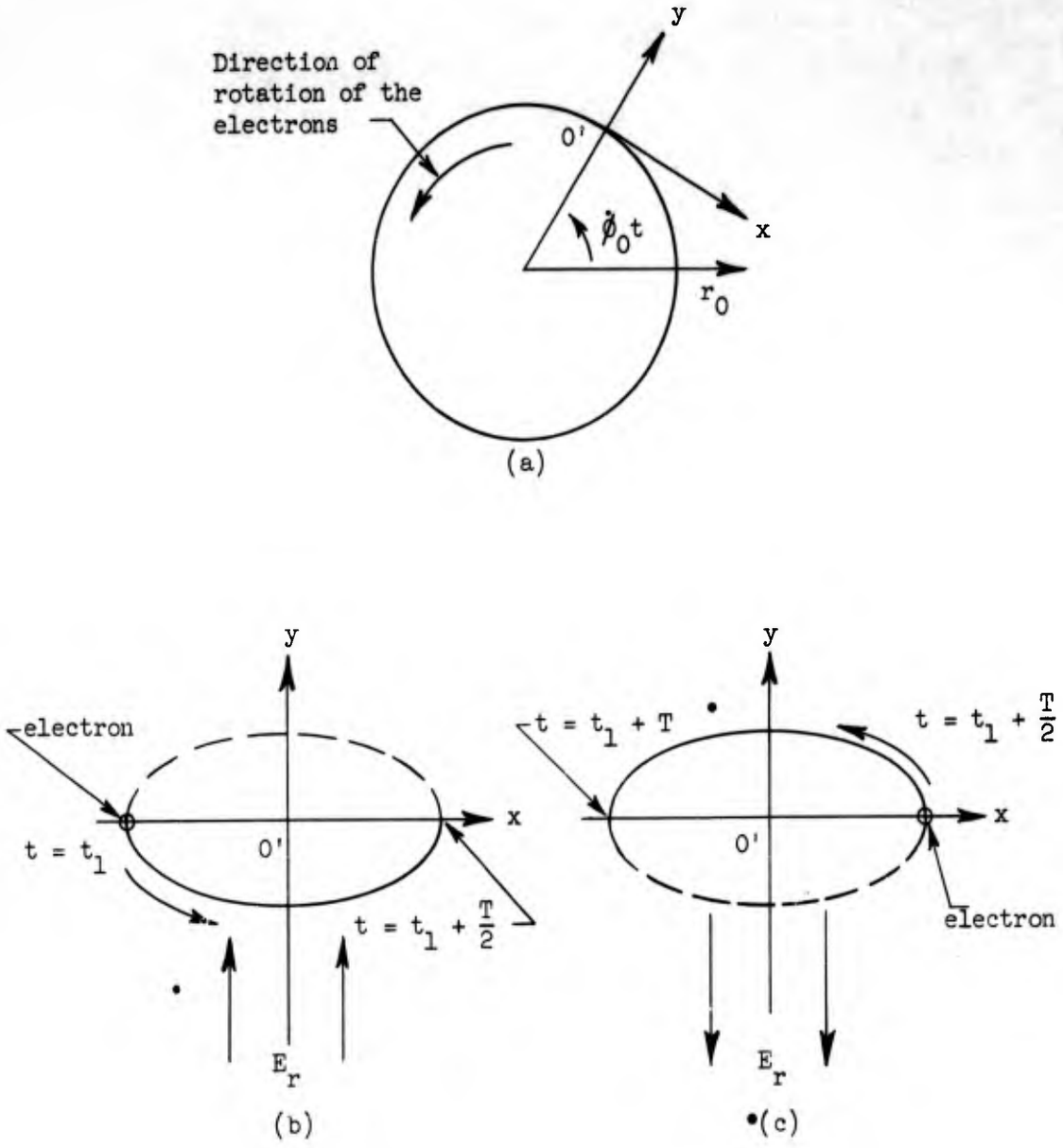

FIG. I.7--Electron trajectory in a frame of reference rotating at the dc angular velocity of the electrons.

(a) New System of Coordinates

(b) Electron trajectory and rf radial field during the first half of a cycle.

(c) Electron trajectory and rf radial field during the second half of a cycle.

Pantell[14] solved these equations and has calculated the circuit field $E_r(z)$ and the time derivative of the radial displacement of the electron $\dot{r}_1(z)$ at any point z inside the coupler. If the coupler is terminated on its characteristic impedance, that is, if the coupler is matched, then the result is

$$E_r(z) = e^{-j\beta z}\left[E_r(0)\cos\beta_e Cz + \frac{2\omega_s C}{\eta}\dot{r}_1(0)\sin\beta_e Cz\right] \qquad (I.10)$$

and

$$\dot{r}_1(z) = e^{-j\beta z}\left[\frac{\eta}{2\omega_s C}E_r(0)\sin\beta_e Cz + \dot{r}_1(0)\cos\beta_e Cz\right] \qquad (I.11)$$

where $E_r(0)$ is the circuit electric field at the input of the coupler,

$\dot{r}_1(0)$ is the time derivative of the radial displacement of the electron at the input of the coupler

C is a parameter defined by

$$C = \left[\frac{\eta I_0 E_{rn}^2}{8P_n\omega_s^2}\right]^{1/2} \qquad (I.12)$$

where I_0 is the dc current

P_n is the power flow associated with the TEM mode

E_{rn} is the circuit field in the absence of the beam.

If the length L of the coupler is such that

$$\beta_e CL = (2n+1)\frac{\pi}{2} \qquad n = 0,1,2\ldots \qquad (I.13)$$

then the result is

$$\left.\begin{aligned} E_r(L) &= e^{-j\beta L}\frac{2\omega_s C}{\eta}\dot{r}_1(0) \\ \dot{r}_1(L) &= e^{-j\beta L}\frac{\eta}{2\omega_s C}E_r(0) \end{aligned}\right\} \qquad (I.14)$$

The signal originally present on the beam $\left[\dot{r}_1(0)\right]$ has been completely transferred to the circuit, and the signal injected into the coupler $\left[E_r(0)\right]$ has been completely transferred to the beam. If the dc longitudinal velocity of the electron is very small compared to the velocity of light, this coupler interacts only with the fast wave.

The bandwidth of this type of coupler is quite small, but it is voltage tunable. For a TEM mode and a small beam pitch angle ψ, Pantell has found that

$$\left.\begin{aligned} r_0 &= \frac{s}{e^{1/2}} \\ \dot{\phi}_0 &= \frac{e^{1/2}}{s}\,\frac{\eta(V_c - V_s)}{\ln(s/c)} \\ \beta_e C &= \frac{1}{u_0}\left[\frac{120\,\eta I_0}{8 r_0^{\,2} P_n s/c}\right]^{1/2} \end{aligned}\right\} \qquad \text{(I.15)}$$

Equations (I.13) and (I.15) define the coupler completely.

C. LUMPED-RESONANT COUPLER

Pantell, following a method similar to the one used by Cuccia, also studied a resonant type of coupler. The coupler represented in Fig. I.4b consists of a short length of open-circuited coaxial transmission line. The line is shorter than a quarter-wavelength and acts like a capacitor. The coupler can be tuned to resonate, at the signal frequency, with an external inductance. In order to transfer all the energy from the fast wave to the circuit, the resonant system must be properly loaded. Pantell[14] derived the expression relating the loaded Q, Q_L, to the length and the frequency:

$$\frac{1}{Q_L} = \frac{L\lambda}{2\pi}(\beta_e C)^2 \qquad \text{(I.16)}$$

where L is the length of the cavity

λ is the wavelength, and

C is the parameter defined by Eq. (I.12).

The loaded Q is inversely proportional to the product $L\lambda$. For a given Q_L the length of the cavity increases with the frequency. At high frequencies the loaded Q must be small in order to maintain reasonably small dimensions of the coupler.

Pantell found that the coupler, which is not voltage tunable, is relatively broad band.

D. COMPARISON OF THE TWO TYPES OF COUPLERS

A concrete example, using numerical values, will be chosen to illustrate the advantages and disadvantages of both couplers.

Consider a coupler where

- s radius of the outer conductor is 0.120"
- c radius of the inner conductor is 0.040"
- I_0 the dc current is 300μA
- u_0 the dc velocity is 1/300 × velocity of light
- f_s the signal frequency is 1.2 kMc/sec
- V_s the outer cylinder potential is zero

From Eqs. (I.10) through (I.16) these characteristics are as follows:

$$\beta_e C = 0.148$$

Traveling-wave coupler	Lumped-resonant coupler
L = 10 cm	L = 1.15 cm
narrow band	with $Q_L = 10$
voltage tunable	2.5 per cent bandwidth
frequency = $1.6V_s^{1/2}$ kMc/sec	

The bandwidth has been defined by the relation

$$\left[\frac{\dot{r}_1(L)}{r_1(0)}\right]^2 < 0.1 \ .$$

Certain conclusions can be drawn from this example:

(1) The traveling-wave coupler is much longer than the resonant coupler.

(2) The traveling-wave coupler has the advantage of being voltage tunable. In practice it may be extremely difficult to match the transmission line, due to the presence of the beam between the two conductors, and electrostatic focusing is difficult to achieve over long distances. The resonant coupler, being short, is then a better choice. Furthermore,

the critical loading of the resonant coupler is easier to achieve than the matching of the traveling-wave coupler. For these reasons, the resonant coupler was chosen for the design of an experimental tube.

CHAPTER III

AMPLIFYING SECTION

A. INTRODUCTION.

The interaction between a fast wave and a circuit wave does not produce any amplification. Pierce's coupled mode theory provides a simple explanation. The power flow in the fast wave and the power flow in the circuit wave are in the same direction[16] and the propagation constants of the coupled waves remain purely imaginary. The rf energy is transferred from one wave to the other. If a parametric amplifying section is inserted after the input coupler, the energy of the rf pump is converted into energy at the signal frequency by means of the nonlinear properties of the electron beam.

It will be shown that the frequency of the rf pump depends on the geometrical configuration of the pump electric field. The ballistic equations governing the motion of an electron in the pump field will be solved and the gain of the amplifying section calculated.

B. DETERMINATION OF THE PUMP FREQUENCY

The signal, idler and pump frequencies are related through Eq. (I.17)

$$\omega_p = \omega_s + \omega_i \tag{I.17}$$

where ω_p is the pump frequency
ω_s is the signal frequency
ω_i is the idler frequency.

To insure a cumulative parametric effect the propagation constants must satisfy the following equation

$$\beta_p = \beta_s + \beta_i \tag{I.18}$$

where $\beta_p = \omega_p/v_p$
$\beta_s = \omega_s/v_s$
$\beta_i = \omega_i/v_i$,

and where

v_p is the phase velocity at the pump frequency

v_s is the phase velocity at the signal frequency

v_i is the phase velocity at the idler frequency.

The rf quantities vary as indicated:

$$\exp(j\omega_s t) \cdot \exp\left(- j \frac{\omega_s}{u_0} z\right) \cdot \exp\left(+ j\sqrt{2} \frac{\dot{\phi}_0}{u_0} z\right)$$

at the signal frequency (I.19)

$$\exp(j\omega_i t) \cdot \exp\left(- j \frac{\omega_i}{u_0} z\right) \cdot \exp\left(+ j\sqrt{2} \frac{\dot{\phi}_0}{u_0} z\right)$$

at the idler frequency (I.20)

$$\exp(j\omega_p t) \cdot \exp\left(+ j \frac{\omega_p}{v_p} z\right) \cdot \exp\left(- jp \frac{\dot{\phi}_0}{u_0} z\right)$$

at the pump frequency (I.21)

where p is the number of azimuthal variations of the pump electric field in the amplifying section. If the phase velocity of the pump electric field is much larger than the dc longitudinal velocity of the electron Eq. (I.21) becomes

$$\exp(j\omega_p t) \cdot \exp\left(- jp \frac{\dot{\phi}_0}{u_0} z\right) . \qquad (I.22)$$

If the signal frequency is equal to $\sqrt{2}\,\dot{\phi}_0$, the phase velocity v_s becomes infinite and

$$\beta_s = 0 .$$

Equation (I.18) yields

$$\beta_p = \beta_i \qquad (I.23)$$

which can be written

$$\omega_s - \omega_i = - \frac{p}{\sqrt{2}} \omega_s \qquad (I.24)$$

Equations (I.17) and (I.24) define the pump frequency ω_p as

$$\omega_p = \left(2 + \frac{p}{\sqrt{2}}\right)\omega_s \quad \text{rad/sec.} \tag{I.25}$$

If the pump electric field has cylindrical symmetry ($p = 0$), the pump frequency is twice the signal frequency: the idler and signal frequencies are the same and the amplifier is called degenerate.

If the pump electric field has p azimuthal variations the pump and signal frequencies are not harmonically related.

C. OUTLINE OF THE INTEGRATION OF THE EQUATIONS OF MOTION.

The equations of motion in cylindrical coordinates are:

$$\ddot{r} - r\dot{\phi}^2 = -\eta E_r(r,\phi,t) \tag{I.26}$$

$$r\ddot{\phi} + 2\dot{r}\dot{\phi} = -\eta E_\phi(r,\phi,t)\ , \tag{I.27}$$

where $E_r(r,\phi,t)$ and $E_\phi(r,\phi,t)$ are the radial and azimuthal components of the pump electric field in the amplifying section.

These equations can be solved with the following assumptions:

(1) All the electrons have the same dc longitudinal velocity u_0 and the same dc angular velocity $\dot{\phi}_0$.

(2) The space-charge forces are neglected.

(3) The theory is limited to the three-frequency case; that is, the important terms are at the signal, idler, and pump frequencies. All the other frequencies are neglected.

(4) The theory is based on a small-signal analysis. The dc and rf components are separated and r and $\dot{\phi}$ are written

$$\begin{aligned} r &= r_0 + r_p + \epsilon r_1 \\ \dot{\phi} &= \dot{\phi}_0 + \dot{\phi}_p + \epsilon\dot{\phi}_1\ . \end{aligned} \tag{I.28}$$

where r_0 is the dc equilibrium radius of the electrons

r_p is the rf displacement of a given electron at the pump frequency

r_1 is the rf displacement of a given electron at the signal frequency

$\dot{\phi}_0$ is the dc angular velocity of the electrons

$\dot{\phi}_p$ is the rf angular velocity of a given electron at the pump frequency

$\dot{\phi}_1$ is the rf angular velocity of a given electron at the signal frequency, and

ϵ is a small positive number.

All the equations are kept linear with respect to ϵ and with respect to the amplitude of the pump electric field.

(4) The electron motion at the pump frequency is not perturbed by the presence of the signal. The perturbation of the dc electron trajectories at the pump frequency is calculated with no signal present, and these calculated values of r_p and $\dot{\phi}_p$ are used in the presence of the signal.

If these assumptions are made, the equations of motion become linear equations with nonconstant coefficients. However, the varying coefficients of the differential equations vary in a harmonic fashion and their amplitude is small compared to the constant coefficients; then, it is possible to solve the equations using the method of the variation of parameters.[17]

In a first step r_p and $\dot{\phi}_p$, the rf displacement and angular velocity at the pump frequency, are calculated by substituting in Eqs.(I.26) and (I.27) the values of

$$r = r_0 + r_p$$

$$\dot{\phi} = \dot{\phi}_0 + \dot{\phi}_p .$$

These calculated values of r_p and $\dot{\phi}_p$ are then substituted back into Eq. (I.28); then the result is

$$\begin{aligned} r &= r_0 + r_p\Big|_{\substack{\text{calculated with} \\ r_1 = \dot{\phi}_1 = 0}} + \epsilon r_1 \\ \dot{\phi} &= \dot{\phi}_0 + \dot{\phi}_p\Big|_{\substack{\text{calculated with} \\ r_1 = \dot{\phi}_1 = 0}} + \epsilon\dot{\phi}_1 . \end{aligned} \tag{I.29}$$

Equations (I.26), (I.27) and (I.29) yield the rf displacement r_1 and the rf angular velocity $\dot{\phi}_1$ at the signal frequency.

The gain of the amplifying section is given by the ratio

$$\left|\frac{r_1(L)}{r_1(0)}\right|^2$$

where $r_1(L)$ is the amplitude of the displacement at the signal frequency at the output end of the coupler, and $r_1(0)$ is the amplitude at the entrance of the coupler.

D. THEORY OF THE AMPLIFYING SECTION

The pump frequency was found to be

$$\omega_p = \left(2 + \frac{p}{\sqrt{2}}\right)\omega_s \ .$$

The equations of motion are then solved for two cases:

(1) The pump electric field has p azimuthal variations,

(2) The amplifying section has cylindrical symmetry (p = 0): the pump frequency is twice the signal frequency.

1. Calculation of the Gain of the Amplifying Section When the Pump Electric Field has p Azimuthal Variations.

The amplifying section consists of a 2p - wire transmission line surrounding a central conductor (Fig. I.8). The 2p wires are connected in a dc manner and they can be assimilated, as far as the dc field is concerned, to a cylindrical conductor if the angle θ_0 is small enough. The solution of Laplace's equation for such a geometry yields the pump potential

$$V(r,\phi) = \sum_p - \frac{2V_p}{\pi} \frac{\sin (p/2)\,\theta_0}{s^p \theta_0\, (p/2)^2}\, r^p \sin p\phi \qquad (I.30)$$

with $p/2 = 1,3,5,\ldots$

where V_p is the amplitude of the pump potential

θ_0 is the width of the slots between the wires.

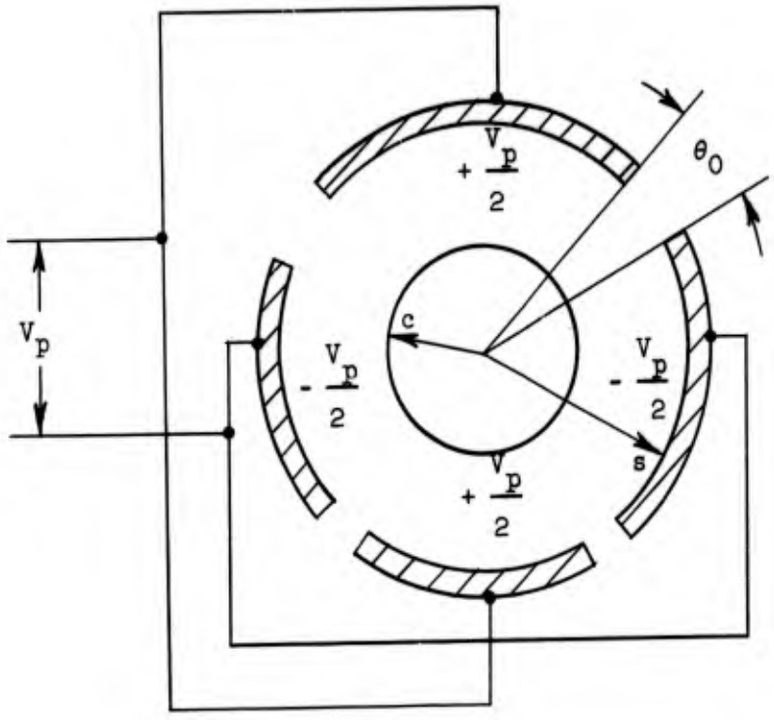

FIG. I.8--Cross section of the amplifying section for $p = 2$.

The term varying as $(c/r)^p$ has been neglected, and the rf connections are those shown in Fig. I.8.

If the fundamental only is taken into account and if the time variation is introduced, Eq. (I.30) becomes

$$V(r,\phi,t) = -2Br^p \sin p\phi \sin \omega_p t \qquad (I.31)$$

with

$$2B = +\frac{2V_p}{\pi} \frac{\sin (p/2)\,\theta_0}{s^p \theta_0 (p/2)^2} . \qquad (I.32)$$

Equation (I.31) can be simplified further by noticing that $V(r,\phi,t)$ can be represented by two circularly polarized waves. The effect of the wave rotating in the opposite direction of the beam can be neglected and the potential becomes

$$V(r,\phi,t) = -Br^p \cos (\omega_p t - p\phi) . \qquad (I.33)$$

As the pump and signal frequencies are not harmonically related, the phase difference between the signal and the pump has no significance when there is no external idler source.

The electric field is easily deduced from Eq. (I.33):

$$\left.\begin{aligned} E_r(r,\phi,t) &= pBr^{p-1} \cos (\omega_p t - p\phi) = pBr^{p-1} \cos (2\omega_s t + p\dot{\phi}_0 t_0) \\ E_\phi(r,\phi,t) &= pBr^{p-1} \sin (\omega_p t - p\phi) = pBr^{p-1} \sin (2\omega_s t + p\dot{\phi}_0 t_0) \end{aligned}\right\} \qquad (I.34)$$

because

$$\omega_p t - p\phi = \left(2\omega_s t + \frac{p}{\sqrt{2}} \omega_s t\right) - p\dot{\phi}_0 (t - t_0) = 2\omega_s t + p\dot{\phi}_0 t_0$$

($\phi = 0$ for $t = t_0$: the electrons enter the amplifying section at the same location all the time.)

The equations of motion Eqs. (I.26) and (I.27) become

$$\left.\begin{aligned} \ddot{r} - r\dot{\phi}^2 &= -\eta\frac{V_0}{r} - \eta B r^{p-1}\cos(\omega_p t - p\phi) \\ r\ddot{\phi} + 2\dot{r}\dot{\phi} &= -\eta B r^{p-1}\sin(\omega_p t - p\phi)\ . \end{aligned}\right\} \tag{I.35}$$

These equations are solved by the method of variations of parameters.[17] Given the condition that

$$\left.\begin{aligned} r &= r_0 + r_p \\ \dot{\phi} &= \dot{\phi}_0 + \dot{\phi}_p\ , \end{aligned}\right\} \tag{I.36}$$

then if r and ϕ are substituted in Eq. (I.35), the motion of an electron at the frequency ω_p can be determined.

At the entrance plane of the amplifying section the electrons have not been subjected to any pump field. If t_0 is the entrance time of an electron in the amplifying section, the boundary conditions can be expressed mathematically by the following expressions:

$$\begin{aligned} r_p(t_0) &= 0 & \dot{r}_p(t_0) &= 0 \\ \phi_p(t_0) &= 0 & \dot{\phi}_p(t_0) &= 0 \end{aligned} \tag{I.37}$$

Equations (I.37), (I.35) and (I.36) yield

$$\begin{aligned} r_p = \frac{C}{V_0} r_0^{p-1} \Bigg\{ & \frac{1-2\sqrt{2}}{6}\cos\omega_s t_0 \cdot \cos(2\omega_s t_o + p\dot{\phi}_0 t_0)\cdot\cos\omega_s t \\ & + \frac{2-\sqrt{2}}{6}\sin\omega_s t_0 \cdot \sin(2\omega_s t_0 + p\dot{\phi}_0 t_0)\cdot\cos\omega_s t \\ & + \frac{1-2\sqrt{2}}{6}\sin\omega_s t_0 \cdot \cos(2\omega_s t_0 + p\dot{\phi}_0 t_0)\cdot\sin\omega_s t \\ & + \frac{\sqrt{2}-2}{6}\cos\omega_s t_0 \cdot \sin(2\omega_s t_0 + p\dot{\phi}_0 t_0)\cdot\sin\omega_s t \\ & + \frac{\sqrt{2}-2}{12}\cos(2\omega_s t + p\dot{\phi}_0 t_0) \\ & + \frac{\sqrt{2}}{4}\cos(2\omega_s t_0 + p\dot{\phi}_0 t_0) \Bigg\} \end{aligned} \tag{I.38}$$

and

$$\dot{\phi}_p = \frac{C}{V_0} r_0^{p-2} \dot{\phi}_0 \left\{ -2 \left[\begin{array}{l} \frac{1-\sqrt{2}}{6} \cos \omega_s t_0 \cdot \cos (2\omega_s t_0 + p\dot{\phi}_0 t_0) \cdot \cos \omega_s t \\ + \frac{2-\sqrt{2}}{6} \sin \omega_s t_0 \cdot \sin (2\omega_s t_0 + p\dot{\phi}_0 t_0) \cdot \cos \omega_s t \\ + \frac{1-2\sqrt{2}}{6} \sin \omega_s t_0 \cdot \cos (2\omega_s t_0 + p\dot{\phi}_0 t_0) \cdot \sin \omega_s t \\ + \frac{\sqrt{2}-2}{6} \cos \omega_s t_0 \cdot \sin (2\omega_s t_0 + p\dot{\phi}_0 t_0) \cdot \sin \omega_s t \end{array} \right] - \frac{\sqrt{2}}{4} \cos (2\omega_s t_0 + p\dot{\phi}_0 t_0) + \frac{4-5\sqrt{2}}{12} \cos (2\omega_s t + p\dot{\phi}_0 t_0) \right\} \tag{I.39}$$

where $C = pr_0^2 B$, B being defined by Eq. (I.32). The detailed calculation is made in Appendix I.A.

The values of r_p and $\dot{\phi}_p$, which represent the rf perturbation of the beam at the pump frequency, are valid in the absence of a signal even when a signal is present. They can be substituted in

$$\left. \begin{array}{l} r = r_0 + r_p + \epsilon r_1 \\ \dot{\phi} = \dot{\phi}_0 + \dot{\phi}_p + \epsilon \dot{\phi}_1 \end{array} \right\} \tag{I.40}$$

and these new values of r and ϕ can be substituted back into the equations of motion Eq. (I.35). The boundary condition is

$$r_1 = r_1(0) \cos \omega_s t_0 \tag{I.41}$$

where $r_1(0)$ is the maximum amplitude of the transverse motion of the electron at the entrance of the coupler.

Then the radial displacement of an electron which has remained a time τ in the amplifying section is found to be (see Appendix I.A)

$$r_1 = r_1(0) \exp \left\{ \left[\frac{C}{V_0} r_0^{p-2} \dot{\phi}_0 \frac{1}{12\sqrt{2}} (9p - 8 + 7\sqrt{2} - 6p\sqrt{2}) \sin p\dot{\phi}_0 t_0 \right] \tau \right\} \cdot \cos \left[\omega_s t - \frac{1}{12\sqrt{2}} \frac{C}{V_0} \dot{\phi}_0 r_0^{p-2} (9p + 16 - 17\sqrt{2} + 6p \quad 2)\tau \right] \tag{I.42}$$

r_1 and $\dot{\phi}_1$ were substituted back into the equations of motion (I.35), and it was found that these values satisfy (I.35) to the first order in C/V_0.

The rf amplitude grows exponentially, and the rate of growth depends on the entrance time t_0 of the electron. Each electron is characterized by a different value of t_0. Some electrons enter the amplifying section at a favorable time, some do not. [A favorable electron receives energy from the pump field during all the time it remains in the amplifying section, that is, when $p\dot{\phi}_0 t_0 = (4n + 1)\pi/2$.] To calculate the gain of the device at the signal frequency, the effect of all the electrons must be included. The average of Eq. (I.42) over all the electrons must be taken. As t_0 appears only as $\sin p\dot{\phi}_0 t_0$ in the exponential, the effect of all the electrons is taken into account by taking the average over one period of $p\dot{\phi}_0 t_0$. The "average" displacement at the signal frequency at the output of the amplifying section is then

$$r_1(L) = \frac{r_1(0)}{2\pi} \left\{ \int_0^{2\pi} \exp \left[L \frac{C}{V_0} \frac{r_0^{p-2}}{u_0} (0.120 + 0.029p) \sin p\dot{\phi}_0 t_0 \right] d(p\dot{\phi}_0 t_0) \right\} \cos \omega_s t \qquad \text{(I.43)}$$

where $r_1(L)$ is the amplitude of the rf radial displacement at the output of the coupler, corresponding to the overall effect of all the electrons

$r_1(0)$ is the amplitude at the entrance of the coupler

L is the length of the coupler

C is given by Eq. (I.39).

The gain of the amplifying section is given by

$$\text{gain} = \frac{r_1(L)^2}{r_1(0)} . \qquad \text{(I.44)}$$

The gain in db is obtained from Eqs. (I.43) and (I.44):

$$\text{gain in db} = 20 \log_{10} \left\{ \frac{1}{2\pi} \int_0^{2\pi} \exp \left[L \frac{C}{V_0} \frac{r_0^{p-2}}{u_0} (0.120 + 0.029p) \sin p\dot{\phi}_0 t_0 \right] d(p\dot{\phi}_0 t_0) \right\} \tag{I.45}$$

This result will be discussed below in paragraph 3, with the gain of the other type of amplifying section.

2. Calculation of the Gain in the Amplifying Section With Cylindrical Symmetry (p = 0).

The pump frequency is twice the signal frequency, and the idler and signal frequencies are the same. The amplifying circuit consists of a length L of coaxial transmission line (Fig. I.5). The pump electric field is

$$\left. \begin{aligned} E_r &= \frac{B}{r} \cos (\omega_p t + X) \\ E_\phi &= 0 \end{aligned} \right\} \tag{I.46}$$

where B represents the strength of the pump field and where X is the phase difference between the signal and the pump.

The equations of motion, for this circuit configuration, are

$$\left. \begin{aligned} \ddot{r} - r\dot{\phi}^2 &= -\eta \frac{V_0}{X} - \eta \frac{B}{r} \cos (\omega_p t + X) \\ r\ddot{\phi} + 2\dot{r}\dot{\phi} &= 0 \, . \end{aligned} \right\} \tag{I.47}$$

The amplitude of the radial displacement of an electron at the signal frequency is obtained by the same method used in paragraph 1 above. The algebra is carried out in detail in Appendix I.B. The value of r_1

derived from Eq. (I.47) is

$$r_1(L) = r_1(0) \exp\left[-\frac{1}{3\sqrt{2}\,u_0}\,\dot{\phi}_0\,\frac{BL}{V_0}\,(\sin X)\right] \cos \omega_s t \qquad (I.48)$$

where B is defined in Eq. (I.44), and where L is the length of the coupler.

The amplitude of the rf displacement is independent of the entrance time of the electron. However, this amplitude depends on the relative phase between the pump and the signal. This result appears in all the degenerate type parametric amplifiers:

if $x = 0$, the signal is not modified by the amplifying section,
if $x = +\pi/2$, the signal decays exponentially, and
if $X = -\pi/2$, the signal grows exponentially.

The maximum gain is deduced from Eq. (I.48) with the condition $x = \pi/2$:

$$\text{gain in db} = 20 \log_{10} \exp\left(-\frac{1}{3\sqrt{2}}\,\dot{\phi}_0\,\frac{B}{V_0}\right)$$

3. Comparison of the Two Types of Amplifying Sections.

a. Relative length of the amplifying section.

A numerical example, using the same numerical values utilized for the fast wave coupler, is more illustrative and will serve as a basis for the discussion:

s the radius of the outer conductor is 0.120"
c the radius of the inner conductor is 0.040"
I_0 the dc durrent is 300μA
u_0 the dc velocity is 1/300 of the velocity of light
f the frequency is 1.2 kMc.

The integral appearing in Eq. (I.43) can be approximated (see Appendix I.C). The gain of the amplifying section with two azimuthal variations of the pump electric field ($p = 2$) can be calculated. An approximate value for the gain is

$$(p = 2) \qquad \text{gain db} = 34\,\frac{V_p}{V_0}\,L - 6 \qquad (I.49)$$

where V_p is the rf pump voltage applied between opposite wires of the transmission line and L is the length of the coupler in cm .

For a gain of 20 db the length of the structure is, with $V_p/V_0 = 0.1$, L = 7.6 cm . The gain of the other amplifying section (p = 0) is given by the following approximate formula:

$$\text{gain db} = 100 \frac{V_p}{V_0} . \qquad \text{(I.50)}$$

With $V_p/V_0 = 0.1$ and a gain of 20 db, the length of this section is L = 2 cm .

b. Advantages of the amplifying section with cylindrical symmetry:

(1) It is shorter.

(2) The amplifier does not require the addition of a fast wave coupler to remove the noise at the idler frequency because the idler frequency is equal to the signal frequency.

(3) This type of coupler is easier to build.

c. Disadvantages of this amplifying section (p = 0):

(1) The gain of the amplifier depends critically on the phase of the pump relative to the phase of the signal.

(2) However, in practice, the pump frequency may be slightly different from twice the signal frequency.

(3) If the difference of frequency between the idler and the signal is well within the limitation of bandwidth of the fast wave coupler, at the signal frequency, the noise will be removed from the idler too.

(4) As $\omega_p \neq 2\omega_c$, the phase restriction is removed and by continuity the performances of the amplifying section must be only slightly perturbed.

For these reasons an amplifying section consisting of a length L of coaxial transmission line (p = 0) is used in the actual amplifier.

CHAPTER IV

DESIGN AND CONSTRUCTION OF THE ELECTROSTATIC PARAMETRIC AMPLIFIER

A. DESIGN

A schematic of the amplifier is shown in Fig. I.9. The injection of the beam and the design of the different components are discussed first.

1. Beam Injection.

The electron beam is cylindrical. The beam must enter the electrostatic-focusing region with the proper azimuthal and longitudinal velocity. The azimuthal motion is created by injecting the beam in a uniform transverse magnetic field.

The electron gun is an Eimac convergent flow gun. An auxiliary anode preceding the magnetic circuit has been added (Fig. I.10). Its purpose is twofold:

(1) It shaves off the beam to the diameter of the center hole of the auxiliary anode which is 0.040" .

(2) It regulates the longitudinal velocity of the electrons without changing the dc current I_0 .

The 0.040" beam enters the region of uniform transverse magnetic field. The width of the pole pieces is d and the magnetic flux density is adjusted to the value B_0 such that

$$d \cong \frac{u_0}{\eta B_0} ,$$

where u_0 is the dc velocity of the electrons. The electrons describe a circle of radius d (Fig. I.10). If B is smaller than B_0 the beam leaves the region of uniform magnetic field with an angle ψ and enters the region of electrostatic focusing. If u_0 and ψ are properly chosen the beam will remain in equilibrium. Then, ψ can be changed by varying B and u_0 can be altered by changing the dc potential on the auxiliary anode.

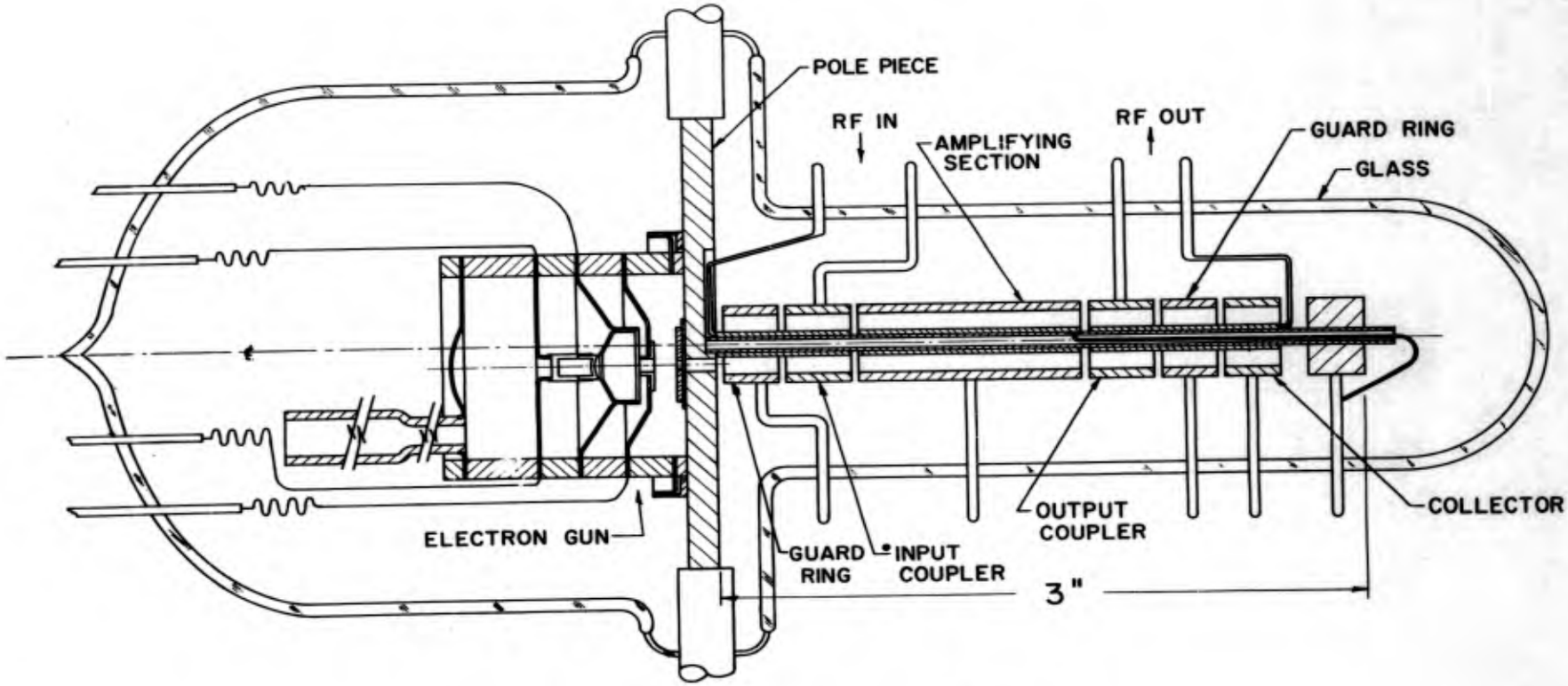

FIG. I.9--Schematic of the amplifier.

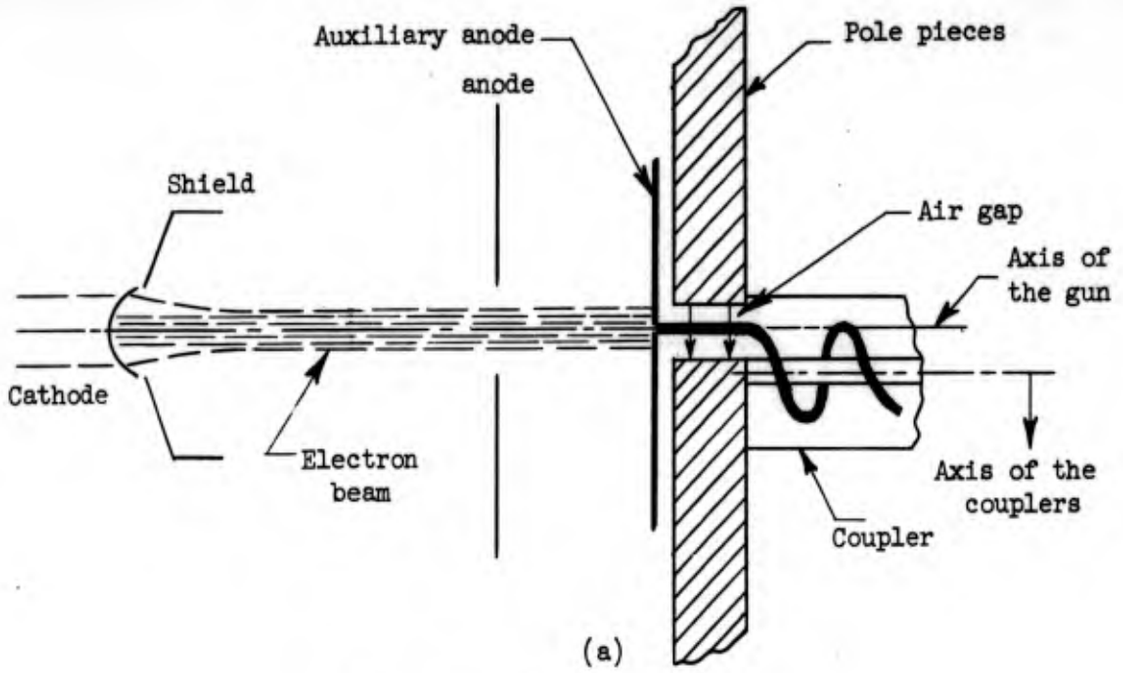

(a)

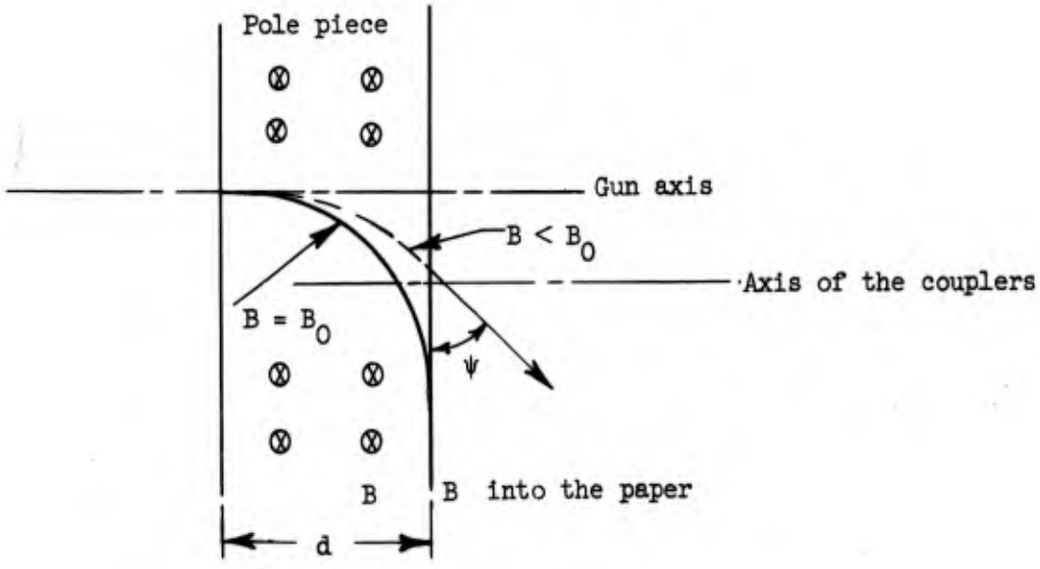

(b)

FIG. I.10--Injection scheme of the electron beam.

(a) Longitudinal View

(b) Top View Across the Magnetic Pole Pieces

2. Fast-Wave Couplers and Amplifying Section.

The amplifier will be designed to operate at 1000 Mc/s with a dc current of 300μA .

a. Couplers.

For practical reasons, after some investigation the following values of the parameters have been selected:

s is the inner radius of the outer conductor: 3.6×10^{-3}m = 0.140"

c is the outer radius of the inner conductor: 1.0×10^{-3}m = 0.040"

ψ is the pitch angle.

In order to minimize the electron interception by the coupler, r_0 , the dc equilibrium radius, will be chosen equal to $(s + c)/2$:

$$r_0 = 2.15 \times 10^{-3}\text{m} ,$$

and ψ and $\dot{\phi}_0$ are given by

$$\dot{\phi}_0 = \frac{e^{1/2}}{s} (\eta V_0)^{1/2}$$

$$\psi = \frac{u_0}{(\eta V_0)^{1/2}} .$$

For $\psi = 8^\circ$ these equations yield

$$V_0 = 518 \text{ volts}$$

$$V_c = 414 \text{ volts}$$

$$u_0 = 1.34 \times 10^6 \text{ m/s} ,$$

and βeC can be calculated from

$$L_{cm} = \frac{10^3}{37.2 Q_L} .$$

The fast-wave couplers are completely determined. They consist of a cylinder, surrounding a central conductor, having the following characteristics:

$$s = 0.140"$$
$$c = 0.040"$$
$$L = 0.300"$$
$$Q_L = 36$$

with $V_c = 414$ volts, $\psi = 8^o$, $I_o = 300\mu A$. } at 1000 Mc.

The two conductors form a short transmission line which looks capacitive. An external inductance and an external resistance must be added to tune the couplers to 1000 Mc/s and to obtain a loaded Q of 36 .

b. Amplifying section.

The amplifying section consists of a cylinder of inner radius $S = 0.140"$. The tube is designed for a gain of 20 db. Then from Eq. (I.48) the length of the couplers will be

$$L_{cm} = 3.75 \left(\frac{10^{-1}}{V_p/V_o} \right).$$

For a ratio $V_p/V_o = 0.1$ the section is 3.75 cm long.

Electron interception by the couplers or the amplifying section must be avoided in order to conserve the low-noise properties of the amplifier. For this reason dc guard rings have been added, as shown in Fig. I.9, in front of the input coupler and after the output coupler. The length of the amplifying section was then reduced to 1 inch in order to maintain a small overall length which is necessary for a good beam transmission.

B. CONSTRUCTION

A photograph of the tube is shown (Fig. I.11). The vacuum envelope is in glass. All the leads coming through the envelope are made out of kovar. This material was chosen for its excellent match with the 7052 type of glass which was used.

The tube consists of two parts: the circuit on one hand, and the electron gun and injection system on the other hand. With the magnetic type of beam injection used, the gun and circuit axes are different. For this reason the tube was mounted in two major steps: in the first step the circuit was built, and in a second step the electron gun and the pole pieces were mounted.

1. Circuit.

The circuit consists of a series of copper rings surrounding a central conductor. The rings were cut from a copper cylinder electroformed on an aluminum mandrel; the aluminum was then etched out after machining. Kovar leads, 0.040" in diameter, with glass beads were brazed to the cylinders.

The glass envelope was mounted at one end of a glass blower's lathe and the holes for the dc and rf leads were made in the glass. The cylinders were then slipped, with the proper spacers, on a steel mandrel (supported at the other end of the lathe) with the kovar leads going through the glass as shown in Fig. I.12. When all the cylinders were in place the leads were sealed to the glass and the steel mandrel was removed.

The central conductor consists of a glass tube 0.060" in diameter to which were cemented three copper sleeves (Fig. I.13). The conducting part of it was made in three different sections in order to provide better rf insulation between the couplers and the amplifying section. The wire connected to each sleeve was spot-welded to a kovar lead going through the vacuum envelope. The central conductor is held in place at the collector end of the tube by a cylinder having a 0.060" hole along its axis. At the gun end it is slipped into a hole in one of the pole pieces.

2. Electron Gun and Pole Pieces.

The electron gun is an Eimac gun which was obtained already mounted.

The pole pieces were made out of a cold rolled steel disk 1/8" thick which was cut in two unequal parts leaving a 0.070" air-gap. Two 1.5" long steel rods with kovar cups were brazed to the pole pieces (Fig. I.14). The steel rods provide the access to the magnetic circuit which is outside the vacuum (the glass envelope being sealed to the kovar cups).

A ring which maintains the electron gun in position was brazed to one of the pole pieces (Fig. I.15). The position of the gun axis is then

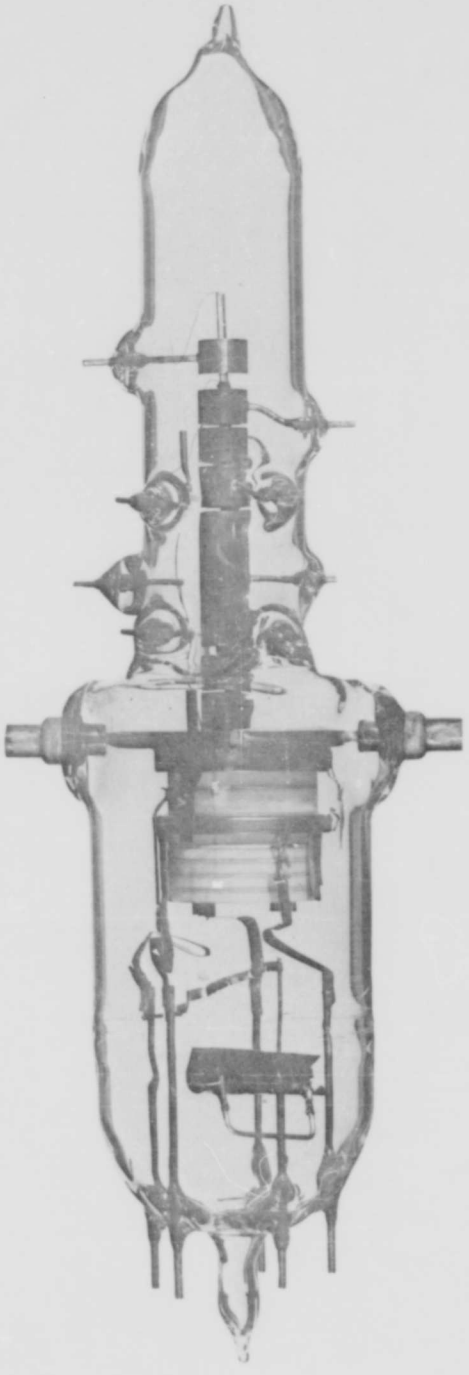

FIG. I.11--Photograph of the tube.

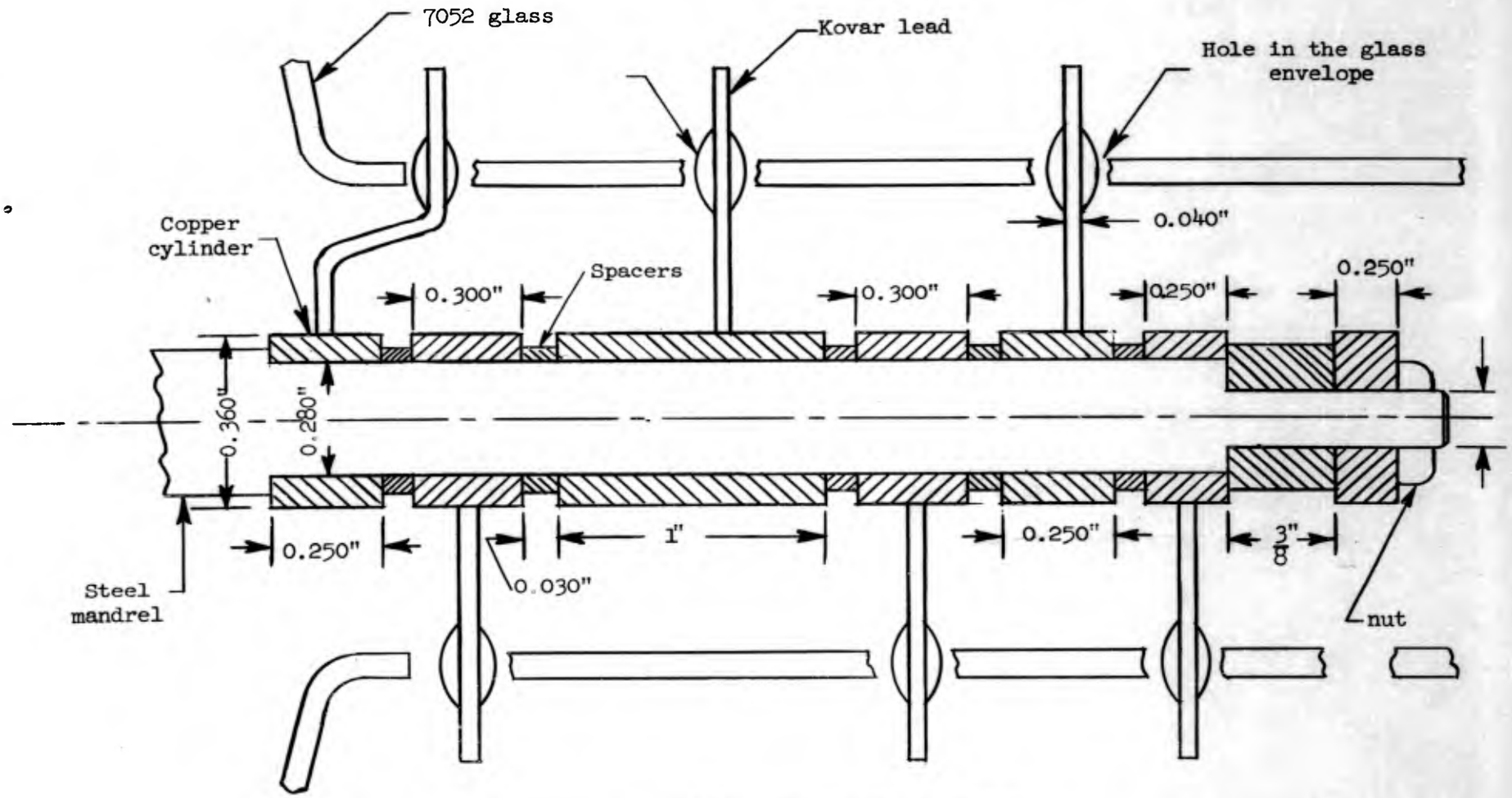

FIG. I.12--Mounting of the cylinders.

The kovar leads shown here in the same plane are actually distributed along the circumference of the glass envelope.

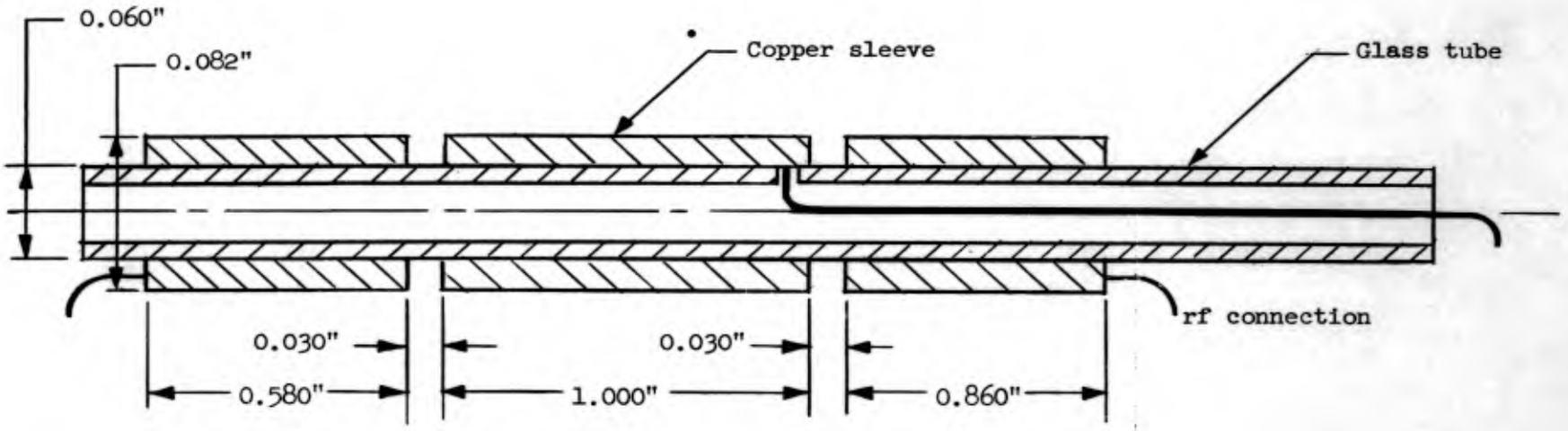

FIG. I.13--Central conductor.

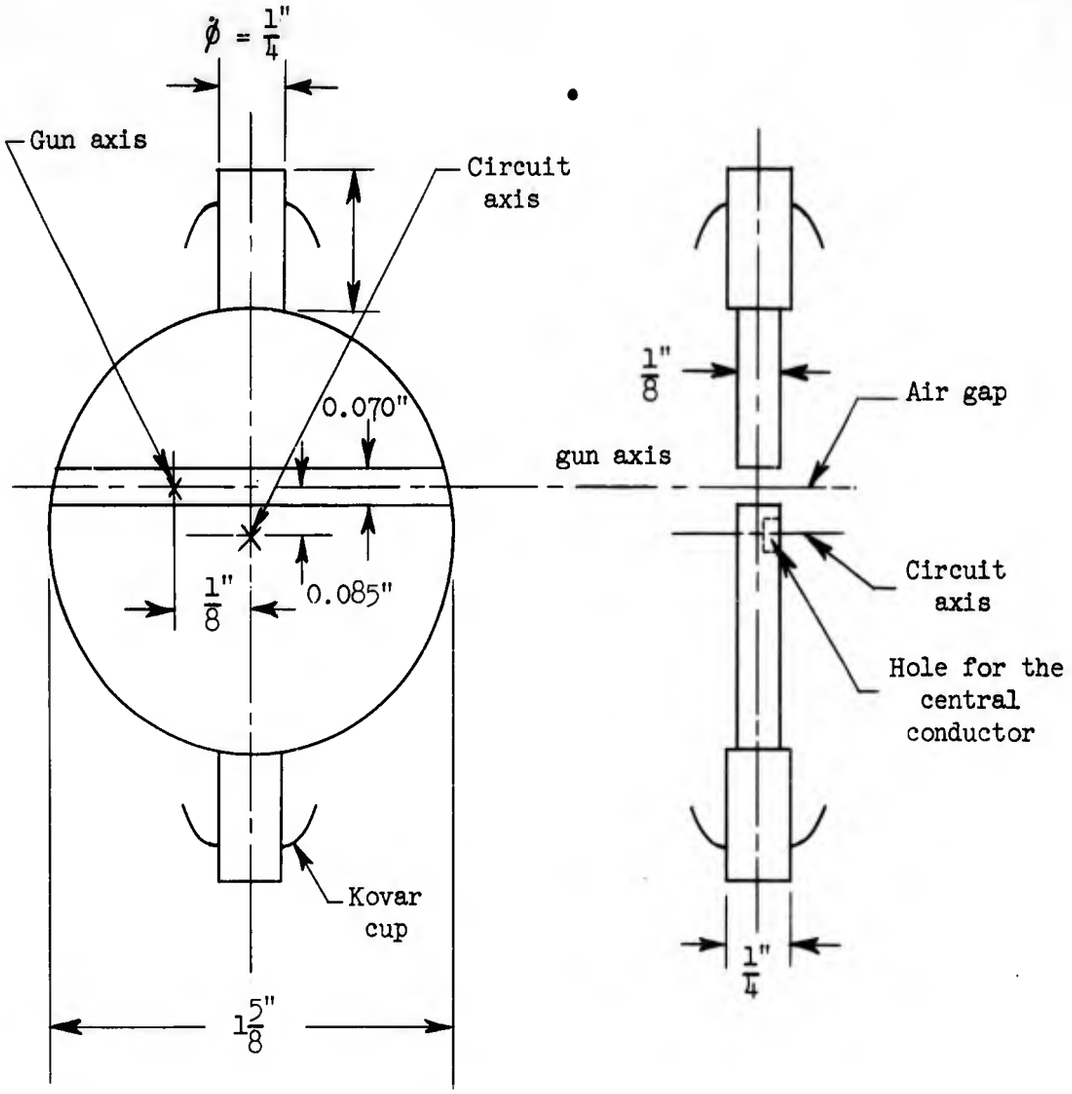

FIG. I.14--Pole pieces.

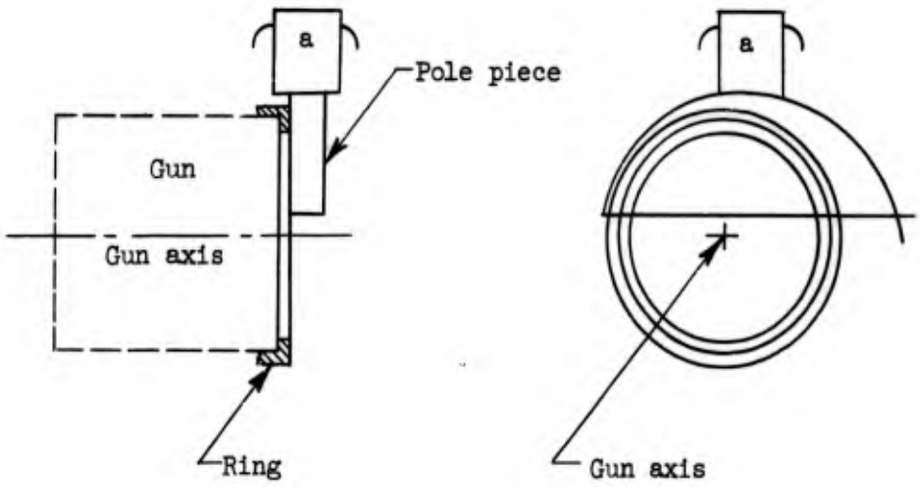

FIG. I.15--Positioning of the electron gun.

fixed relative to the pole pieces. A special mounting jig is then used to maintain the two pole pieces in position relative to the lathe axis and the envelope was sealed to the kovar cups (Fig. I.9).

A small copper disk was mounted with screws in front of the pole pieces and was isolated from it with mica, (Figs. I.9 and I.10). This disk is the auxiliary anode described in paragraph 1, section A, chapter IV, entitled "Beam Injection." All the necessary dc leads were connected and the tube was sealed except for the pumping tubulation.

The experiments with the electrostatic parametric amplifier will be undertaken in the Microwave Laboratory in the near future.

CHAPTER V

CONCLUSION

It was shown that it is possible to design and build a low-noise electrostatically-focused microwave tube using parametric amplification. After a brief summary of the analogies between electrostatic waves and cyclotron waves, the same conditions which led Pantell to the idea of the electrostatic parametric amplifier, a brief description of the couplers designed by Pantell was given.

The work presented here was the logical continuation for the design of a parametric amplifier, that is, the study of the motion of electrons in an amplifying section. The beam modulated at the signal frequency in the form of a fast electrostatic wave is injected in the region where a pump field is applied. The pump frequency depends on the geometrical configuration of the amplifying section, and it should be noted that a quadrupole type section does not correspond to a pump frequency which is twice the signal frequency. A kinetic analysis of the electron motion in this section showed that the radial transverse motion of the electron could be amplified by the pump field, and if all the electrons are taken into account gain can be obtained. As could be predicted the gain depends on the length of the amplifying section and on the strength of the pump field. Two main amplifying structures were studied. In the first case the structure which has no variation of the electric field in the azimuthal direction led to a pump frequency equal to twice the signal frequency which is a degenerate parametric amplifier, and in this case the amplifying structure is simply a given length of coaxial structure. If the amplifying structure has p azimuthal variations of the pump electric field, it was found that the pump frequency was not harmonically related to the signal frequency.

A parametric electrostatic amplifier was designed and built using Pantell's fast-wave couplers for the case where the pump frequency is twice the signal frequency.

The experimental check of the theory, which is outside the scope of this work, remains to be done. Future theoretical work may include the

study of:

(1) the influence of the pump field on the dc motion of the electrons,

(2) the effect of space-charge forces, and

(3) the study of such means of amplification as dc pumping.

APPENDIX I.A

INTEGRATION BY THE METHOD OF VARIATION OF THE PARAMETERS

Consider the two second order differential equations

$$\left.\begin{aligned} a\ddot{x}(t) + b\dot{y}(t) &= c_1(t)x(t) + c_2(t)y(t) \\ d\ddot{y}(t) + e\dot{x}(t) &= f_1(t)x(t) + f_2(t)y(t) \end{aligned}\right\} \qquad \text{(I.A.1)}$$

where $c_1(t)$, $c_2(t)$, $f_1(t)$, $f_2(t)$ are harmonic functions of t whose amplitudes are small compared with the constant coefficients of the equations. In the first step the following system will be solved:

$$\left.\begin{aligned} a\ddot{x}(t) + b\dot{y}(t) &= 0 \\ d\ddot{y}(t) + c\dot{x}(t) &= 0 \end{aligned}\right\} . \qquad \text{(I.A.2)}$$

Its solution is

$$\left.\begin{aligned} x &= x_0(t,A,B,D,F) \\ y &= y_0(t,A,B,D,F) \end{aligned}\right\} \qquad \text{(I.A.3)}$$

where A , B , D , and F are the constants of integration to be determined by the boundary conditions. With the change of variable,

$$\left.\begin{aligned} \alpha &= \dot{x} \\ \beta &= \dot{y} \end{aligned}\right\} \qquad \text{(I.A.4)}$$

Eq. (I.A.1) becomes

$$\left.\begin{aligned} a\dot{\alpha}(t) + b\beta(t) &= c_1(t)x(t) + c_2(t)y(t) \\ d\dot{\beta}(t) + e\beta(t) &= f_1(t)x(t) + f_2(t)y(t) \end{aligned}\right\} \qquad \text{(I.A.5)}$$

As the c's and the f's are small, the following condition exists:

$$\left.\begin{aligned} \alpha = \dot{x} &= \frac{\partial}{\partial t}\, x_0(t,A,B,D,F) = \alpha_0(t,A,B,D,F) \\ \beta = \dot{y} &= \frac{\partial}{\partial t}\, y_0(t,A,B,D,F) = \beta_0(t,A,B,D,F) \end{aligned}\right\} \qquad \text{(I.A.6)}$$

At this point A , B , D and F are allowed to be functions of time. The system of Eqs. (I.A.5) becomes a system of coupled linear equations

in which A , B , D , and F can be solved with the relations of the type

$$\dot{\alpha} = \frac{\partial}{\partial t}\alpha_0 + \dot{A}\frac{\partial \alpha_0}{\partial A} + \dot{B}\frac{\partial \alpha_0}{\partial B} + \dot{D}\frac{\partial \alpha_0}{\partial D} + \dot{F}\frac{\partial \alpha_0}{\partial F} .$$

If $\overline{A}$, $\overline{B}$, $\overline{D}$ and $\overline{F}$ are the time averages of A , B , D and F , the solution of the system of Eqs. (I.A.1) is

$$x = x_0(t,\overline{A},\overline{B},\overline{D},\overline{F}; K,L,M,N)$$

$$y = y_0(t,\overline{A},\overline{B},\overline{D},\overline{F}; K,L,M,N) ,$$

where K , L , M and N are constants of integration.

APPENDIX I.B

CALCULATION OF THE RF PERTURBATION IN THE AMPLIFYING SECTION

1. The following discussion is for the case of $p \neq 0$.

Equations (I.34) and (I.35) yield:

$$\left.\begin{aligned} \ddot{R}_p - 2\dot{\phi}_0\dot{\phi}_p - 2\dot{\phi}_0^2 R_p &= \frac{C}{V_0}\dot{\phi}_0^2\,[1 + (p-1)R_p]\, r_0^{p-2} \cos(2\omega_s t + p\dot{\phi}_0 t_0) \\ \ddot{\phi}_p + 2\dot{\phi}_0\dot{R}_p &= \frac{C}{V_0}\dot{\phi}_0^2\,[1 + (p-1)R_p]\, r_0^{p-2} \sin(2\omega_s t + p\dot{\phi}_0 t_0) \end{aligned}\right\} \quad \text{(I.B.1)}$$

where $R_p = r_p/r_0$.

Equation (I.B.1) can be simplified. The interaction terms

$$\frac{C}{V_0}\dot{\phi}_0^2 R_p \cos(2\omega_s t + p\dot{\phi}_0 t_0)$$

and

$$\frac{C}{V_0}\dot{\phi}_0^2 R_p \sin(2\omega_s t + p\dot{\phi}_0 t_0) ,$$

which give components proportional to $(C/V_0)^2$, are neglected:

$$\left.\begin{aligned} \ddot{R}_p - 2\dot{\phi}_0\dot{\phi}_p - 2\dot{\phi}_0^2 R_p &= \frac{C}{V_0}\dot{\phi}_0^2 r_0^{p-2} \cos(2\omega_s t + p\dot{\phi}_0 t_0) \\ \ddot{\phi}_p + 2\dot{\phi}_0\dot{R}_p &= \frac{C}{V_0}\dot{\phi}_0^2 r_0^{p-2} \sin(2\omega_s t + p\dot{\phi}_0 t_0) \end{aligned}\right\} \quad \text{(I.B.2)}$$

The general solution of the system I.B.2 is

$$\left.\begin{aligned} R_p &= A\cos\omega_s t + B\sin\omega_s t \\ &\quad + \frac{\sqrt{2}-2}{12}\,\frac{C}{V_0}\, r_0^{p-2}\cos(2\omega_s t + p\dot{\phi}_0 t_0) + D \\ \dot{\phi}_p &= -2A\dot{\phi}_0\cos\omega_s t - 2B\dot{\phi}_0\sin\omega_s t \\ &\quad + \frac{4-5\sqrt{2}}{12}\,\frac{C}{V_0}\, r_0^{p-2}\cos(2\omega_s t + p\dot{\phi}_0 t_0) + D \end{aligned}\right\} \quad \text{(I.B.3)}$$

At the entrance time of the electrons t_0 , the following boundary condi-

tions must be satisfied

$$R_p(t_0) = 0 \qquad \dot{R}_p(t_0) = 0$$
$$\phi_p(t_0) = 0 \qquad \dot{\phi}_p(t_0) = 0 \tag{I.B.4}$$

The terms A , B and D are calculated from Eq. (I.B.4) and

$$\left.\begin{aligned} A &= \frac{C}{V_0} r_0^{p-2} \left[\frac{1-2\sqrt{2}}{6} \cos \omega_s t_0 \cos (2\omega_s t_0 + p\dot{\phi}_0 t_0) + \frac{2-\sqrt{2}}{6} \sin \omega_s t_0 \sin (2\omega_s t_0 + p\dot{\phi}_0 t_0)\right] \\ B &= \frac{C}{V_0} r_0^{p-2} \left[\frac{1-2\sqrt{2}}{6} \sin \omega_s t_0 \cos (2\omega_s t_0 + p\dot{\phi}_0 t_0) + \frac{\sqrt{2}-2}{6} \cos \omega_s t_0 \sin (2\omega_s t_0 + p\dot{\phi}_0 t_0)\right] \\ D &= \frac{C}{V_0} r_0^{p-2} \frac{\sqrt{2}}{4} \cos (2\omega_s t_0 + p\dot{\phi}_0 t_0) \end{aligned}\right\} \tag{I.B.5}$$

Equations (I.B.3) and (I.B.5) yield Eqs. (I.38) and (I.39) which give r_p and $\dot{\phi}_p$. These values of r_p and of $\dot{\phi}_p$ are substituted in Eq. (I.40) and r and ϕ are in turn substituted back into Eq. (I.35) which gives

$$\ddot{R}_1 - 2\dot{\phi}_0\dot{\phi}_1 - 2\dot{\phi}_0^2 R_1 = \frac{C}{V_0} \dot{\phi}_0^2 r_0^{p-2} \left[p\phi_1 \sin (2\omega_s t + p\dot{\phi}_0 t_0) + (p-1) R_1 \cos (2\omega_s t + p\dot{\phi}_0 t_0)\right]$$
$$+ 2\dot{\phi}_p\dot{\phi}_1 + 2\dot{\phi}_0\dot{\phi}_1 R_p + 2\dot{\phi}_0\dot{\phi}_p R_1 - 2R_1 R_p \dot{\phi}_0^2 \tag{I.B.6}$$

$$\ddot{\phi}_1 + 2\dot{\phi}_0\dot{R}_1 = \frac{C}{V_0} \dot{\phi}_0^2 r_0^{p-2} \left[(p-1) R_1 \sin (2\omega_s t + p\dot{\phi}_0 t_0) - p\phi_1 \cos (2\omega_s t + p\dot{\phi}_0 t_0)\right]$$
$$- R_p\ddot{\phi}_1 - R_1\ddot{\phi}_p - 2\dot{R}_p\dot{\phi}_1 - \dot{R}_1\dot{\phi}_p \tag{I.B.7}$$

where $R_1 = r_1/r_0$ and where all the terms not linear in ϵ and C/V_0 have been neglected. Equations (I.B.6) and (I.B.7) are solved by the method of variation of parameters as the amplitude of the time varying coefficient is proportional to $C/V_0 \ll 1$. Their homogeneous

solution is

$$\left.\begin{aligned} R_1 &= L\cos(\omega_s t + \zeta) + M \\ \phi_1 &= -\sqrt{2}\,L\sin(\omega_s t + \zeta) - \dot{\phi}_0 M t + N \end{aligned}\right\} \qquad \text{(I.B.8)}$$

With the change of variables

$$\left.\begin{aligned} \beta &= \dot{R}_1 = -\sqrt{2}\,L\dot{\phi}_0 \sin(\omega_s t + \zeta) \\ \alpha &= \dot{\phi}_1 = -2\dot{\phi}_0 L\cos(\omega_s t + \zeta) - \dot{\phi}_0 D \\ \psi &= (\omega_s t + \zeta) \\ \xi &= 2\omega_s t + p\dot{\phi}_0 t_0 \end{aligned}\right\} \qquad \text{(I.B.9)}$$

Eqs. (I.B.6) and (I.B.7) become

$$\left.\begin{aligned} -\sqrt{2}(\sin\psi)\,\dot{L} - \sqrt{2}\,L(\cos\psi)\,\dot{\zeta} &= \frac{C}{V_0}\dot{\phi}_0\left[p\phi_1\sin\xi + (p-1)R_1\cos\xi\right] \\ &\quad + \frac{C}{V_0}\dot{\phi}_0 L\frac{(1+\sqrt{2})}{3}\cos\psi\cos\xi - 2AL\dot{\phi}_0\cos\psi\cos\omega_s t \\ &\quad - 2BL\dot{\phi}_0\cos\psi\sin\omega_s t - 4DL\dot{\phi}_0\cos\psi \end{aligned}\right\}$$

$$\left.\begin{aligned} -(\cos\psi)\,\dot{L} + L(\sin\psi)\,\dot{\zeta} &= \frac{C}{V_0}\dot{\phi}_0\left[(p-1)R_1\sin\xi - p\phi_1\cos\xi\right] \\ &\quad + r_0^{p-2}\frac{C}{V_0}L\dot{\phi}_0\begin{bmatrix}(+\sqrt{2}-2)\cos\xi\sin\psi \\ +(2\sqrt{2}-3)\cos\psi\sin\xi\end{bmatrix} \\ &\quad - 6\sqrt{2}\,\dot{\phi}_0 LA\sin\psi\cos\omega_s t \\ &\quad - 6\sqrt{2}\,\dot{\phi}_0 LB\sin\psi\sin\omega_s t - 4\sqrt{2}\,\dot{\phi}_0 LD\sin\dot{\psi} \\ &\quad - 6\sqrt{2}\,\dot{\phi}_0 LA\cos\psi\sin\omega_s t + 6\sqrt{2}\,\dot{\phi}_0 LB\cos\psi\cos\omega_s t \end{aligned}\right\}$$

$$\left.\begin{aligned} \dot{M} &= L(\sin\psi)\,\dot{\zeta} - \dot{L}\cos\psi \\ \dot{N} &= \sqrt{2}\,L(\cos\psi)\,\dot{\zeta} + \sqrt{2}(\sin\psi)\,\dot{L} + \dot{\phi}_0 M t \end{aligned}\right\}$$

(I.B.10)

where A, B and D are given by Eq. (I.B.5). The first two equations give $\dot{L}$ and $\dot{\zeta}$ and the last two give $\dot{M}$ and $\dot{N}$. After some straight-

forward algebra it is found that

$$\left.\frac{\dot{L}}{L}\right|_{\text{average}} = \frac{C}{V_0} r_0^{p-2}\dot{\phi}_0 \frac{1}{12\sqrt{2}} (9p - 8 + 7\sqrt{2} - 6p\sqrt{2}) \sin p\dot{\phi}_0 t_0$$

$$\left.\zeta\right|_{\text{average}} = -\frac{C}{V_0} r_0^{p-2}\dot{\phi}_0 \frac{1}{12\sqrt{2}} (9p + 16 - 17\sqrt{2} + 6p\sqrt{2}) \cos p\dot{\phi}_0 t_0$$

$$\left.\dot{M}\right|_{\text{average}} = 0$$

$$\left.\dot{N}\right|_{\text{average}} = 0 \qquad \text{(I.B.11)}$$

The other term $r_1(L)$ is easily calculated from Eqs. (I.B.8), (I.B.11) and the boundary condition (I.41)

2. The following discussion is for the case of $p = 0$.
With the same method, the values of R_p and $\dot{\phi}_p$ are easily found to be

$$\left.\begin{aligned} R_p &= \frac{1}{6}\frac{C'}{V_0}\cos(2\omega_s t + X) \\ \dot{\phi}_p &= -\frac{1}{3}\frac{C'}{V_0}\dot{\phi}_0 \cos(2\omega_s t + X) \end{aligned}\right\} \qquad \text{(I.B.12)}$$

where $C' = B$ and where X is the phase of the pump relative to the phase of the signal.

The differential equations in R_1 and ϕ_1 are

$$\ddot{R}_1 - 2\dot{\phi}_0\dot{\phi}_1 - 2R_1\dot{\phi}_0^2 = +\frac{C'}{V_0}\dot{\phi}_0^2 (R_1)\cos(2\omega_s t + X)$$

$$-\frac{1}{3}\frac{C'}{V_0} L\dot{\phi}_0^2 \cos\psi \cos(2\omega_s t + X) \qquad \text{(I.B.13)}$$

$$\ddot{\phi}_1 + 2\dot{\phi}_0\dot{R}_1 = -\frac{C'}{V_0} L\dot{\phi}_0^2 [\sqrt{2}\sin\psi\cos(2\omega_s t + X) + 2\sqrt{2}\cos\psi\sin(2\omega_s t + X)].$$

Their homogeneous solution is

$$\left.\begin{aligned} R_1 &= L\cos(\omega_s t + \zeta) + M \\ \phi_1 &= -\sqrt{2}\, L\sin(\omega_s t + \zeta) - \dot{\phi}_0 M t + N . \end{aligned}\right\} \qquad \text{(I.B.14)}$$

Applying the method of variation of parameters yields

$$-\sqrt{2}\,(\sin\psi)\,\dot{L} - \sqrt{2}\,L\,(\cos\psi)\,\dot{\zeta} = -\frac{2}{3}\frac{C'}{V_0}L\dot{\phi}_0\cos\psi\cos(2\omega_s t + X)$$

$$-(\cos\psi)\,\dot{L} + L\,(\sin\psi)\,\dot{\zeta} = -\frac{C'}{V_0}L\dot{\phi}_0\left[\begin{array}{l}\sqrt{2}\sin\psi\cos(2\omega_s t + X)\\ +\,2\sqrt{2}\cos\psi\sin(2\omega_s t + X)\end{array}\right]$$

$$\dot{M} = L\,(\sin\psi)\,\dot{\zeta} - \dot{L}\cos\psi$$

$$\dot{N} = 2L\,(\cos\psi)\,\dot{\zeta} + 2\,(\sin\psi)\,\dot{L} + \dot{\phi}_0 t\dot{M}\,. \qquad \text{(I.B.15)}$$

This system is solved for $\dot{L}$, $\dot{M}$, $\dot{N}$ and $\dot{\zeta}$ and their time average calculated is the following

$$\left.\begin{array}{l}\dfrac{\dot{L}}{L}\Big|_{\text{average}} = -\dfrac{1}{3\sqrt{2}}\dfrac{C'}{V_0}\dot{\phi}_0\sin X\\[2ex] \dot{\zeta}\Big|_{\text{average}} = -\dfrac{5}{3\sqrt{2}}\dfrac{C'}{V_0}\dot{\phi}_0\cos X\\[2ex] \dot{M}\Big|_{\text{average}} = 0\\[2ex] \dot{N}\Big|_{\text{average}} = 0\,.\end{array}\right\} \qquad \text{(I.B.16)}$$

Equation (I.48) is obtained by calculating L, ζ, M and N from (I.B.16) and by substituting them back into Eq. (I.B.14).

APPENDIX I.C

NUMERICAL CALCULATION OF THE INTEGRAL $\int_0^{2\pi} \exp(a \sin u)\, du$

The term $r_1(L)$ is given by

$$r_1(L) = r_1(0) \left[\frac{1}{2\pi} \int_0^{2\pi} \exp\left(\frac{L}{u_0} \frac{10 - 5\sqrt{2}}{12\sqrt{2}} \sin 2\dot{\phi}_0 t_0 \right) d(2\dot{\phi}_0 t_0) \right] \cos \omega_s t \, .$$

Let a be the quantity

$$a = \frac{10 - 5\sqrt{2}}{12\sqrt{2}} \frac{L}{u_0} \, .$$

In practice a is larger than 2, and the curve representing $\exp(a \sin 2\dot{\phi}_0 t_0)$ can be approximated by the triangle B, C, O. The integral is then approximately equal to

$$\frac{1}{2\pi} \int_0^{2\pi} \exp\left(\frac{10 - 5\sqrt{2}}{12\sqrt{2}} \frac{L}{u_0} \sin 2\dot{\phi}_0 t_0 \right) d(2\dot{\phi}_0 t_0) \simeq \frac{1}{2\pi} \left(\frac{1}{2} \pi \times e^a \right) = \frac{e^a}{4}$$

and

$$r_1(L) \simeq \frac{r_1(0)}{4} \exp\left(\frac{10 - 5\sqrt{2}}{12\sqrt{2}} \frac{L}{u_0} \right) \cos \omega_s t \, .$$

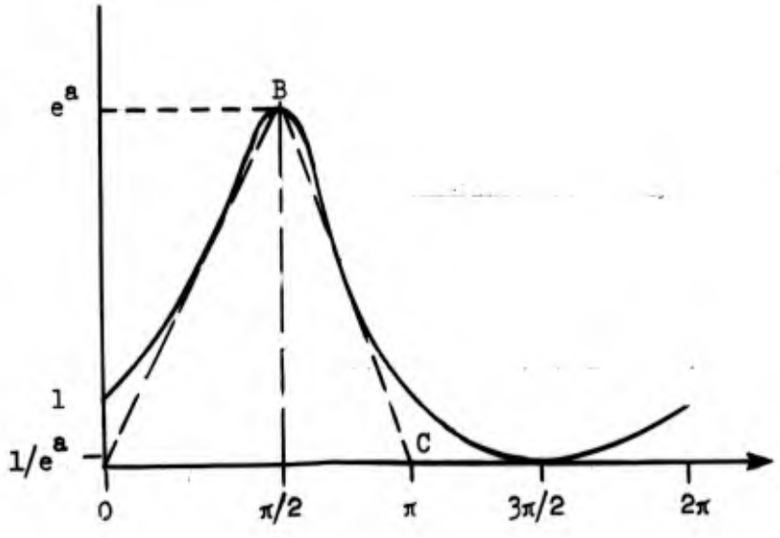

PART II

STUDY OF A FAST SPACE-CHARGE WAVE PARAMETRIC AMPLIFIER

PART II: STUDY OF A FAST SPACE-CHARGE WAVE PARAMETRIC AMPLIFIER

CHAPTER VI
INTRODUCTION

A. HISTORY

Bridges[5] built the first beam-type parametric amplifier using space-charge waves. He injected an electron beam, which had been modulated at twice the signal frequency, through a "floating drift tube" klystron cavity. The pumped beam modulated the beam-loading susceptance, existing across the second gap of the cavity, at twice the signal frequency. Thus a negative conductance was created and amplification could occur. Bridges, however, did not use fast space-charge waves and the device had no low-noise properties. Ashkin,[9,10] using a theory developed by Louisell and Quate,[6] built an amplifier using the exponential growth of the fast wave due to parametric pumping. A first tube was built on the model of a klystron where the output cavity was movable and the presence of gain was established. Other tubes using fast-wave couplers were built; these couplers consisted either of double-gap klystron cavities[18] or of "Kompfner dip" helices followed by a velocity jump.[19] The experimental results were satisfactory, except for the noise figure. It was shown theoretically and experimentally, by Ashkin, Cook and Louisell, that the higher than expected noise level was due to interaction of higher harmonics.

The theory of a different space-charge wave amplifier will be developed. The amplifier is of the klystron type. Long interaction cavities, studied by Wessel-Berg,[15] will be used as fast-wave couplers. The amplification of the signal lies, as in Bridges' amplifier, in the creation of a negative beam-loading conductance across the cavity. It was hoped that gain could occur without any growing waves by the proper combination of the four running waves which can exist in the parametrically pumped beam. This would differentiate this amplifier from other space-charge wave parametric amplifiers.

B. DESCRIPTION OF THE AMPLIFIER

The amplifier uses a cylindrical electron beam immersed in a large magnetic field which prevents any transverse motion of the electrons. As in Part I, the different components of the amplifier, i.e., the fast-

wave couplers and the amplifying section, will be briefly discussed.

1. Fast-Wave Coupler.

Wessel-Berg has studied long interaction cavities which support a resonant longitudinal electric field. He calculated the coupling coefficient between an electron beam and such a cavity. By a proper choice of the parameters these resonant cavities can couple only to the fast wave and the power carried by the fast wave can be entirely transferred to the load.

Such a cavity can be constructed with a helix, shorted at both ends (Fig. II.1).

2. Amplifying Mechanism.

An electron beam injected through a narrow-gap klystron cavity creates a beam loading across the cavity which is proportional to the dc current I_0. If the beam is 100 per cent modulated at twice the signal frequency, that is, if the current varies as $I_0 \cos 2\omega_s t$, the beam loading in turn will be proportional to $I_0 \cos 2\omega_s t$. The cavity is shunted by a susceptance varying at twice the signal frequency and amplification can be achieved.

The same principle, extended to long interaction cavities, is used in this amplifier. An rf pumped electron beam is injected into a cavity. The beam loading is calculated and it is shown that under certain conditions the real part of the beam loading admittance can be negative.

The amplifier consists of 3 parts:

(1) an input fast-wave coupler,

(2) a fast-wave cavity which modulates the beam at the pump frequency in the form of a fast space-charge wave, and

(3) an output fast-wave coupler.

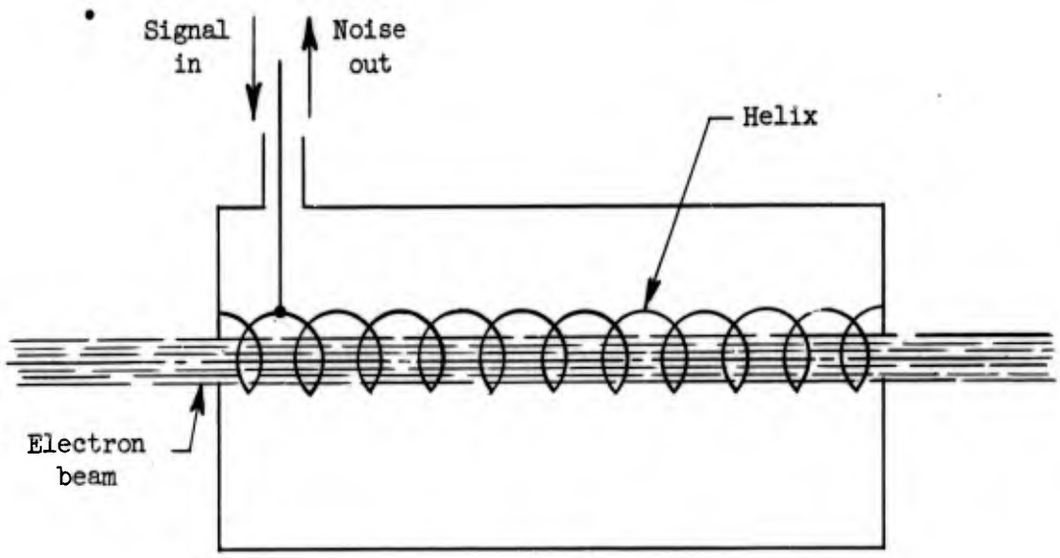

FIG. II.1--Fast-wave coupler.

CHAPTER VII

FAST-WAVE COUPLERS

The fast-wave coupler consists of a "long interaction" klystron cavity which supports a longitudinal resonant electric field (Fig. II.1). Wessel-Berg[15] has made a detailed study of cavities of this type. His theory can be applied directly to the design of fast-wave couplers.

A. COUPLING COEFFICIENT

In a linear theory the rf current can be represented by a sum of space-charge waves:

$$I(z) = \sum_{\ell} I_{\ell} \exp(-jk_{\ell}z) \exp(j\omega t) , \qquad (II.1)$$

where $I(z)$ is the rf current at a given frequency ω, at the plane z,
I_{ℓ} is the amplitude of the ℓ th space-charge wave, and
k_{ℓ} is the propagation constant of the ℓ th space-charge wave.

The complex power flow between the beam and the cavity is

$$P = 1/2 \int_0^L E(z) I^*(z) dz \qquad (II.2)$$

where P is the complex power flow,
$E(z)$ is the longitudinal electric field on the beam axis at the frequency ω, and
L is the length of the cavity.

If the theory is linear any of the ℓ space-charge waves can be excited alone if the proper boundary conditions are satisfied. Wessel-Berg has normalized the electric field and has defined $F(z)$ by the relation

$$E(z) = AV_0 F(z) \qquad (II.3)$$

with

$$\int_0^L F(z)F^*(z)dz = 1$$

where $E(z)$ is the electric field,

V_0 is the beam voltage,

A is a complex coefficient, and

L is the length of the cavity.

Wessel-Berg has defined the coupling coefficient $\beta(k_\ell)$ as

$$\beta(k_\ell) = \int_0^L F(z) \exp(-jk_\ell z)\, dz .$$

If $|\beta(k_\ell)| = 0$ there is no current wave with a propagation constant k_ℓ leaving the cavity. He has shown that the beam-loading conductance corresponding to the ℓ th wave is proportional to the absolute value of the coupling coefficient, $|\beta(k_\ell)|$. The integral

$$\beta = \int_0^L F(z) \exp(-jk_\ell z)\, dz$$

is a complex number. If both the real and the imaginary part are zero, that is, if its absolute value is zero, there is no exchange of real energy, on the average, over the whole length of the cavity, between the field in the cavity and the ℓ th space-charge wave of the beam.

With Wessel-Berg's normalization the absolute value of β , β_0 , which is called the coupling coefficient, is always smaller or equal to one; $\beta_{0\ell} = |\beta| \leq 1$. Then if

$$\beta_{0\ell} = \left| \int_0^L F(z) \exp(-jk_\ell z)\, dz \right| = 0 \qquad \text{(II.4)}$$

there is no coupling between the circuit and the ℓ th space-charge wave.

B. FAST-WAVE COUPLER

Wessel-Berg has calculated β_0 , the coupling coefficient, for a structure supporting a resonant longitudinal electric field

$$E(z) = AV_0 \frac{\sqrt{2}}{L} \cos \frac{n\pi}{L} z , \qquad \text{(II.5)}$$

where n is the length of the cavity in half-circuit wave length. One of Wessel-Berg's curves is reproduced, Fig. II.2, and β_0 is plotted as

These curves are reproduced from Wessel-Berg (reference 15, page 80).

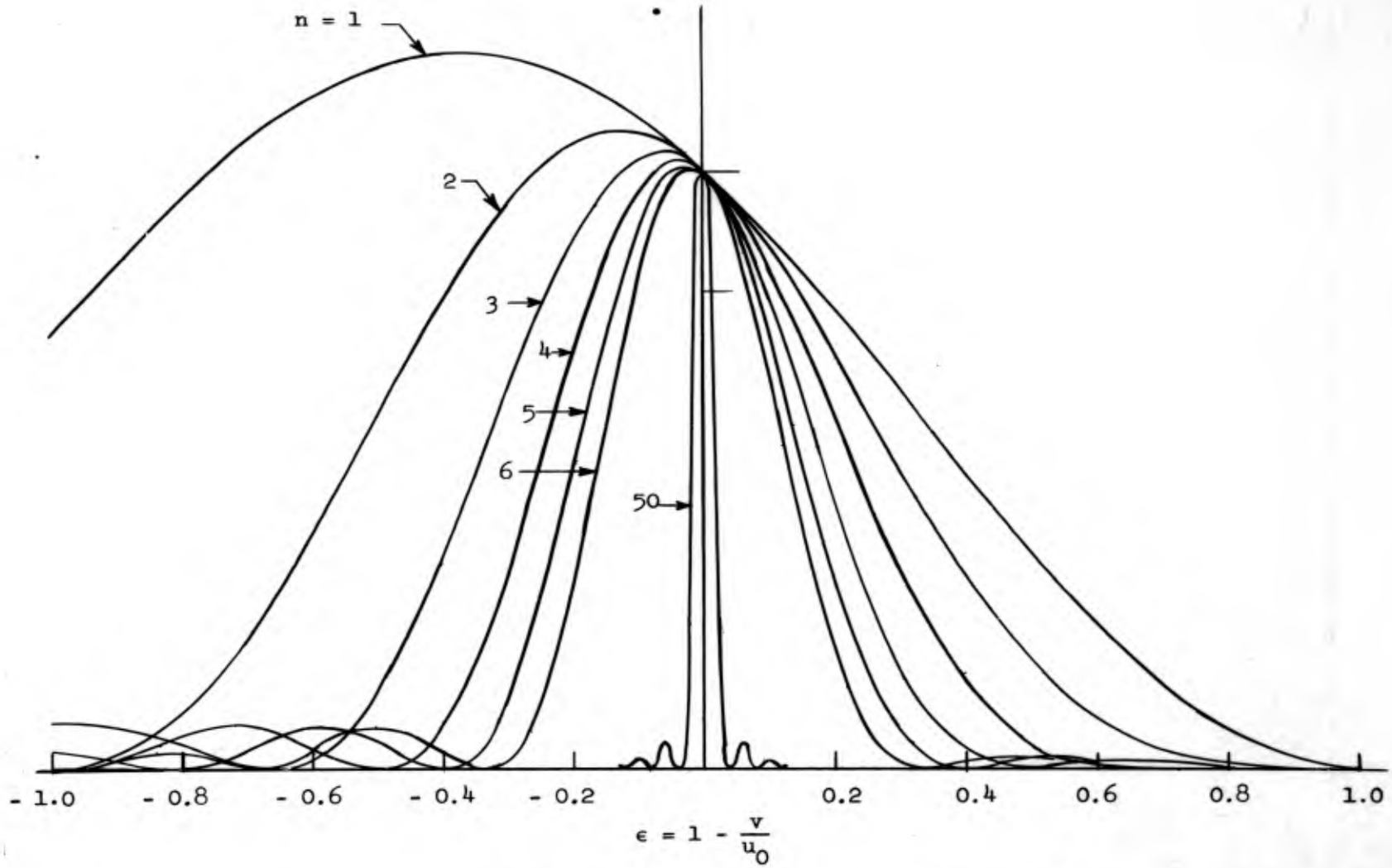

FIG. II.2--Square of the coupling coefficient for a resonant longitudinal sinusoidal electric field.

a function of a parameter ϵ for different values of n :

$$\epsilon = 1 - \frac{v_{ph}}{u} \tag{II.6}$$

where v_{ph} is the phase velocity of the circuit, and
u is the phase velocity of the space-charge wave, then
β_0 is equal to zero, if ϵ has the following value:

$$\epsilon = -\frac{2}{n} . \tag{II.7}$$

If u_s , phase velocity of the slow space-charge wave, satisfies the equation

$$1 - \frac{v_{ph}}{u_s} = -\frac{2}{n} , \tag{II.8}$$

then there is no coupling between the slow wave and the circuit. The phase velocities of the slow and fast space-charge waves are

$$\left.\begin{aligned} u_s &= \frac{u_0}{1 + \omega_q/\omega} \\ u_f &= \frac{u_0}{1 - \omega_q/\omega} \end{aligned}\right\} \tag{II.9}$$

where ω is the frequency of the signal, and
ω_q is the reduced plasma frequency.

The amount of coupling to the fast wave is determined easily from the curve (Fig. II.2) with

$$\epsilon_f = 1 - \frac{v_{ph}}{u_f} . \tag{II.10}$$

Two curves are reproduced (Fig. II.3) which give the coupling coefficient β_0 as a function of ϵ for two values of n . If the cavity is short, $n = 2$ for example, the minimum (point A), which gives no coupling to the slow wave, is very flat. If the frequency is changed, Eq. (II.8) is still

These curves are reproduced from Wessel-Berg (reference 15, page 80).

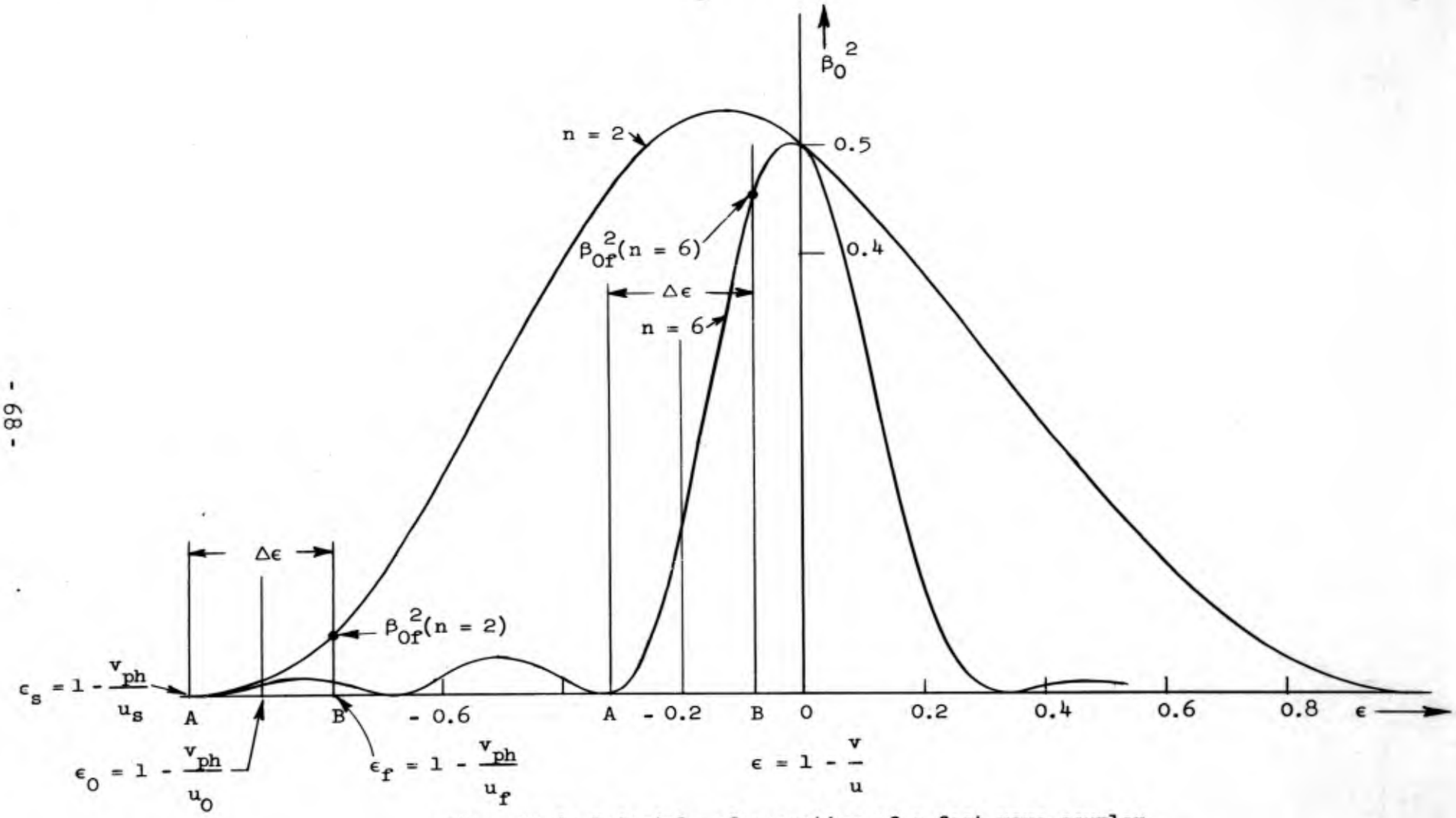

FIG. II.3--Principle of operation of a fast-wave coupler.

(a) n = 2 [β_{0f}^2 (coupling coefficient for the fast wave) = 0.06].

(b) n = 6 [for the same ω_q/ω, that is the same $\Delta\epsilon$, $\beta_{0f}^2 = 0.46$].

true for all practical purposes, and a relatively large bandwidth can be expected. This bandwidth is counterbalanced by poor coupling to the fast wave, the curve rises very slowly, and the coupling coefficient for the fast wave (point B) is small. If the value of n is large, $n = 6$ for example, the minimum is much sharper: the bandwidth will be reduced because the relation [Eq. (II.8)] is satisfied only for a relatively small change in frequency. But as the curve rises faster for the same value of ω_q/ω, the coupling to the fast wave is much larger. This is a design alternative: the bandwidth can be increased to the detriment of the amount of coupling to the fast wave or the bandwidth can be reduced and the coupling to the fast wave is much greater.

C. REMOVAL OF THE NOISE FROM THE FAST WAVE

The noise at the frequency ω can be represented by a current source at this frequency. The noise carried by the fast wave is identified with an rf current I_a. In order to extract all the noise from the fast wave, at the signal frequency, the total power carried by the fast wave must be set equal to the total power absorbed by the cavity. The power absorbed will be dissipated in the shunt resistance of the cavity and in the load.

Haus[19] has shown that the power carried by fast space-charge waves is given by

$$P = 1/2\ Y_0 V_f^2 , \qquad \text{(II.11)}$$

where V_f is the kinetic voltage associated with the fast wave. The term Y_0 is an admittance defined by

$$Y_0 = \frac{I_0}{2V_0}\,\omega/\omega_q , \qquad \text{(II.12)}$$

where I_0 is the dc beam current, and where V_0 is the dc beam voltage. The kinetic voltage V_f is equal to

$$V_f = + \frac{m}{e}\, u_0 u_f . \qquad \text{(II.13)}$$

Replacing the kinetic voltage V_f by the current I_f Eq. (II.11) becomes

$$P = 1/2 \frac{I_a^2}{Y_0} . \tag{II.14}$$

The power absorbed in the cavity is given by[15]

$$P = 1/2 |V|^2 \left(\frac{Q}{R_{sh}}\right) \frac{1}{Q_L} , \tag{II.15}$$

where Q is the Q of the cavity
R_{sh} is the shunt resistance
Q_L is the loaded Q .

The term $|V|^2$ has been calculated by Wessel-Berg as

$$\left.\begin{aligned} V^2 &= \frac{1}{|N|^2}\left(\frac{R_{sh}}{Q}\right)^2 (Q_L)^2 (\beta_{0f})^2 I_a^2 \\ \text{and} \qquad N &= 1 + 1/8 \left(\frac{R_{sh}}{Q}\right) Q_L \left(\frac{I_0}{V_0}\right)\left(\frac{\omega}{\omega_q}\right) (\beta_{0f})^2 \end{aligned}\right\} \tag{II.16}$$

where β_{0f} is the coupling coefficient to the fast wave. The two powers defined in Eqs. (II.14) and (II.15) must be equal. From this condition the loaded Q , Q_L , is given by

$$Q_L = 8 \left(\frac{\omega_q}{\omega}\right)\left(\frac{V_0}{I_0}\right)\left(\frac{Q}{R_{sh}}\right) \frac{1}{(\beta_{0f})^2} . \tag{II.17}$$

The fast-wave coupler can be designed from Eqs. (II.8) and (II.17).

D. APPLICATION: DESIGN OF A FAST-WAVE COUPLER USING A SHORTED HELIX

A possible design of a coupler of this type is shown in Fig. II.1. It consists of a helix shorted at both ends which is enclosed in a cylindrical cavity. Normally a structure having transverse planes of symmetry should be used in order to satisfy the boundary conditions at each end. However, a single helix was used here because of the simple formulas which describe its properties. If the phase velocity of the helix

is small enough, the helix can be characterized by the following equations:

$$\frac{v_{ph}}{c} = \text{tg}\psi \ , \qquad \text{(II.18)}$$

where c is the velocity of light

ψ is the pitch angle of the helix;

$$L = N2\pi a\,\text{tg}\psi \ , \qquad \text{(II.19)}$$

where L is the length of the helix

a is the radius of the helix

N is the number of turns; and

$$\frac{n}{N} = 2\,\frac{\omega a}{c} \ , \qquad \text{(II.20)}$$

where n is the length of the helix in half-wave length. If ω_q, the reduced plasma frequency, is expressed as a function of the perveance K and if Eqs. (II.18) through (II.20) are used, Eq. (II.8) becomes

$$\frac{u_0}{c} = \frac{n\,\text{tg}\psi}{n + 2 - n(\text{tg}\psi)(R/b)(c/\omega)\sqrt{3.03 \times 10^4 K}} \ , \qquad \text{(II.21)}$$

where R is the plasma reduction factor

b is the beam radius

ω is the frequency in radians/s .

1. Example: Design of a Fast-Wave Coupler Operating At 900 Mc/s.

After some investigation the following parameters were chosen:

$$\frac{\omega a}{c} = 0.039 \qquad K = 6 \times 10^{-7}$$

$$\frac{u_0}{c} = 0.077 \qquad n = 4$$

$$\frac{b}{a} = 0.4$$

Then from Eq. (II.20), we find

$$N = 26$$

$$a = 2 \times 10^{-3} m$$

and, from Eq. (II.7)

$$\epsilon_s = -\frac{2}{n} = -\frac{1}{2} .$$

From Eq. (II.21) the pitch angle can be determined as $tg\psi = 0.11$. And the pitch of the helix is

$$P = 2\pi a tg\psi = 1.4 \times 10^{-3} m .$$

From the value of ϵ_s and $\epsilon_0 = 1 - v_{ph}/u_0$ and from

$$|\epsilon_s - \epsilon_0| = |\epsilon_0 - \epsilon_f|$$

the value of ϵ_f can be calculated as $\epsilon_f = -0.34$ and $\beta_{0f} = 0.08$. The R_{sh} can be calculated from curves in Pierce's book. Then Eq. (II.17) yields $Q_L = 35$. The coupler is completely determined by

radius of the helix $a = 2 \times 10^{-3} m$

pitch of the helix $p = 1.4 \times 10^{-3} m$

number of turns of the helix $N = 26$

Q_L loaded $Q = 35$.

The beam must furthermore satisfy the following conditions:

K: perveance $= 6 \times 10^{-7}$

beam diameter: $= 1.6 \times 10^{-3} m$

V_0 beam potential = 1500 volts .

2. Bandwidth of the Fast-Wave Coupler.

The amplitude of the coupling coefficient has been calculated by Wessel-Berg. For a structure supporting a sinusoidal resonant field he

has found that

$$\beta_0(\epsilon) = \frac{1}{\sqrt{2}} \frac{1 - \epsilon}{1 - \epsilon/2} \frac{\sin n\pi\epsilon/2}{n\pi\epsilon/2} . \qquad (II.22)$$

At the design frequency ω ,

$$\beta_0(\epsilon_s) = 0 \qquad (II.23)$$

and there is no coupling to the slow wave. At a different frequency, $\omega + \Delta\omega$ Eq. (II.23) may not be satisfied any more, and a certain amount of coupling to the slow wave is introduced.

The bandwidth of the coupler is defined as the frequency range over which the ratio β_{0s}/β_{0f} of the amplitudes of the coupling coefficients to the slow wave and to the fast wave is smaller than a fixed number M .

The calculation of the bandwidth is made in Appendix II.A where it is found that

$$\frac{\Delta\omega}{\omega} \leq 7 \frac{\sin \pi [(1 - \omega_q/\omega)\, n]}{\pi [(1 - \omega_q/\omega)\, n]} \frac{1}{n} M . \qquad (II.24)$$

Eq. (II.24) is only approximate and only an order of magnitude of the bandwidth may be deducted from it. For the best coupling to the fast wave, that is, when $\epsilon_f = 0$ (Fig. II.3) and for $M = 10^{-2}$, the bandwidth becomes

$$\frac{\Delta\omega}{\omega} \leq \frac{7M}{n} . \qquad (II.25)$$

As was described qualitatively, the bandwidth is inversely proportional to the number n . For $n = 4$, as in the example, the bandwidth is 1.7% with $M = 10^{-2}$. For real, low-noise properties M should be kept at a smaller level than 10^{-2} in order to have very little coupling to the slow wave. The bandwidth becomes then extremely small, being 0.17% only for $M = 10^{-3}$.

CHAPTER VIII

AMPLIFYING MECHANISM

A. INTRODUCTION

If an electron beam is injected through a cavity with a narrow gap resonant at the frequency ω, the effect of the beam in the cavity can be accounted for by introducing an admittance Y called beam-loading admittance. This admittance is proportional to the dc current I_0. If the gap is sufficiently small and if the beam is 100% modulated at the frequency 2ω, the beam-loading admittance will be proportional to $I_0 \cos 2\omega t$. The cavity can be represented by the equivalent circuit of Fig. II.4. Since the beam loading admittance, Y, varies at twice the

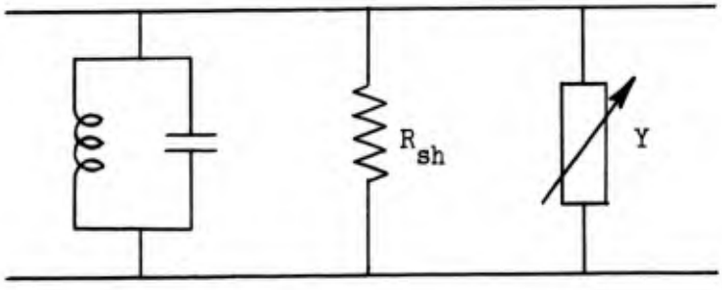

FIG. II.4--Equivalent circuit for the cavity:

R_{sh} is the shunt resistance of the cavity,

Y is the beam-loading admittance.

resonant frequency, parametric amplification occurs.

The same process can be used with a long-interaction cavity even when the pump is not equal to twice the signal frequency. An electron beam is injected through a fast-wave coupler designed to operate at the pump frequency ω_p. The pump electric field in this cavity excites only a fast space-charge wave at the frequency ω_p. This beam then enters a long-interaction cavity resonant at the signal frequency. The current at the signal frequency can be calculated. The power flow between the beam and the cavity can be derived and the beam-loading admittance found. It will be shown that under certain conditions its real part can be negative if the pump power is large enough. Amplification (or oscillations) occur if the negative beam-loading conductance is smaller (or equal) to the combined conductance of the cavity and the load.

In a first step the differential equation relating the current at the signal frequency to the electric field in a resonant cavity will be derived. The equation is a fourth-order linear differential equation with constant coefficients. Four space-charge waves are present, instead of the usual two waves which exist when there is no pumping. The differential equation is solved and the beam-loading admittance is calculated in two cases:

1. Floating Drift-Tube Klystron Cavity (Fig. II.5).

This cavity was used by Bridges[5] in his amplifier. An electron beam is injected through this cavity with the following conditions:

(1) a fast wave at the pump frequency exists on the beam,

(2) the first gap creates only velocity modulation at the signal frequency, and

(3) there are no initial currents at the signal and idler frequencies and there is no initial velocity at the idler frequency.

It will be found that the signal current will not always be 90° out of phase with the signal velocity. Then, for conditions which in the absence of pump give a reactive beam loading, it is possible to obtain a negative conductance giving rise to amplification.

2. Long-Interaction Klystron Cavity (Fig. II.1).

A sinusoidal, resonant, electric field exists on the beam axis. The current at the signal frequency will be calculated in order to obtain

the complex power flow between the beam and the cavity. From the power flow the beam loading can be calculated. For very small pump power the beam-loading admittance coincides with the values calculated by Wessel-Berg in the nonparametric cases. If the pump power is increased, it is possible to obtain, under certain conditions, a negative beam-loading conductance.

B. DERIVATION OF THE DIFFERENTIAL EQUATIONS GOVERNING THE CURRENT DENSITIES

1. Assumptions.

The usual small-signal theory[15] is generalized in order to include the parametric effect of the pump. The following assumptions are made:

(1) The beam is immersed in an infinite longitudinal magnetic field which forbids any transverse motion of the electrons.

(2) Even though the beam is of finite size, only the first pair of space-charge modes are excited.

(3) The average charge density in the beam region is zero. The dc potential is constant in the cross-section of the beam, and all the electrons have the same dc velocity u_0 .

(4) The theory is limited to the three frequencies interaction case; that is, the only effects considered are at the pump, idler, and signal frequencies. Terms at the pump frequency arise only from sources at that frequency. Terms at the signal and idler frequencies may arise from sources at these respective frequencies or from first order interaction between the pump and the idler, or between the pump and the signal, respectively.

(5) All second order terms are neglected at the signal and idler frequencies. However, all the terms at the pump frequency compatible with assumption (4), are kept.

(6) The pump field is injected in order to create only the fast space-charge wave at the pump frequency.

(7) The dc kinetic energy of the beam is constant.

2. Derivation of the Differential Equations.

It is possible to separate the time and z dependence. The total

current density $I(z,t)$ can then be written,

$$I(z,t) = I_0' + \left.\begin{aligned} &\tfrac{1}{2}\left[I_1(z)\exp(j\omega_1 t) + I_1^*(z)\exp(-j\omega_1 t)\right] \\ &+ \tfrac{1}{2}\left[I_2(z)\exp(j\omega_2 t) + I_2^*(z)\exp(-j\omega_2 t)\right] \\ &+ \tfrac{1}{2}\left[I_3(z)\exp(j\omega_3 t) + I_3^*(z)\exp(-j\omega_3 t)\right] \end{aligned}\right\} \quad \text{(II.26)}$$

where I_0' is the dc current density
$I_1(z)$ is the current density at the signal frequency
$I_2(z)$ is the current density at the idler frequency, and
$I_3(z)$ is the current density at the pump frequency.

The subscript 1 refers to the signal frequency, the subscript 2 to the idler frequency, and the subscript 3 to the pump frequency. The asterisk represents the complex conjugate.

The total electron velocity $u(z,t)$ and the total charge density $\rho(z,t)$ are:

$$u(z,t) = u_0 + \frac{1}{2}\sum_{\ell}\left[u_\ell(z)\exp(j\omega_\ell t) + u_\ell^*(z)\exp(-j\omega_\ell t)\right] \quad \text{(II.27)}$$

$$(\ell = 1,2,3)$$

where u_0 is the dc velocity of the electrons and $u_\ell(z)$ the rf velocity at the frequency ω_ℓ.

$$\rho(z,t) = \rho_0 + \frac{1}{2}\sum_{\ell}\left[\rho_\ell(z)\exp(j\omega_\ell t) + \rho_\ell^*(z)\exp(-j\omega_\ell t)\right], \quad \text{(II.28)}$$

where ρ_0 is the dc charge density and
$\rho_\ell(z)$ is the rf charge density at the frequency ω_ℓ.

The current density is related to the charge density and the electron velocity by the relation

$$I(z,t) = \rho(z,t)\, u(z,t) . \quad \text{(II.29)}$$

The values of $I(z,t)$, $\rho(z,t)$ and $u(z,t)$ are calculated from Eqs. (II.26), (II.27), (II.28) and are substituted in Eq. (II.29), then

$$I(z,t) = I_0' + \frac{1}{2} \sum_{\ell} \left[I_\ell(z) \exp(j\omega_\ell t) + I_\ell^*(z) \exp(-j\omega_\ell t) \right]$$

$$= \left\{ u_0 + \frac{1}{2} \sum_{m} \left[u_m(z) \exp(j\omega_m t) + u_m^*(z) \exp(-j\omega_m t) \right] \right\} \qquad \text{(II.30)}$$

$$\times \left\{ \rho_0 + \frac{1}{2} \sum_{n} \left[\rho_n(z) \exp(j\omega_n t) + \rho_n^*(z) \exp(-j\omega_n t) \right] \right\} .$$

$$\ell, m, n = 1, 2, 3$$

Equation (II.30) is an identity in time; the terms of same time dependance can be identified. The dc term gives

$$I_0' = \rho_0 u_0 + \frac{1}{4} \left[u_3(z)\, \rho_3^*(z) + \rho_3(z)\, u_3^*(z) \right] . \qquad \text{(II.31)}$$

The term at the signal frequency is

$$I_1(z) = u_0 \rho_1(z) + \rho_0 u_1(z) + \frac{1}{2} \left[u_3(z)\, \rho_2^*(z) + \rho_3(z)\, u_2^*(z) \right] . \qquad \text{(II.32)}$$

The first two terms of the right hand side are the small-signal terms which are usually found; the last term represents the interaction between the pump and the idler. In the same way it is found that

$$I_2(z) = u_0 \rho_2(z) + \rho_0 u_2(z) + \frac{1}{2} \left[u_3(z)\, \rho_1^*(z) + \rho_3(z)\, u_1^*(z) \right] . \qquad \text{(II.33)}$$

The current density at the pump frequency is

$$I_3(z) = u_0 \rho_3(z) + \rho_0 u_3(z) . \qquad \text{(II.34)}$$

To neglect the second order terms at the signal and idler frequency is equivalent to state that as far as Eq. (II.34) is concerned, the pump wave is not perturbed by the presence of the signal or the idler.

The rf velocity at the idler frequency, $u_2^*(z)$, can be calculated from the complex conjugate of Eq. (II.33) and substituted in Eq. (II.32).

Then the result is

$$I_1(z) = \rho_1 \left[u_0 - \frac{1}{4} \frac{\rho_3(z)\, u_3^*(z)}{\rho_0} \right] + u_1(z) \left[\rho_0 - \frac{1}{4} \frac{\rho_3(z)\, \rho_3^*(z)}{\rho_0} \right] \tag{II.35}$$

$$+ \frac{1}{2} \left[u_3(z) - \frac{u_0}{\rho_0} \rho_3(z) \right] \rho_2^*(z) + \frac{1}{2\rho_0} \rho_3(z)\, I_2^*(z) \ ,$$

where $I_1(z)$ is the current density at the signal frequency. The equation of continuity,

$$\vec{\nabla} \cdot \vec{I}(z,t) = - \frac{\partial \rho}{\partial t} (z,t) \ , \tag{II.36}$$

where $I(z,t)$ is the total current density, and $\rho(z,t)$ the total charge density, can be split in its different time varying components. Thus

$$\frac{\partial I_\ell(z)}{\partial z} = \frac{dI_\ell(z)}{dz} = - j\omega_\ell \rho_\ell(z) \tag{II.37}$$

$$\ell = 1,2,3$$

where the partial derivatives have been replaced by the total derivative, $I_\ell(z)$ being now a function of one variable only.

The equation of motion is

$$\frac{du(z,t)}{dt} = \frac{e}{m} E_T'(z,t) \ , \tag{II.38}$$

where $u(z,t)$ is the total electron velocity and

$E_T'(z,t)$ is the total electric field, in the z direction. Thus $E_T'(z,t)$ can be written

$$E_T'(z,t) = E'(z,t) + E_s'(z,t) \ , \tag{II.39}$$

where $E'(z,t)$ is the total external electric field, and

$E_s'(z,t)$ is the total space-charge field.

The space-charge field is related to the charge density by the equation

$$\vec{\nabla} \cdot \vec{E}_s'(z,t) = \frac{\rho(z,t)}{\epsilon_0} , \tag{II.40}$$

when ϵ_0 is the dielectric constant of free space. Equation (II.40) can be separated in its various time dependent components, so that

$$\frac{d}{dz} [E_{s\ell}(z)] = \frac{\rho_\ell(z)}{\epsilon_0} \tag{II.41}$$

$$\ell = 1,2,3$$

where $E_{s\ell}(z)$ is the electric space-charge field varying at the frequency ω_ℓ . Then $\rho_\ell(z)$ can be expressed as a function of $I_\ell(z)$ from Eq. (II.37). Equation (II.41) becomes

$$E_s'(z,t) = \frac{1}{2} \sum_\ell \left[\frac{j}{\omega_\ell} I_\ell(z) \exp (j\omega_\ell t) - \frac{j}{\omega_\ell} I_\ell^*(z) \exp (- j\omega_\ell t) \right] \tag{II.42}$$

$$\ell = 1,2,3 .$$

The terms $E_\ell(z)$ and $E_\ell^*(z)$ are defined by the following equation:

$$E_s'(z,t) = \frac{1}{2} \sum_\ell \left[E_{s\ell}(z) \exp (j\omega_\ell t) + E_{s\ell}^*(z) \exp (- j\omega_\ell t) \right] \tag{II.43}$$

$$\ell = 1,2,3$$

and can be written, from Eq. (II.42), as

$$E_{s\ell}(z) = \frac{j}{\omega_\ell} I_\ell(z)$$

and (II.44)

$$E_{s\ell}^*(z) = - \frac{j}{\omega_\ell} I_\ell^*(z) .$$

In the same fashion, $E'(z,t)$ may be defined as

$$E'(z,t) = \frac{1}{2} \sum_{\substack{\ell \\ \ell = 1,2}} \left[E_\ell(z) \exp (j\omega_\ell) + E_\ell^*(z) \exp (- j\omega_\ell t) \right] . \tag{II.45}$$

It has been assumed that there is no applied field at the pump frequency.

The equation of motion (II.38) can now be separated in its various time varying components

$$j\omega_\ell u_\ell(z) + u_0\left[\frac{du_\ell(z)}{dz}\right] + \frac{1}{2}\frac{d}{dz}\left[u_3(z)\, u_\ell^*(z)\right] = \frac{e}{m}\left[\frac{jI_\ell(z)}{\epsilon_0\omega_\ell} + E_\ell(z)\right]$$

$$\ell = 1,2 \qquad \text{(II.46)}$$

for the signal frequency ($\ell = 1$) and the idler frequency ($\ell = 2$). With the first order approximation of this theory (assumption 5) the equation for the pump frequency is

$$j\omega_3 u_3(z) + u_0\left[\frac{du_3(z)}{dz}\right] = \frac{e}{m}\left[\frac{jI_3(z)}{\epsilon_0\omega_3}\right] \qquad \text{(II.47)}$$

Equation (II.47) is the usual small-signal equation one would obtain without parametric effect. The terms $u_3(z)$ and $\rho_3(z)$ can be calculated from Eqs. (II.34) and (II.37)

$$u_3(z) = \frac{1}{\rho_0}\left[I_3(z) - u_0\rho_3(z)\right]$$

$$u_3(z) = \frac{1}{\rho_0}\left[I_3(z) - \left(\frac{ju_0}{\omega_3}\right)\frac{dI_3(z)}{dz}\right] . \qquad \text{(II.48)}$$

It has been assumed that the pump field is applied to the beam in such a way that only the fast space-charge wave is excited. This can be achieved by a fast-wave coupler, and it follows that

$$I_3(z) = mI_0 \exp\left[-j(k_3 - k_{q3})z\right] , \qquad \text{(II.49)}$$

where m is a complex number independent of z

I_0 is equal to the product $\rho_0 u_0$ (which is different from the total dc current I_0')

k_3 is the propagation constant at the pump frequency $k_3 = \omega_3/u_0$

k_{q3} is the reduced plasma propagation constant at the pump frequency

$$k_{q3} = R_3\frac{\omega_p}{u_0} \qquad \omega_p = \sqrt{\frac{\rho_0 e}{m\epsilon_0}} \qquad \text{(II.50)}$$

where R_3 is the plasma reduction factor. Then from Eqs. (II.37) and (II.48), it follows that

$$\left.\begin{aligned} u_3(z) &= \frac{\omega_{q3}}{\omega_3}\, mI_0 \exp\left[-j\,(k_3 - k_{q3})\,z\right] \\ \rho_3(z) &= \left(1 - \frac{\omega_{q3}}{\omega_3}\right)\left(\frac{mI_0}{u_0}\right) \exp\left[-j\,(k_3 - k_{q3})\,z\right] \end{aligned}\right\}. \qquad \text{(II.51)}$$

It has been implicitly assumed that the fast wave at the pump frequency is identical to the wave obtained in a nonparametric beam under small-signal assumptions. As a consequence, m is not dependent on z, and the products $u_3(z)\, u_3^*(z)$ and $u_3(z)\, \rho_3^*(z)$ are independent of z. This assumption is compatible with the assumptions made before. In particular, the dc kinetic energy is constant along the beam

$$\frac{1}{2}\, m \left[u_0^{\,2} + u_3^*(z)\, u_3(z)\right] = \text{constant}.$$

Some new parameters used by Louisell and Quate will be introduced:

$$\left.\begin{aligned} \alpha_3 &= \frac{\omega_{q3}}{\omega_3} \\ \alpha_2 &= \frac{\omega_{q2}}{\omega_2} \\ \alpha_1 &= \frac{\omega_{q1}}{\omega_1} \end{aligned}\right\} \qquad \text{(II.52)}$$

and

$$\left.\begin{aligned} a_1 &= \frac{\alpha_3}{\alpha_1} = \frac{\omega_{q3}}{\omega_{q1}} \cdot \frac{\omega_1}{\omega_3} \\ a_2 &= \frac{\alpha_3}{\alpha_2} = \frac{\omega_{q3}}{\omega_{q2}} \cdot \frac{\omega_2}{\omega_3} \end{aligned}\right\}. \qquad \text{(II.53)}$$

Since the different quantities vary like $\exp\left[-jk_3(1 - \alpha_3)\, z\right]$ at the

pump frequency, the result is

$\exp [- jk_1 (1 \pm \alpha_1) z]$ at the signal frequency

$\exp [- jk_2 (1 \pm \alpha_2) z]$ at the idler frequency (without parametric effect).

The parameters a_1 and a_2 measure the difference in phase velocity between the pump, on one hand, and the unperturbed signal and idler, on the other hand. Then, a_1 and a_2 are calculated approximately with the relations used by Louisell:[7]

$$\left.\begin{aligned} a_1 &\simeq \frac{\nu}{1+\nu} \frac{1 - \exp\left\{- 0.7\left[(1+\nu)/\nu\right] k_1 b\right\}}{1 - \exp\left(- 0.7\, k_1 b\right)} \\ a_2 &\simeq \frac{1}{1+\nu} \frac{1 - \exp\left\{- 0.7\left[(1+\nu)/\nu\right] k_1 b\right\}}{1 - \exp\left(- 0.7\, k_1 b/\nu\right)} \end{aligned}\right\} \qquad \text{(II.54)}$$

where b is the beam radius, $\nu = \omega_1/\omega_2$. A differential equation in $I_1(z)$ and $E_1(z)$ can be derived from Eqs. (II.35), (II.37), and (II.51). The algebra is carried out in detail in Appendix II.B. The final result with the following change of variables,

$$\left.\begin{aligned} I_1(z) &= i_1(z) \exp\left[- jk_1(1 - \alpha_3)z\right] \\ I_2^*(z) &= i_2^*(z) \exp\left[+ jk_2(1 - \alpha_3)z\right] \end{aligned}\right\}, \qquad \text{(II.55)}$$

is

$$\frac{d^4 i_1(z)}{dz^4} + 2j\,(\alpha_3 k_1)\left(1 - \frac{1}{\nu}\right)\frac{d^3 i_1(z)}{dz^3}$$

$$+ \frac{(k_1\alpha_3)^2}{\nu}\left\{4 - \frac{1}{2}|m|^2 - \left[\left(1 - \frac{1}{a_2^2}\right)\frac{1}{\nu} + \nu\left(1 - \frac{1}{a_1^2}\right)\right]\right\}\frac{d^2 i_1(z)}{dz^2}$$

$$+ 2j\,\frac{(k_1\alpha_3)^3}{\nu}\left\{1 - \frac{|m|^2}{4} - \frac{1}{a_1^2}\left(1 + \frac{|m|^2}{4}\right) - \frac{1}{\nu}\left[1 - \frac{|m|^2}{4} - \frac{1}{a_2^2}\left(1 + \frac{|m|^2}{4}\right)\right]\right\}\frac{di_1(z)}{dz}$$

$$+ \frac{(k_1\alpha_3)^4}{\nu^2}\left[1 - \frac{|m|^2}{2} + \frac{|m|^4}{16} - \left(\frac{1}{a_1^2} + \frac{1}{a_2^2}\right)\left(1 + \frac{3}{4}|m|^2\right) + \frac{1}{a_1^2 a_2^2}\left(1 - \frac{|m|^2}{4}\right)\right] i_1(z)$$

$$= \eta\,\frac{\rho_0}{u_0}\left\{\begin{array}{l} k_1\left\{j\,\dfrac{d^2}{dz^2} + 2\,\dfrac{(\alpha_3 k_1)}{\nu}\left(1 + \dfrac{|m|^2}{4}\right)\dfrac{d}{dz} - j\,\dfrac{(k_1\alpha_3)^2}{\nu^2}\left[1 - \dfrac{1}{a_2^2}\left(1 - \dfrac{|m|^2}{4}\right) + \dfrac{3}{4}|m|^2\right]\right\} \\ \quad \times\left\{E_1(z)\,\exp\left[+ jk_1\,(1 - \alpha_3)\,z\right]\right\} \\ -\dfrac{m}{2}k_1\left[\begin{array}{l} -j\,\dfrac{d^2}{dz^2} + 2\alpha_3 k_1\left(1 - \dfrac{1}{\nu}\right)\dfrac{d}{dz} \\ +j\,\dfrac{(k_1\alpha_3)^2}{\nu}\left(-3 - \dfrac{|m|^2}{4}\right)\end{array}\right] E_2^*(z)\,\exp\left[-jk_2\,(1 - \alpha_3)\,z\right]\ . \end{array}\right\} \qquad \text{(II.56)}$$

If an external field at the idler frequency exists, the current at the signal frequency depends on m instead of depending on $|m|^2$. With

$$\nu = 1 \quad \text{and} \quad E_1(z) = E_2^*(z) = 0 ,$$

the equation is the same as the one derived by Louisell and Quate. As a check on the equation let

$$\nu = 1 \qquad m = 0 ;$$

then Eq. (II.56) must reduce to the ordinary equation

$$\frac{d^2 I_1}{dz^2} + 2jk_1 \frac{dI_1}{dz} - \left(k_1^2 - k_{ql}^2\right) I_1(z) = jk_1 \frac{I_0}{2V_0} E_1(z) . \quad \text{(II.57)}$$

With $\nu = 1$ and $m = 0$, Eq. (II.56) becomes

$$\frac{d^4 i_1(z)}{dz^4} + 4k_{ql}^2 \frac{d^2 i_1(z)}{dz^2} = jk_1 \frac{I_0}{2V_0} \left(\frac{d^2}{dz^2} - 2jk_{ql} \frac{d}{dz}\right) E_1(z) \exp\left[+ jk_1(1 - \alpha_1)z\right]. \quad \text{(II.58)}$$

Equations (II.57) and (II.58) have the same homogeneous solution. To check the inhomogeneous part,

$$E(z) \exp\left[+ jk_1 (1 - \alpha_3) z\right]$$

can be calculated from Eq. (II.57) and substituted in Eq. (II.58). If this is done, the result is the identity $0 = 0$ which proves that the two equations have the same solutions.

C. CALCULATION OF THE BEAM-LOADING ADMITTANCE IN A "FLOATING DRIFT TUBE" KLYSTRON CAVITY

1. Description of the Problem.

Bridges' parametric amplifier[5] consisted of two cavities. The first cavity modulated the beam at the pump frequency. This beam was then injected through a "floating drift tube" klystron cavity (Fig. II.5). It is shown that parametric pumping can create a negative beam-loading conductance across the second gap leading to amplification (or oscillations).

A "floating drift tube" klystron cavity consists of one resonant cavity with two narrow gaps (Fig. II.5). Depending on the resonant mode of the cavity, the rf voltage V_1 across the first gap and the rf voltage V_2 across the second gap have a constant phase difference. For example, the phase difference between V_1 and V_2 can be 0° for the "0" mode of oscillation or 180° for the "π" mode of oscillation. The two gaps are infinitely narrow; that is, the dc transit time of an electron through the gap will be much smaller than an rf cycle at the pump frequency.

2. Derivation of the Current Density.

The z axis of coordinates is the electron beam axis. The first gap is located at the plane $z = 0$, the second gap at the plane $z = L$.

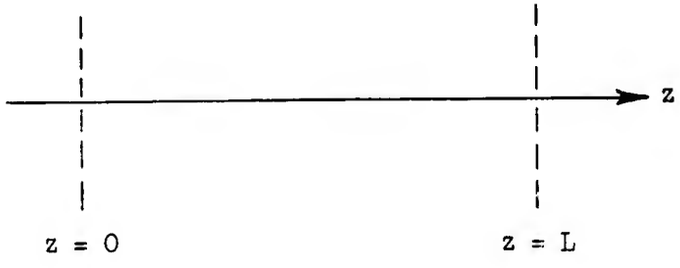

At the first gap $(z = 0)$ the following boundary conditions exist:

the current density at the signal frequency is $i_1(0)$
the current density at the idler frequency is $i_2^*(0)$
the rf velocity at the signal frequency is $v_1(0)$
the rf velocity at the idler frequency is $v_2^*(0)$.

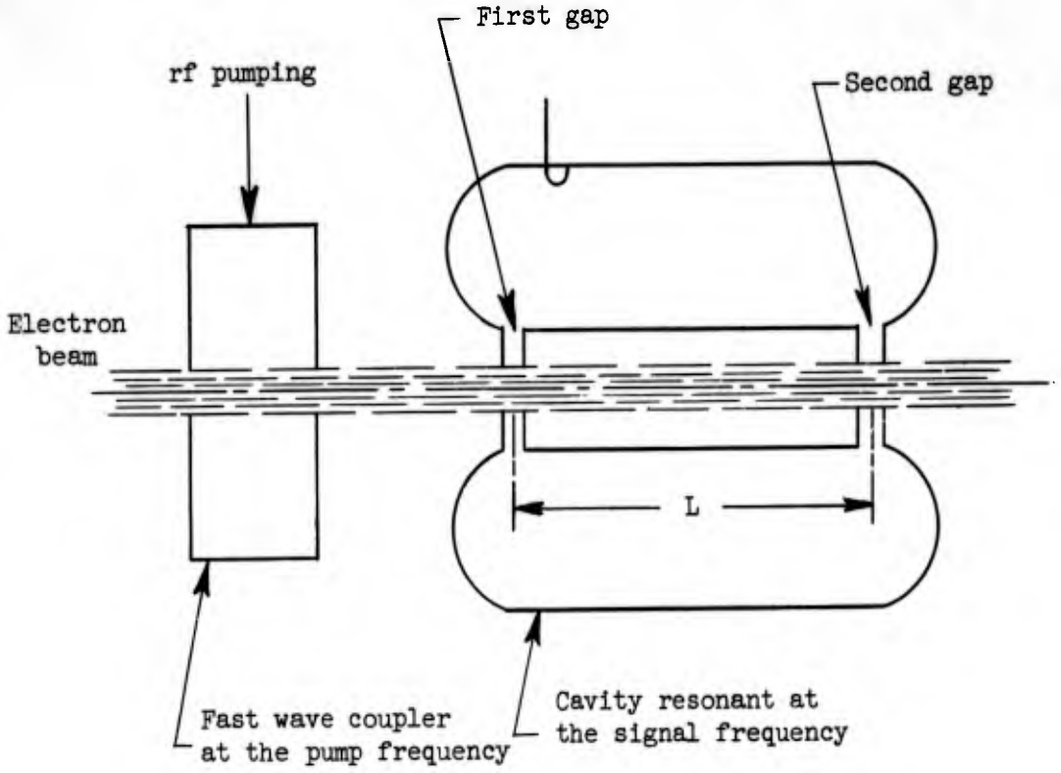

FIG. II.5--"Floating drift tube" klystron cavity.

Between gap I and gap II the electron beam drifts and is not subjected to any rf field. Equations (II.B.5) and (II.B.6) in Appendix II.B give

$$\left.\begin{aligned} & j\frac{d^2 i_1(z)}{dz^2} + 2(\alpha_3 k_1)\left(1 + \frac{|m|^2}{4}\right)\frac{di_1(z)}{dz} \\ & \quad + j(k_1\alpha_3)^2\left[1 - \frac{1}{a_1^2}\left(1 - \frac{|m|^2}{4}\right) + \frac{3}{4}|m|^2\right] i_1(z) \\ & \quad + \frac{m}{2}\left[-j\nu\frac{d^2 i_2^*(z)}{dz^2} + 2(\alpha_3 k_1)(\nu - 1)\frac{di_2^*(z)}{dz}\right. \\ & \quad \left. + j(k_1\alpha_3)^2\left(-3 - \frac{|m|^2}{4}\right)\right] i_2^*(z) = 0 \end{aligned}\right\} \quad (II.59)$$

$$\left.\begin{aligned} & -j\nu\frac{d^2 i_2^*(z)}{dz^2} + 2(\alpha_3 k_1)\left(1 + \frac{|m|^2}{4}\right)\frac{di_2^*(z)}{dz} \\ & \quad - \frac{j}{\nu}(k_1\alpha_3)^2\left[1 - \frac{1}{a_2^2}\left(1 - \frac{|m|^2}{4}\right) + \frac{3}{4}|m|^2\right] i_2^*(z) \\ & \quad + \frac{m^*}{2}\left[+j\frac{d^2 i_1(z)}{dz^2} + 2(\alpha_3 k_1)\left(\frac{1}{\nu} - 1\right)\frac{di_1(z)}{dz}\right. \\ & \quad \left. - j\frac{(k_1\alpha_3)^2}{\nu}\left(-3 - \frac{|m|^2}{4}\right) i_1(z)\right] = 0 \end{aligned}\right\} \quad (II.60)$$

[The same approximations leading to Eq. (II.B.10) have been made.] The amplitudes of the four waves, which then exist at the signal frequency, will be calculated as a function of the boundary conditions. The quantities $i_\ell(z)$ $(\ell = 1,2,3)$ were defined by the relation

$$I_\ell(z) = i_\ell(z) \exp\left[-jk_\ell(1 - \alpha_3)z\right] \quad (II.61)$$

where $I_\ell(z)$ is the current density at the frequency ω_ℓ. It should

be pointed out that each of the four waves can exist independently with the proper boundary conditions. The amplitudes $i_1^{(n)}$ of the modified current density at the signal frequency, which were defined by

$$i_1(z) = \sum_{(n)} i_1^{(n)}(z) = \sum_{(n)} i_1^{(n)} \exp\left[j\alpha_3 k_1 w^{(n)} z\right] \qquad (II.62)$$

$$(n) = 1,2,3,4$$

will be calculated. The straightforward algebra is carried out in Appendix II.C. The four equations defining the four $i_1^{(n)}$ are:

$$\left.\begin{aligned} \sum_{(n)} i_1^{(n)} &= i_1(0) \\ \sum_{(n)} A^{(n)} i_1^{(n)} &= m i_2^*(0) \\ \sum_{(n)} B^{(n)} i_1^{(n)} &= \frac{I_0}{\alpha_3 u_0} v_1(0) \\ \sum_{(n)} C^{(n)} i_1^{(n)} &= \frac{m I_0}{\alpha_3 u_0} v_2^*(0) \\ (n) &= 1,2,3,4 \ . \end{aligned}\right\} \qquad (II.63)$$

The special case,

$$i_1(0) = i_2^*(0) = v_2^*(0) = 0 \quad \text{and} \quad v_1(0) \neq 0 \ ,$$

is studied in detail. There exists no current modulation initially on the beam and the first gap produces only velocity modulation at the signal frequency. The system of Eq. (II.63) becomes

$$\left.\begin{aligned} \sum_{(n)} i_1^{(n)} &= 0 \qquad \sum_{(n)} C^{(n)} i_1^{(n)} = 0 \\ \sum_{(n)} A^{(n)} i_1^{(n)} &= 0 \qquad \sum_{(n)} B^{(n)} i_1^{(n)} = \frac{I_0}{\alpha_3 u_0} v_1(0) \\ (n) &= 1,2,3,4 \ . \end{aligned}\right\} \qquad (II.64)$$

The A's , the C's and the B's are defined in Appendix II.C. The total current density at the signal frequency is

$$I_1(z) = \left\{ \sum_{(n)} i_1^{(n)} \exp \left[+ j\alpha_3 k_1 w^{(n)} z \right] \right\} \exp \left[- jk_1 (1 - \alpha_3) z \right] . \quad \text{(II.65)}$$

As a check, it can easily be shown that the system (II.63) reduces to the equations obtained in the normal space-charge wave theory when $\nu = 1$, $a_1 = a_2 = 1$ and $m = 0$.

3. Discussion of the Results.

The fast and slow space-charge wave combine in such a way that the current is always 90° out of phase with the velocity if allowance is made for the phase shift due to the dc transit time, $\exp (- jk_1 z)$. The current components due to the two space-charge waves, in absence of parametric pumping are shown in vector form, Fig. II.9. The current is maximum for a drift space length of an odd number of quarter reduced plasma wavelength,

$$L = p \frac{\lambda_{q1}}{4} \qquad p = 1,3,5 \ldots$$

By changing the dc velocity, the dc transit angle α can be changed.

If the cavity oscillates in a zero mode of oscillation, that is if the voltages across the first and second gap, V_1 and V_2 , are in phase, it can be shown that for

(a). $\alpha = \left(2n + \frac{3}{2}\right) \pi$ radians

$n = 0,1,2,3 \ldots$

the current i_1 at the second gap is 180° out of phase with the voltage V_2 across the second gap. The ratio i_1/V_2 is real and negative: the tube works as an oscillator. It can be shown that for

(b). $\alpha = (2n + 1) \pi$ radians

$n = 0,1,2,3 \ldots$,

the ratio i_1/V_2 is now imaginary and positive. The beam-loading

admittance is purely reactive. For the case

(c). $\alpha = (2n + 2)\,\pi$ radians

$n = 1,2,3 \ldots ,$

again the beam-loading admittance is imaginary but negative.

If the pump power is applied to the beam, instead of the two normal space-charge waves, there exist four waves. These waves, components of the current density at the signal frequency, are shown in vector form, Fig. II.6. It can be seen that when the pump power is increased the total current at the signal frequency is not always 90° out of phase with the velocity modulation at the first gap. As a consequence for a cavity of length $p\,\lambda_{q1}/4$ in the zero mode of oscillation and a transit angle $\alpha = (2n \pm 1)\,\pi$, the current can be decomposed into two components; one component is 90° out of phase with the voltage across the second gap and one component is 180° out of phase with the voltage V_2 across the second gap. Then, for a given set of parameters which in the absence of pump gives rise to a purely reactive beam loading (i_1/V_2 purely imaginary), the presence of the pump gives rise to a beam loading which is complex, the real part being negative. Thus, parametric amplification may be obtained. This phenomenon was first seen by Bridges, who designed and built parametric amplifiers based on this principle.

4. Example.

Equation (II.C.9) was solved on a Burroughs 220 digital computer and the values $w^{(n)}$ were used to solve the system of Eq. (II.64). The amplitude and the phase of the $i_1^{(n)}$ were calculated, with the condition

$$\frac{I_0}{\alpha_3 u_0}\, v_1(0) = 1 .$$

The origin of phase was $v_1(0)$ (or V_1 voltage across the first gap). The current density at the signal frequency was calculated for several values of L : distance between the gaps. A specific example was chosen; that is, the values of $1/\nu = \omega_2/\omega_1$, $|m|$ and $k_1 b$ were defined to be

$$\frac{1}{\nu} = \frac{\omega_2}{\omega_1} = 2.0 \qquad |m| = 0.04 , 0.6 , 0.92 \qquad k_1 b = 1.0 .$$

Figure II.6 gives the amplitude and the phase of the current density at the signal frequency as a function of L, distance between the gaps, for three values of $|m|$. These results are plotted in Fig. II.7. In the calculations the variation $\exp(-jk_1L)$ which represents the dc transit time has been omitted.

For a small value of the pump power ($|m| = 0.02$) the current and the velocity are always 90° out of phase as in the nonparametric case. When the pump level is increased, the amplitude of the current increases and the phase angle between the current and the velocity is not always 90°. The amplitude and the angle difference increase with the pump power.

Figure II.8 gives the amplitude and the phase of the four space-charge waves. By adding the phasors representing these waves, the total current density at the signal frequency is obtained (Fig. II.6 and Fig. II.7). The phasors are drawn in Fig. II.9. It can be seen that, for low pump power, two of the current waves are similar to the normal slow and fast space-charge waves and that the patterns of Fig. II.9a and II.9b are similar. But in Fig. II.9c and in Fig. II.9d the pattern is different. At $L = 0$, for example, the total current density is zero due to the coalescence of three waves, two of which are off the axis, (the fourth wave is of negligible amplitude).

It should be noted, furthermore, that the maximum amplitude of the current occurs, in the example chosen, for a drift space which is longer than a quarter-plasma wavelength when the pump power is at a high level.

For a drift space $1/4$ of a plasma wavelength long and a dc transit angle of $(2n \pm 1)$ radians $(n = 1,2,3 \ldots)$, the ratio i_1/V_2 of the current to the voltage across the second gap has a real part which is negative. Amplification (or oscillations) at the signal frequency becomes possible if the cavity is in the "0" mode.

D. CALCULATION OF THE BEAM-LOADING ADMITTANCE IN A LONG INTERACTION CAVITY SUPPORTING A SINUSOIDAL AXIAL ELECTRIC FIELD

1. Definition of the Beam-Loading Admittance.

The electric field will be written using Wessel-Berg's normalization

$$E(z) = AV_0F(z) , \qquad (II.66)$$

where A is a complex normalizing constant

Pump Amplitude $\|m\|$	$L = \alpha_1 k_1 L = 0$	$L = \lambda_{q1}/10$	$L = 0.15\lambda_{q1}$	$L = 0.2\lambda_{q1}$	$L = \lambda_{q1}/4$	$L = 0.3\lambda_{q1}$	$L = 0.35\lambda_{q1}$	$L = 0.4\lambda_{q1}$	$L = 0.45\lambda_{q1}$
$\|m\| = 4 \times 10^{-2}$	$0 \angle$	$0.34 \angle 90°$	$0.47 \angle 90°$	$0.55 \angle 90°$	$0.58 \angle 90°$	$0.55 \angle 90°$	$0.47 \angle 90°$	$0.34 \angle 90°$	$0.18 \angle 90°$
$\|m\| = 0.6$	$0 \angle$	$0.35 \angle 87°$	$0.49 \angle 85°$	$0.59 \angle 83°$	$0.65 \angle 82°$	$0.66 \angle 81°$	$0.61 \angle 82°$	$0.52 \angle 85°$	$0.38 \angle 91°$
$\|m\| = 0.92$	$0 \angle$	$0.36 \angle 82°$	$0.52 \angle 78°$	$0.66 \angle 75°$	$0.76 \angle 73°$	$0.83 \angle 73°$	$0.86 \angle 75°$	$0.83 \angle 80°$	$0.78 \angle 91°$

$$\begin{cases} \dfrac{1}{v} = \dfrac{\omega_2}{\omega_1} = 2.0 \\ k_1 b = 1.0 \end{cases} \qquad \begin{cases} \alpha_3 = 0.166 \\ a_1 = 0.581 \end{cases}$$

FIG. II.6--Amplitude and phase of the current density at the signal frequency at the second gap as a function of the distance L between the gaps.

The results are expressed in the form $A \angle \theta$ where A is the amplitude of the current density, θ the phase angle relative to the voltage V_1 across the first gap.

$|m| = 4 \times 10^{-2}$

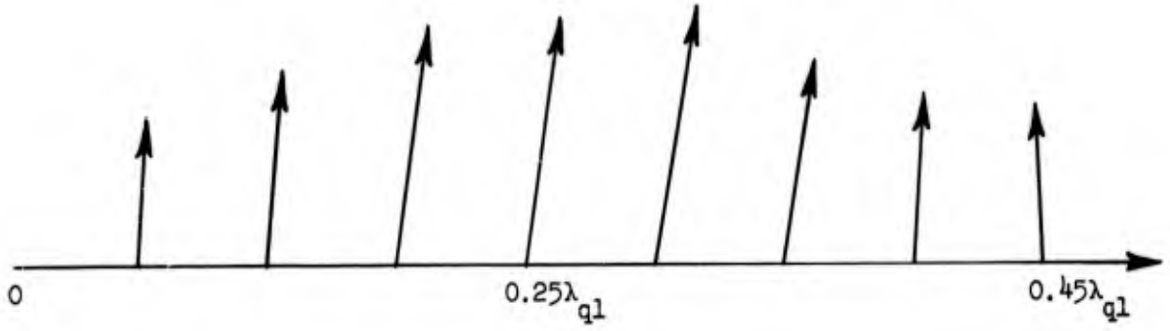

$|m| = 0.6$

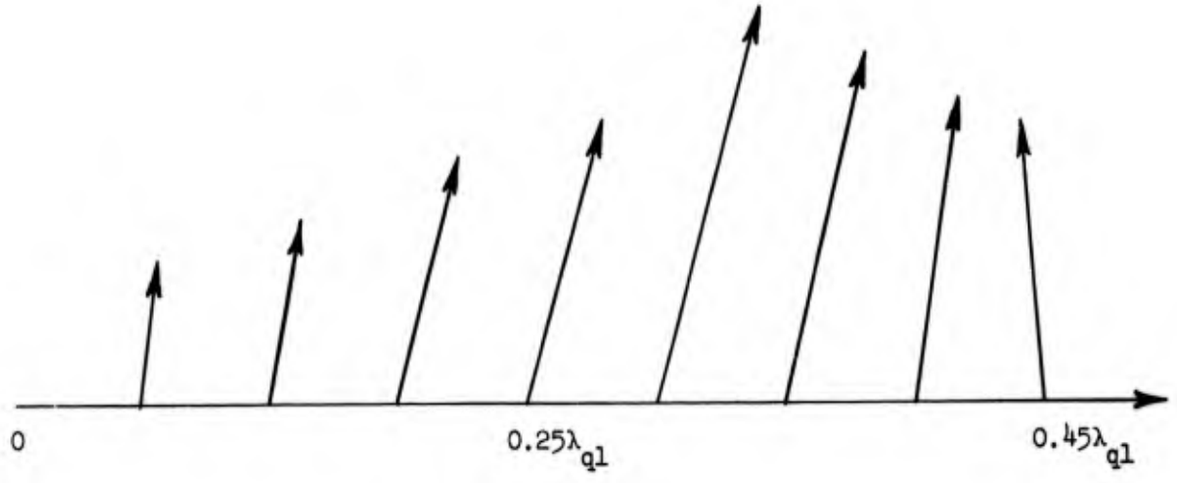

$|m| = 0.92$

FIG. II.7--Current density at the signal frequency as a function of the length of the drift space, for different amplitudes of the pump.

Pump Amplitude $\|m\|$	$k_1 L$ / L		0	$0.10\lambda_{q1}$	$0.15\lambda_{q1}$	$0.20\lambda_1$	$0.25\lambda_{q1}$	$0.30\lambda_{q1}$	$0.35\lambda_{q1}$	$0.40\lambda_{q1}$	$0.45\lambda_{q1}$
$\|m\| = 4 \times 10^{-2}$	Wave no.	1	$5 \times 10^{-6} \angle 0°$	$5 \times 10^{-6} \angle 117°$	$5 \times 10^{-6} \angle 174°$	$5 \times 10^{-6} \angle 233°$	$5 \times 10^{-6} \angle 291°$	$5 \times 10^{-6} \angle 349°$	$5 \times 10^{-6} \angle 410°$	$5 \times 10^{-6} \angle 467°$	$5 \times 10^{-6} \angle 525°$
		2	$0.29 \angle 180°$	$0.29 \angle 144°$	$0.29 \angle 126°$	$0.29 \angle 108°$	$0.29 \angle 90°$	$0.29 \angle 72°$	$0.29 \angle 54°$	$0.29 \angle 36°$	$0.29 \angle 18°$
		3	$0.29 \angle 0°$	$0.29 \angle 36°$	$0.29 \angle 54°$	$0.29 \angle 72°$	$0.29 \angle 90°$	$0.29 \angle 108°$	$0.29 \angle 126°$	$0.29 \angle 104°$	$0.29 \angle 162°$
		4	$2 \times 10^{-4} \angle 180°$	$2 \times 10^{-4} \angle 189°$	$2 \times 10^{-4} \angle 193°$	$2 \times 10^{-4} \angle 198°$	$2 \times 10^{-4} \angle 202°$	$2 \times 10^{-4} \angle 206°$	$2 \times 10^{-4} \angle 211°$	$2 \times 10^{-4} \angle 216°$	$2.10^{-4} \angle 220°$
	I_t Total current density		$0 \angle$	$0.34 \angle 90°$	$0.47 \angle 90°$	$0.55 \angle 90°$	$0.58 \angle 90°$	$0.55 \angle 90°$	$0.47 \angle 90°$	$0.34 \angle 90°$	$0.18 \angle 90°$
$\|m\| = 0.6$	Wave no.	1	$10^{-3} \angle 0°$	$10^{-3} \angle 117°$	$10^{-3} \angle 175°$	$10^{-3} \angle 233°$	$10^{-3} \angle 292°$	$10^{-3} \angle 350°$	$10^{-3} \angle 409°$	$10^{-3} \angle 468°$	$10^{-3} \angle 526°$
		2	$0.305 \angle 180°$	$0.305 \angle 143°$	$0.305 \angle 124°$	$0.305 \angle 106°$	$0.305 \angle 87°$	$0.305 \angle 68°$	$0.305 \angle 50°$	$0.305 \angle 31°$	$0.305 \angle 13°$
		3	$0.217 \angle 314°$	$0.187 \angle 337°$	$0.173 \angle 349°$	$0.161 \angle 0°$	$0.149 \angle 12°$	$0.138 \angle 23°$	$0.128 \angle 35°$	$0.119 \angle 46°$	$0.110 \angle 57°$
		4	$0.217 \angle 46°$	$0.252 \angle 69°$	$0.272 \angle 80°$	$0.293 \angle 91°$	$0.316 \angle 103°$	$0.341 \angle 114°$	$0.367 \angle 126°$	$0.396 \angle 137°$	$0.427 \angle 149°$
	I_t Total current density		$0 \angle$	$0.35 \angle 87°$	$0.49 \angle 85°$	$0.59 \angle 83°$	$0.65 \angle 82°$	$0.66 \angle 81°$	$0.61 \angle 82°$	$0.52 \angle 85°$	$0.38 \angle 91°$
$\|m\| = 0.92$	Wave no.	1	$2 \times 10^{-3} \angle 0°$	$2 \times 10^{-3} \angle 117°$	$2 \times 10^{-3} \angle 176°$	$2 \times 10^{-3} \angle 235°$	$2 \times 10^{-3} \angle 293°$	$2 \times 10^{-3} \angle 352°$	$2 \times 10^{-3} \angle 411°$	$2 \times 10^{-3} \angle 469°$	$2 \times 10^{-3} \angle 528°$
		2	$0.32 \angle 180°$	$0.32 \angle 141°$	$0.32 \angle 122°$	$0.32 \angle 103°$	$0.32 \angle 84°$	$0.32 \angle 64°$	$0.32 \angle 45°$	$0.32 \angle 26°$	$0.32 \angle 7°$
		3	$0.162 \angle 350°$	$0.115 \angle 13°$	$0.10 \angle 25°$	$0.08 \angle 37°$	$0.07 \angle 48°$	$0.06 \angle 60°$	$0.05 \angle 72°$	$0.04 \angle 83°$	$0.03 \angle 94°$
		4	$0.162 \angle 10°$	$0.230 \angle 34°$	$0.274 \angle 45°$	$0.326 \angle 57°$	$0.388 \angle 69°$	$0.462 \angle 80°$	$0.55 \angle 92°$	$0.64 \angle 103°$	$0.78 \angle 115°$
	I_t Total current density		$0 \angle$	$0.36 \angle 83°$	$0.52 \angle 78°$	$0.66 \angle 75°$	$0.76 \angle 73°$	$0.83 \angle 73°$	$0.86 \angle 75°$	$0.83 \angle 80°$	$0.78 \angle 91°$

FIG. II.8--Amplitude and phase of the four space-charge waves for different values of L (L = distance between the two gaps).

$$\frac{1}{\nu} = \frac{\omega_2}{\omega_1} = 2.0$$

$$k_1 b = 1.0$$

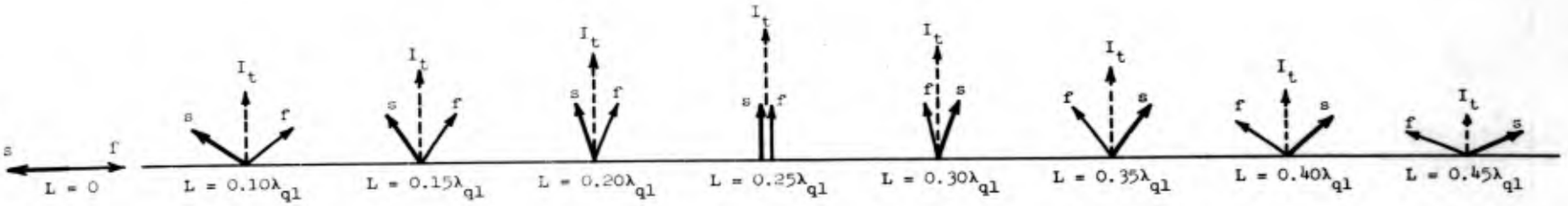

No Parametric Pumping: f refers to the fast space-charge wave.
s refers to the slow space-charge wave.

(a) No Parametric Pumping

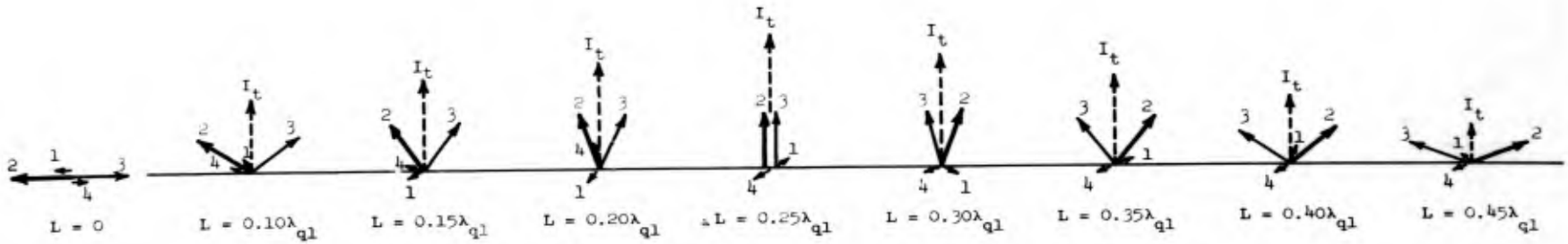

The numbers 1, 2, 3, 4 identify the four waves, λ_{ql} is the reduced plasma wavelength at the signal frequency, and I_t is the total current density at the signal frequency.

(Waves 1 and 4 are not drawn to scale.)

(b) Low Pump Power m = 0.04

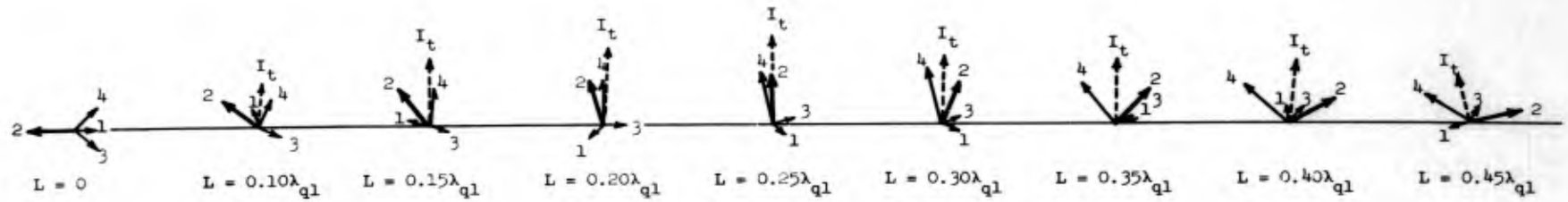

(Wave 1 is not drawn to scale.)

(c) m = 0.60

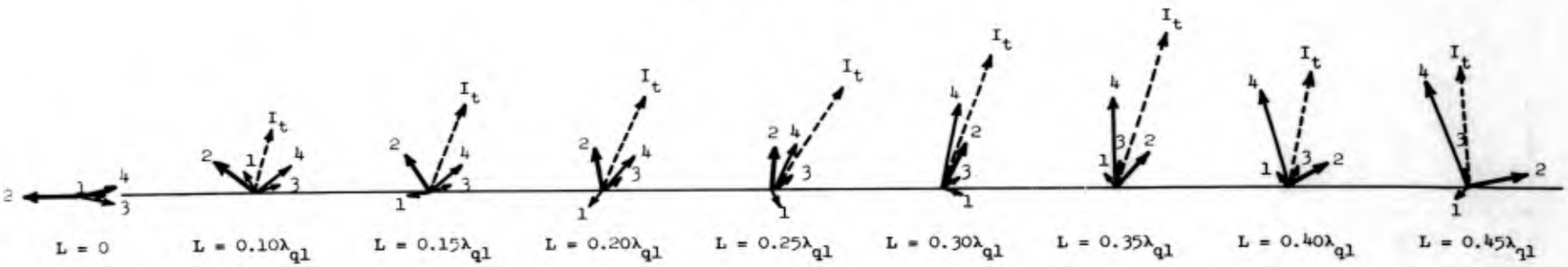

(Wave 1 is not drawn to scale.)

(d) m = 0.90

FIG. II.9--Phasor representation of the four current waves.

V_0 is the dc potential of the cavity

$F(z)$ is the normalized longitudinal electric field.

It is assumed that the electric field in the cavity varies as

$$E_1(z) = AV_0 \frac{\sqrt{2}}{L} \cos \frac{n\pi}{L} z \ , \tag{II.67}$$

where L is the length of the cavity in meters, and

n is the length of the cavity in half-circuit wavelength.

The voltage "across" the cavity is defined by the following equation:

$$V_1^2 = L \int_0^L E_1(z) E_1^*(z) \, dz \ . \tag{II.68}$$

This definition coincides with the usual one

$$V = \int_0^L \vec{E}(z) \cdot \vec{dz} \ , \tag{II.69}$$

when the electric field is a constant. Using Eq. (II.67) the square of the voltage becomes

$$V_1^2 = \frac{2}{L^2} A^2 V_0^2 \int_0^L \cos^2 \frac{n\pi z}{L} \, dz = A^2 V_0^2 \ . \tag{II.70}$$

Let P_1 be the time average of the complex power flow between the beam and the cavity at the signal frequency

$$P_1 = \frac{1}{2} \int_0^L I_1(z) E_1^*(z) \, dz \ . \tag{II.71}$$

With these definitions, the beam-loading admittance is

$$Y_1 = \frac{2P_1}{V_1^2} \ . \tag{II.72}$$

If the real part of Y_1 is positive, the cavity delivers energy to the beam, and if it is negative, the beam delivers energy to the circuit.

Equations (II.70) and (II.72) yield

$$Y_1 = \frac{2P_1}{A^2 V_0^2} . \qquad \text{(II.73)}$$

It is helpful, furthermore, to normalize the beam-loading admittance to the beam admittance $G_0 = I_0/V_0$; then

$$\frac{Y_1}{G_0} = \frac{2P}{A^2 V_0 I_0} . \qquad \text{(II.74)}$$

2. Calculation of the Beam-Loading Admittance.

This calculation will be made in two steps:

(1) calculation of the current, at the signal frequency, in the cavity, and

(2) computation of the complex power flow.

In the calculation of the current density at the signal frequency, the current will be obtained by solving Eq. (II.56):

$$\frac{d^4}{dz^4} i_1(z) + 2j\,(\alpha_3 k_1)\left(1 - \frac{1}{\nu}\right)\frac{d^3 i_1(z)}{dz^3} + \frac{(k_1\alpha_3)^2}{\nu}\left\{4 - \frac{1}{2}|m|^2 - \left[\left(1 - \frac{1}{a_2^2}\right)\frac{1}{\nu} + \nu\left(1 - \frac{1}{a_1^2}\right)\right]\right\}\frac{d^2 i_1(z)}{dz^2} + 2j\,\frac{(k_1\alpha_3)^3}{\nu^2}\left\{1 - \frac{|m|^2}{4} - \frac{1}{a_1^2}\left(1 + \frac{|m|^2}{4}\right) - \frac{1}{\nu}\left[1 - \frac{|m|^2}{4} - \frac{1}{a_2^2}\left(1 + \frac{|m|^2}{4}\right)\right]\right\}\frac{di_1(z)}{dz} + \frac{(k_1\alpha_3)^4}{\nu^2}\left[1 - \frac{|m|^2}{2} + \frac{|m|^4}{16} - \left(\frac{1}{a_1^2} + \frac{1}{a_2^2}\right)\left(1 + \frac{3}{4}|m|^2\right) + \frac{1}{a_1^2 a_2^2}\left(1 - \frac{|m|^2}{4}\right)\right] i_1(z)$$

$$= \frac{k_1 I_0}{2V_0}\left\{ j\frac{d^2}{dz^2} + 2\frac{(\alpha_3 k_1)}{\nu}\left(1 + \frac{|m|^2}{4}\right)\frac{d}{dz} - j\frac{(k_1\alpha_3)^2}{\nu^2}\left[1 - \frac{1}{a_2^2} \times \left(1 - \frac{|m|^2}{4}\right) + \frac{3}{4}|m|^2\right]\right\} E_1(z) \exp\left[+ jk_1(1 - \alpha_3)\, z\right] \qquad \text{(II.75)}$$

This equation will be solved by using the Laplace transform method which takes the boundary conditions directly into account.

It is assumed that there is no initial current and no initial velocity at the signal and idler frequencies. This statement is expressed mathematically by the following equations:

$$\left.\begin{aligned} I_1\,(z=0) &= 0\,, \\ I_2^*\,(z=0) &= 0\,, \\ \frac{dI_1}{dz}\,(z=0) &= 0\,, \\ \frac{dI_2^*}{dz}\,(z=0) &= 0\,, \end{aligned}\right\} \qquad \text{(II.76)}$$

where the plane $z = 0$ is the input plane.

The lengthy but straightforward algebra is carried out in Appendix II.D. It is found that the current density at the signal frequency is given by

$$I_1(z) = \frac{jA\sqrt{2}}{2L}\,\frac{I_0}{k_1}\sum_{(n)}\left\{\begin{aligned} &K^{(n)}\,\exp\left[j(\alpha_3 w^{(n)} - 1 + \alpha_3)\,k_1 z\right] \\ &- G^{(n+)}\,\exp\,(+\,jyk_1 z) - G^{(n-)}\,\exp\,(-\,jyk_1 z)\end{aligned}\right\}$$
$$(n) = 1,2,3,4\,. \qquad \text{(II.77)}$$

where $w^{(n)}$, $K^{(n)}$, $G^{(n+)}$ and $G^{(n-)}$ are given in Appendix II.D.

The complex power flow between the cavity and the beam can easily be calculated from Eq. (II.74), as both the electric field $E_1(z)$ and the current density $I_1(z)$ are known.

The beam-loading admittance defined by Eq. (II.74) can easily be

calculated, and it is found that

$$\frac{Y}{G_0} = j \frac{1}{2k_1^2 L^2} \sum_{(n)} \left\{ \begin{array}{l} P^{(n+)} \left[\exp \left[j(\alpha_3 w^{(n)} - 1 + \alpha_3 + y) \, Lk_1 \right] - 1 \right] \\ + P^{(n-)} \left[\exp \left[j(\alpha_3 w^{(n)} - 1 + \alpha_3 - y) \, Lk_1 \right] - 1 \right] \\ - Lk_1 Q^{(n)} \end{array} \right\}$$

$$(n) = 1,2,3,4$$

$$G_0 = I_0/V_0 \quad \text{beam admittance} \qquad \text{(II.78)}$$

where

$$\left. \begin{array}{l} P^{(n+)} = \dfrac{K^{(n)}}{j[\alpha_3 w^{(n)} - 1 + \alpha_3 + y]} \\ P^{(n-)} = \dfrac{K^{(n)}}{j[\alpha_3 w^{(n)} - 1 + \alpha_3 - y]} \\ Q^{(n)} = G^{(n+)} + G^{(n-)} \end{array} \right\} \qquad \text{(II.79)}$$

The beam-loading admittance is the sum of four terms. Each term corresponds to one of the four space-charge waves. The situation is identical to the nonparametric case where the total beam-loading admittance is the sum of two terms: one corresponds to the fast space-charge wave, the other to the slow space-charge wave. The fast space-charge wave which carries positive power gives rise to a positive beam-loading conductance; the slow space-charge wave which carries negative power creates a negative beam-loading conductance. The sign of the total beam-loading conductance depends on the amount of coupling to each wave. If the coupling is primarily to the fast wave, it is positive, and if it is primarily to the slow wave, it is negative.

For the parametric case there exist four waves, and the sign of the beam-loading admittance depends on the amount of coupling to each wave. Numerical calculations were made for a cavity designed to couple only to the unperturbed fast wave.

3. Discussion of the Results.

The beam-loading admittance was calculated from Eq. (II.78) with an IBM 650 and a Burroughs 220 digital computer.

Five normalized parameters are necessary to define the problem; these are:

(1) $\nu = \omega_1/\omega_2$, the ratio of the signal to the idler frequency,

(2) $|m|^2$, the amplitude of the pump signal,

(3) n , the length of the cavity in half-circuit wavelength,

(4) $1/y = u_0/v_{ph}$, the ratio of the dc velocity of the electrons to the phase velocity of the circuit,

(5) $k_1 b$, where b is the beam radius and $k_1 = \omega_1/u_0$.

The real and imaginary parts of the normalized beam-loading admittance Y/G_0 can be calculated for different values of the parameters. If three of the parameters are held constant, the real and imaginary part of the admittance can be plotted as a function of a fourth parameter for different values of the last unused parameter.

a. Beam-loading admittance as a function of $\nu = \omega_1/\omega_2$.

The normalized beam radius, the normalized phase velocity of the circuit and the length of the cavity are held constant. The beam-loading admittance can be plotted as a function of $\nu = \omega_1/\omega_2$ for different values of the pump power.

For very small pump power, the admittance must be equal to the values found in the nonparametric case, and its value should be independent of the parameter ν .

Figures II.10 and II.11 give the beam-loading conductance and susceptance as a function of ν for the following values of the parameters:

$$n = 4$$

$$y = 0.75$$

$$k_1 b = 1 .$$

For a small pump power ($|m|^2 = 1.6 \times 10^{-4}$) the conductance and susceptance are independent of ν and their value is the same as the ones found by Wessel-Berg. If the pump strength is increased to $|m|^2 = 0.84$, both the real and imaginary part of the beam-loading admittance vary with ν .

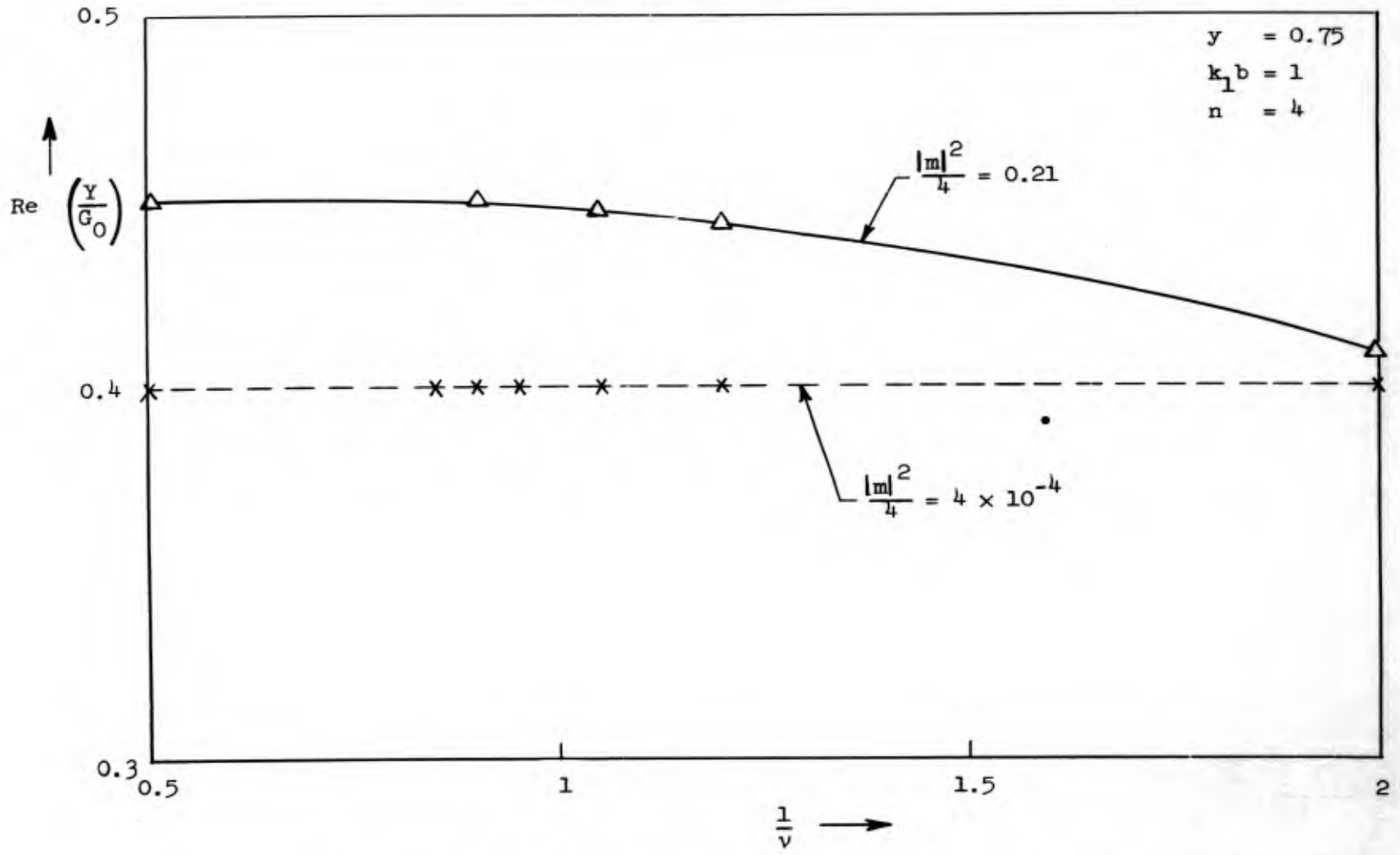

FIG. II.10--Beam-loading conductance versus frequency $1/\nu = \omega_2/\omega_1$.

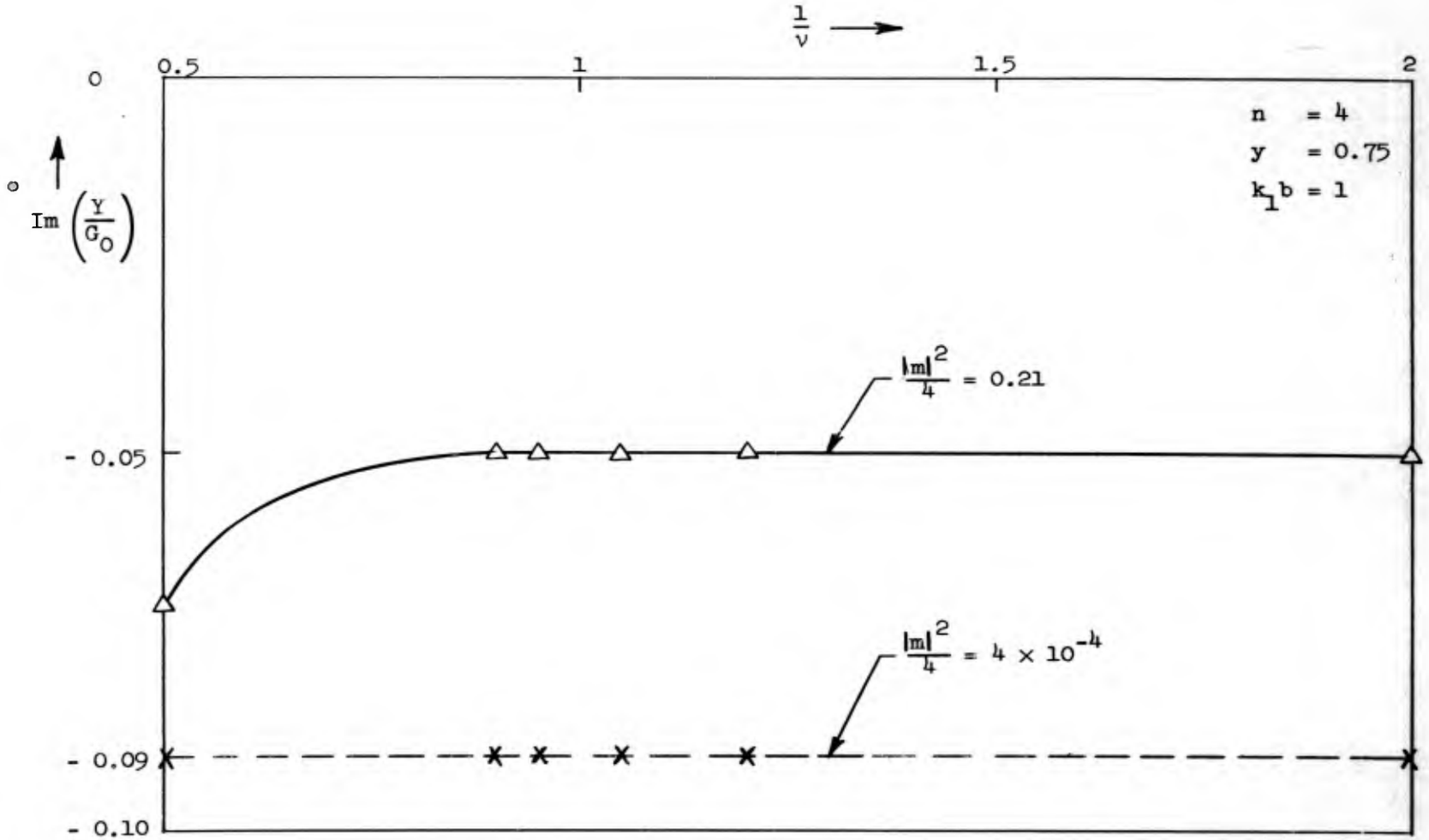

FIG. II.11--Beam-loading susceptance versus frequency $1/\nu = \omega_2/\omega_1$.

b. Beam-loading admittance as a function of n length of the cavity; the quantities ν, $|m|^2$, y and $k_1 b$ are held constant. The following values of the parameters have been chosen:

$$\nu = 0.95$$

$$|m|^2 = 1.6 \times 10^{-3}$$

$$y = 1$$

$$k_1 b = 10^{-3} \quad \text{(thin beam)}.$$

The beam-loading admittance has been plotted as a function of the length n of the cavity, Figs. II.12 and II.13. The small value of $|m|^2$ was chosen in order to check that the beam-loading obtained was the same as the one obtained by Wessel-Berg in the nonparametric case. It was found that for the very small value of $|m|^2$ used this was true.

c. Beam-loading admittance as a function of $y = u_0/v_{ph}$.

The ratio $\nu = \omega_1/\omega_2$ of the signal to the idler frequency, the length of the cavity n, and the beam dimension $k_1 b$ are held constant; the beam-loading is plotted against y for different values of $|m|^2$.

These curves can easily be compared to Wessel-Berg's, as his parameter ϵ is related to y by

$$\epsilon = 1 - \frac{1}{y}.$$

It is found that for small values of $|m|^2$ the values of the beam-loading admittance check extremely well with the values obtained for the nonparametric case. The beam-loading conductance is positive (as should be expected because the cavity couples only to the unperturbed fast space-charge wave) except for the values of y which give zero conductance in the nonparametric case.

For small values of n, relatively short cavities, the effect of the parametric pumping remains small even for large values of the pump power (Figs. II.14 and II.15).

Parametric pumping creates four waves propagating as $\exp[j\Gamma^{(n)}z]$. Two waves always have a real Γ and the two others may have real or

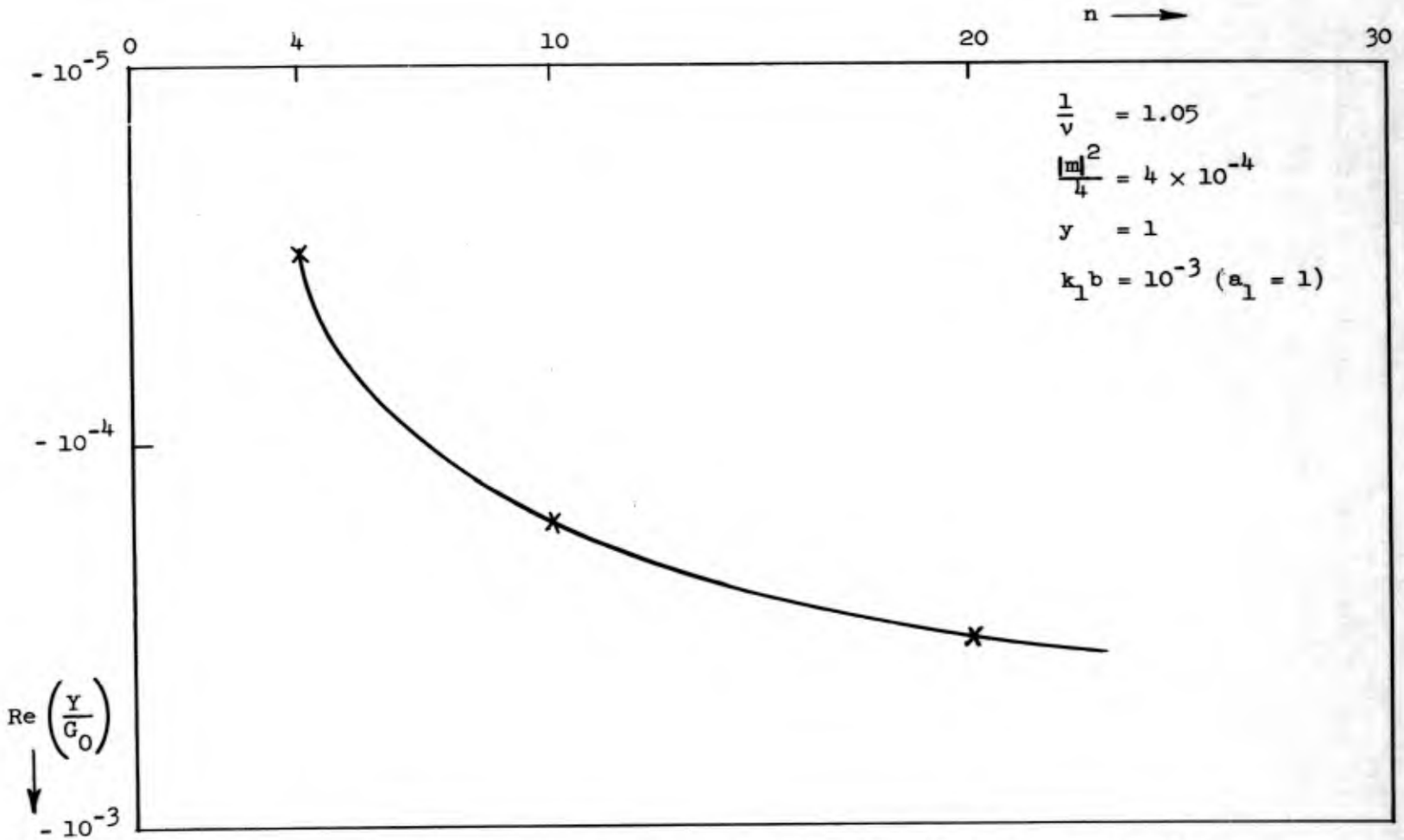

FIG. II.12--Beam-loading conductance versus length of the cavity (n).

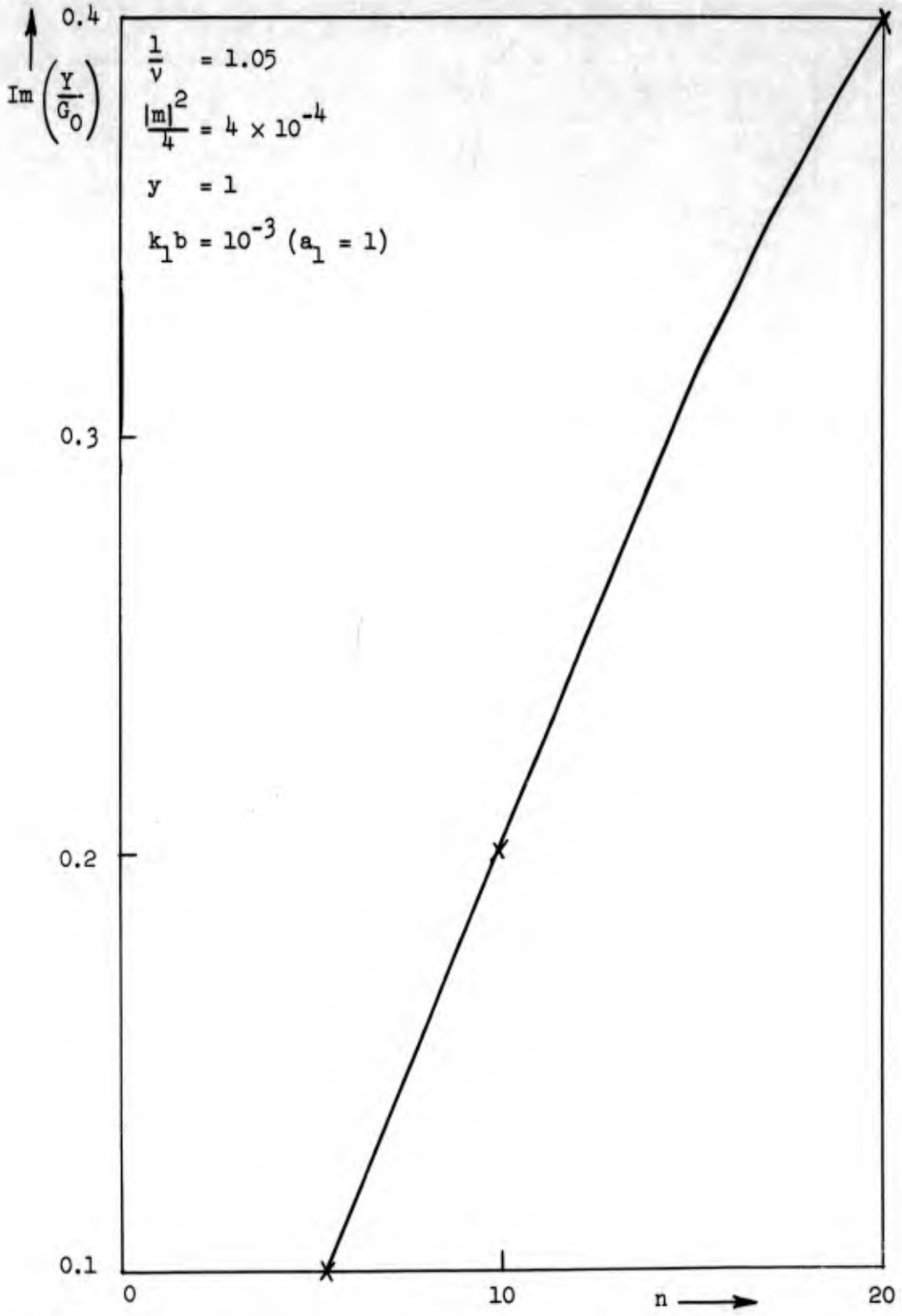

FIG. II.13--Beam-loading susceptance versus length of the cavity (n).

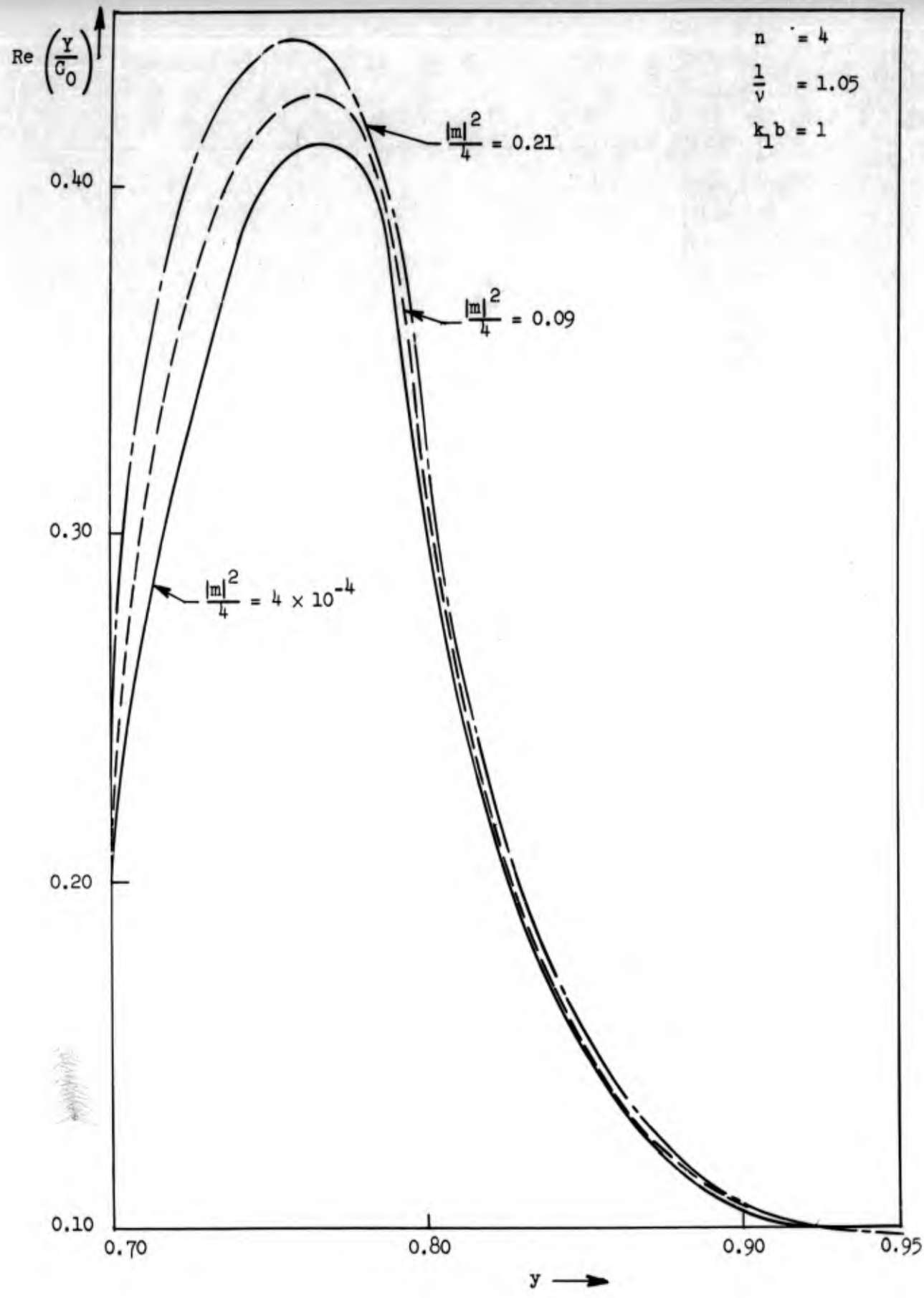

FIG. II.14--Beam-loading conductance versus circuit phase velocity (y).

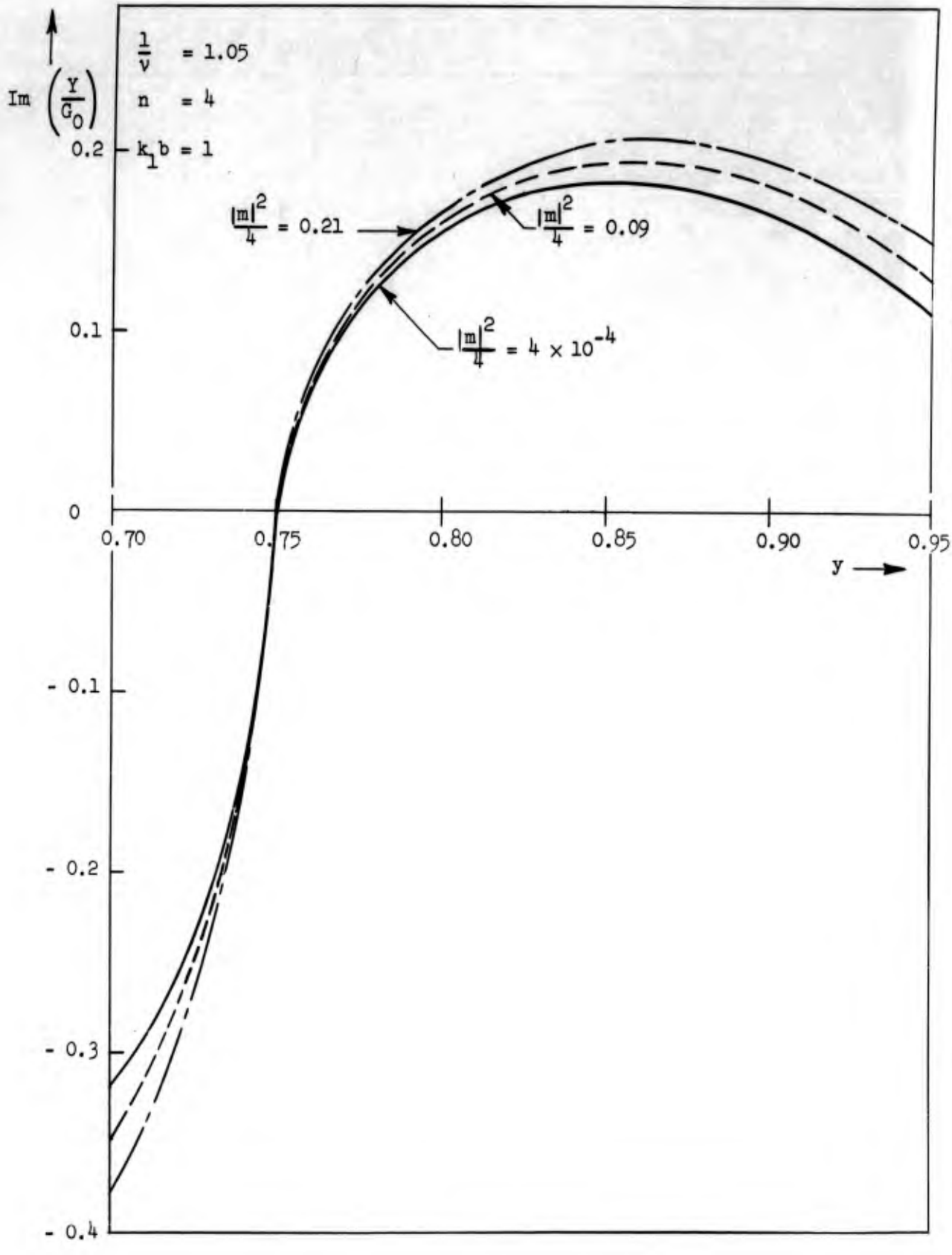

FIG. II.15--Beam-loading susceptance versus circuit phase velocity (y).

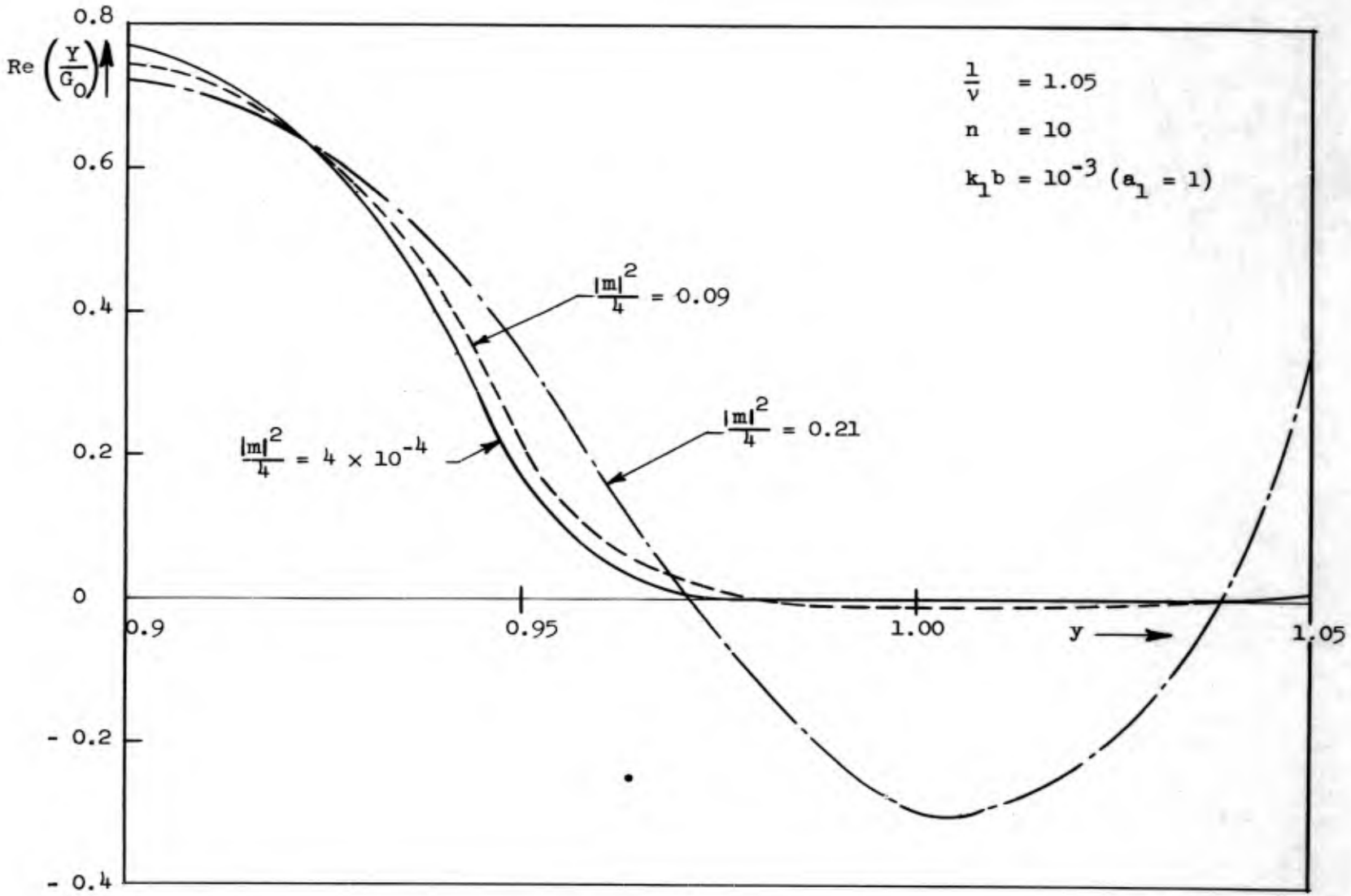

FIG. II.16--Beam-loading conductance versus circuit phase velocity (y)

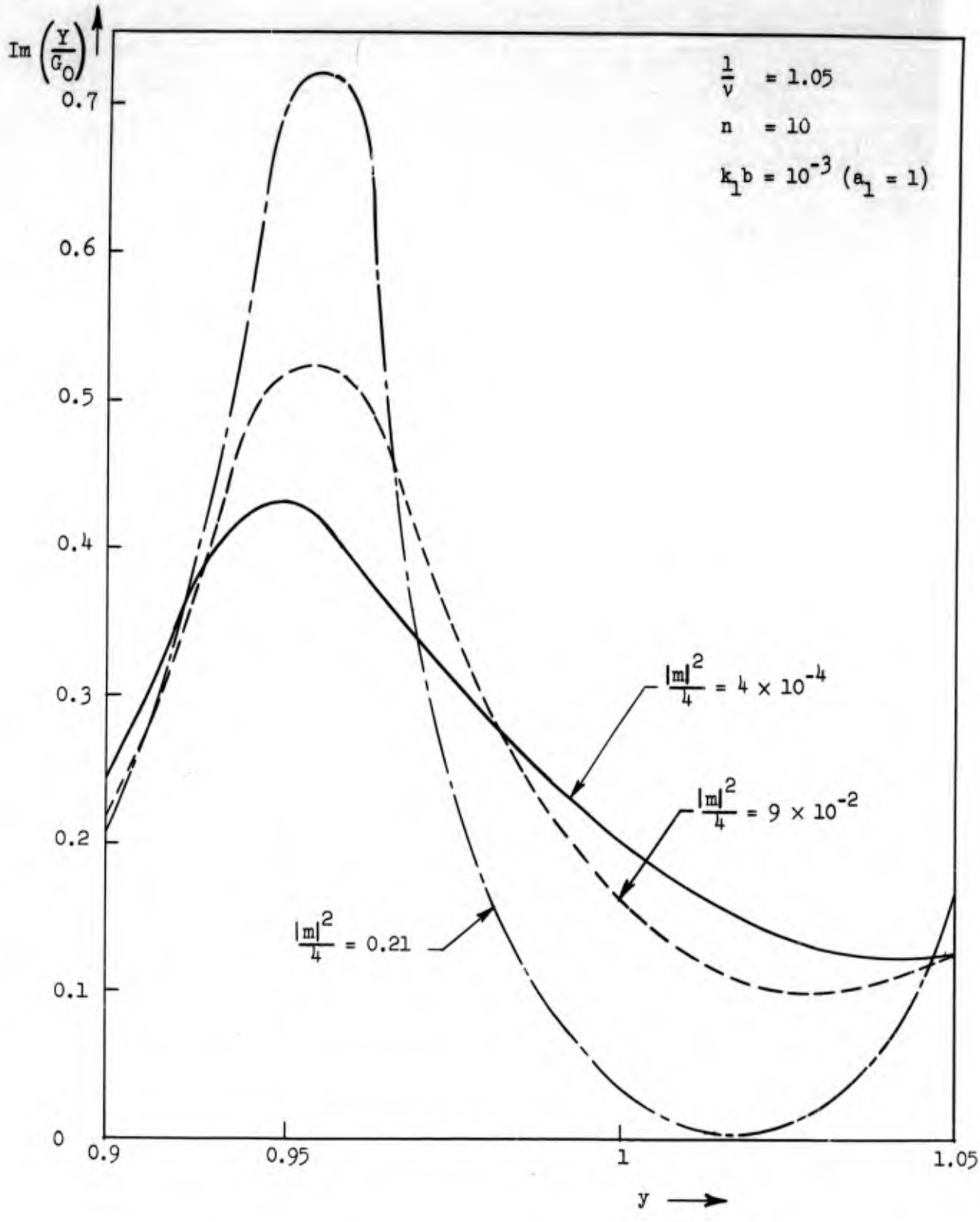

FIG. II.17--Beam-loading susceptance versus circuit phase velocity (y).

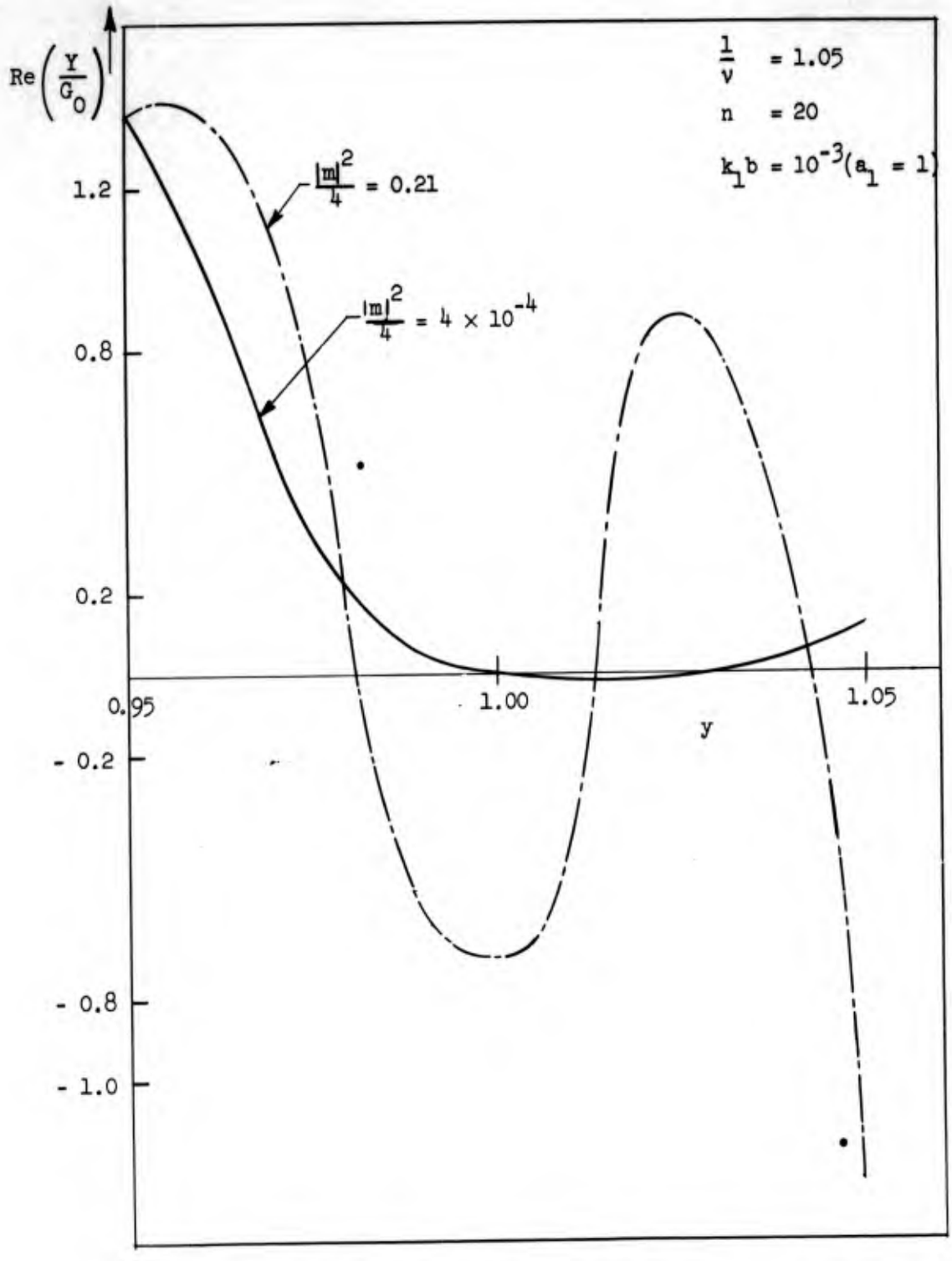

FIG. II.18--Beam-loading conductance versus circuit phase velocity (y).

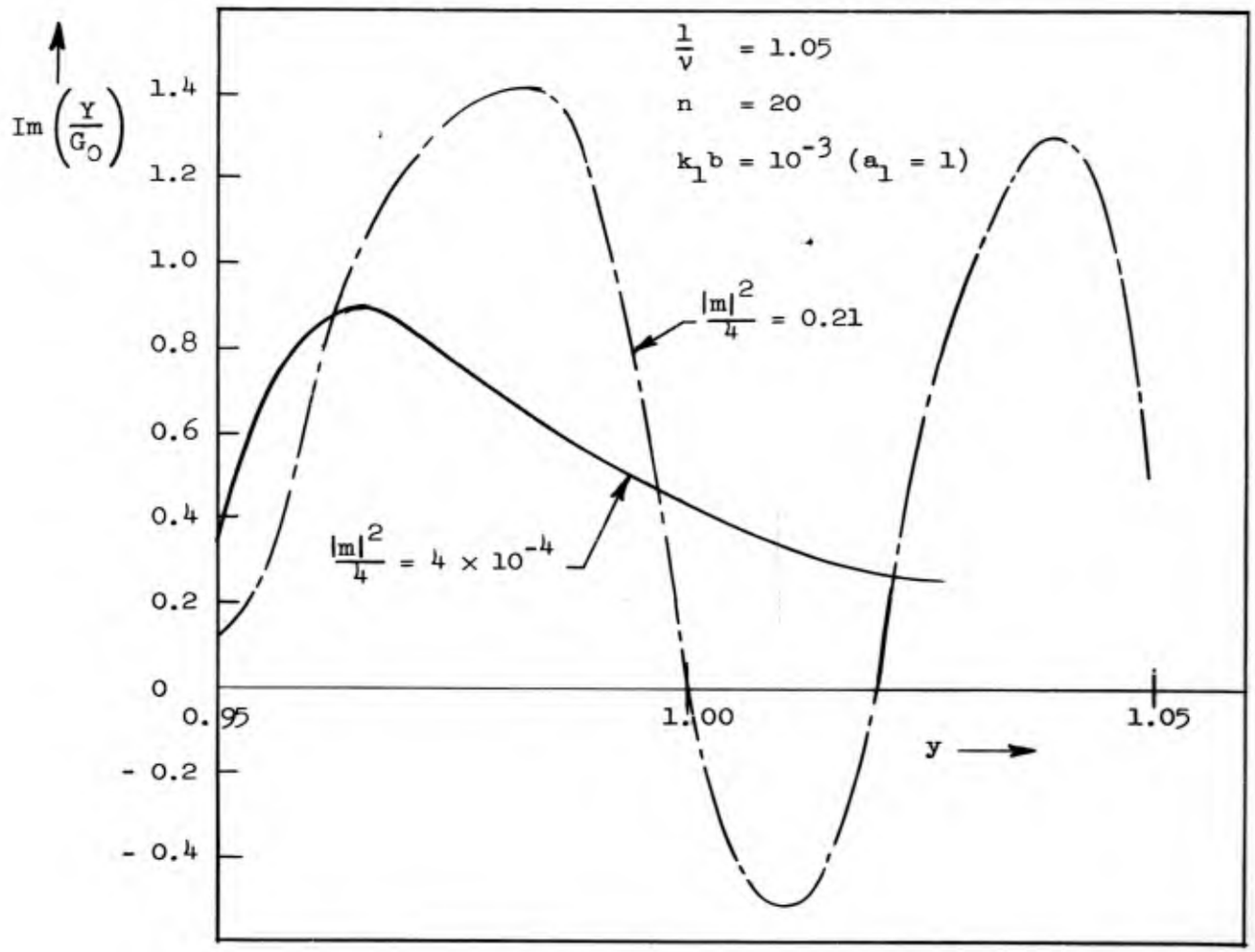

FIG. II.19--Beam-loading susceptance versus circuit phase velocity (y).

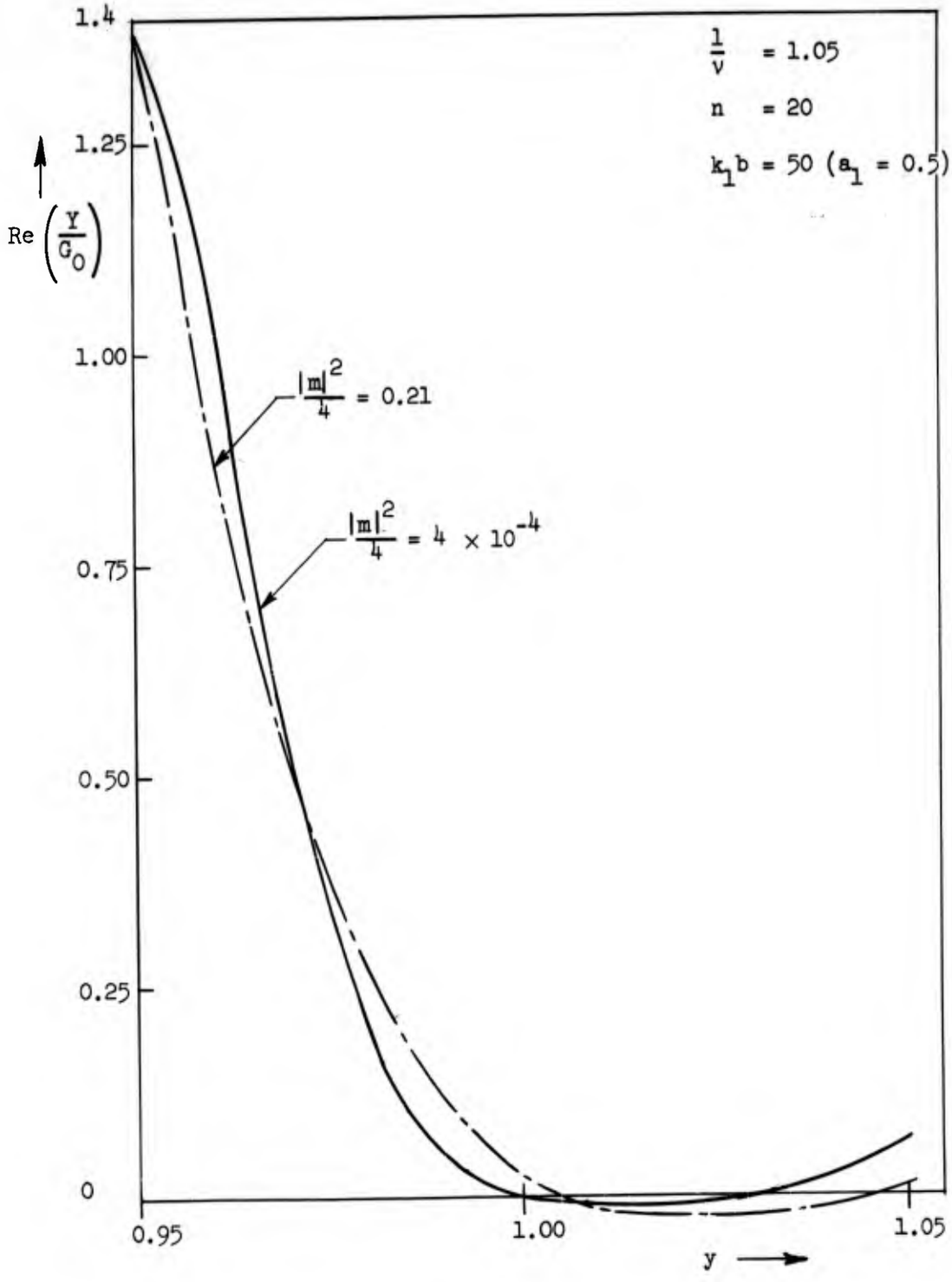

FIG. II.20--Beam-loading conductance versus circuit phase velocity (y).

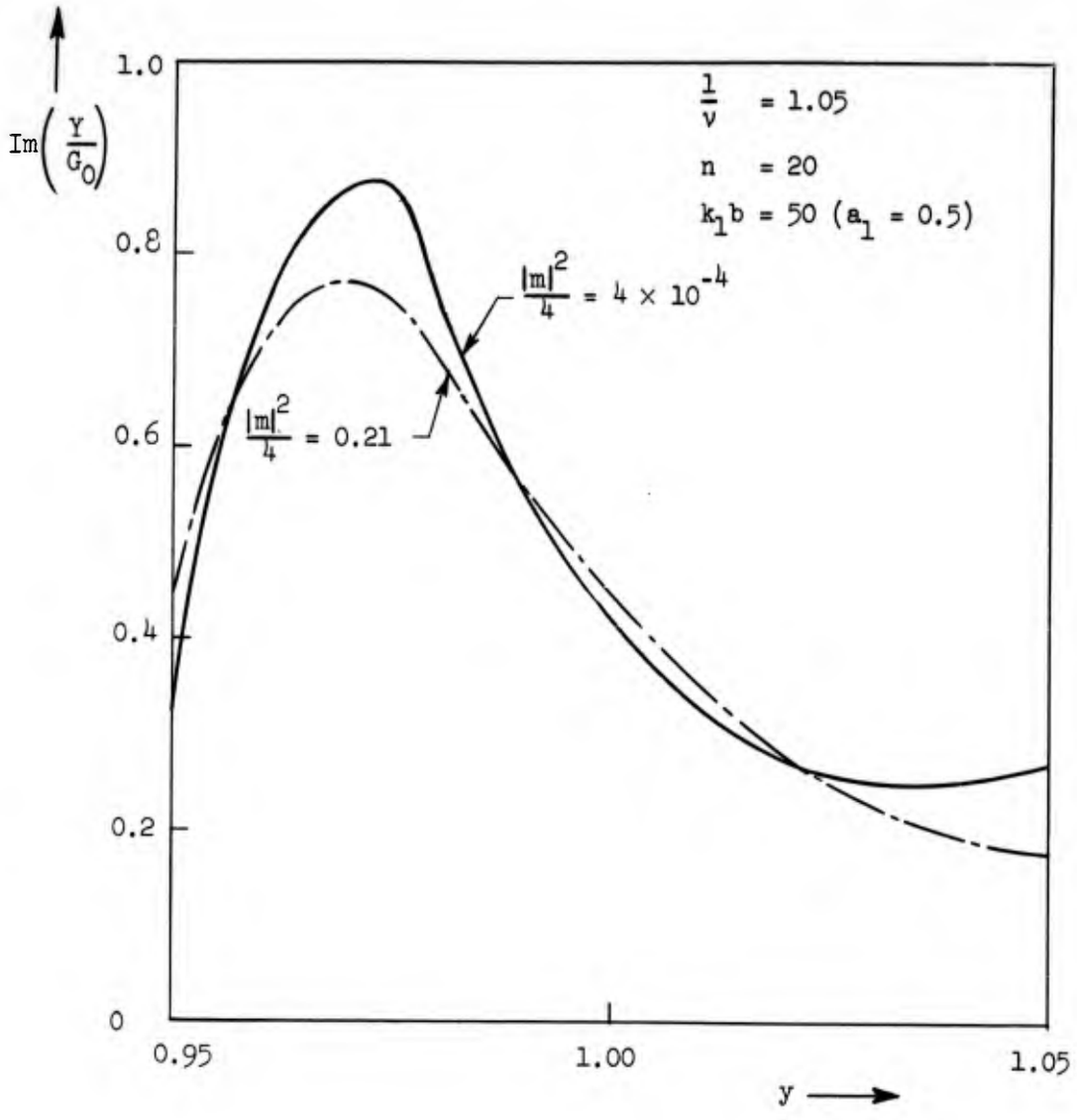

FIG. II.21--Beam-loading susceptance versus circuit phase velocity (y).

complex propagation constants. In either case, if the cavity is short, the parametric effect cannot become very large.

When the length of the cavity increases, as for example, when $n = 10$ (Figs. II.16 and II.17), the difference between the beam-loading admittance for small and large values of $|m|^2$ increases. In the case where $1/\nu = 1.05$, $n = 10$, $k_1 b = 10^{-3}$ a large negative value of the beam-loading conductance can be obtained for $y = 1$. It should be noticed that the parametric effect on the conductance which is a second order effect becomes large only in a region where the beam-loading conductance in the absence of parametric pumping is small. It corresponds too, to a region where the coupling coefficient is small.

For large values of n ($n = 20$ for example) a large effect of the pumping may be noticed in Figs. II.18 and II.19 and a very small change in the beam loading exists in Figs. II.20 and II.21. The difference is due to the fact that for a thin beam ($k_1 b = 10^{-3}$) two of the waves are growing and decaying waves, whereas in the thick beam ($k_1 b = 50$) the propagation constants of the four waves are real. The change in phase velocity of the waves due to parametric pumping is not large enough to create a substantial change in the beam loading, even though the beam-loading conductance becomes slightly negative (Fig. II.20).

For the thin beam (Fig. II.18) there exists a large change in the beam-loading conductance, due to the presence of the growing and decaying wave.

A cavity can be built with the following parameters (Figs. II.18 and II.19):

$$\nu = 0.95$$

$$n = 20$$

$$k_1 b = 10^{-3}$$

$$y = 1$$

For these values the beam-loading conductance is $R_e\,(Y/G_0) \simeq -0.75$ and the imaginary part is $I_m\,(Y/G_0) \simeq 0$. The large negative beam-loading conductance is the basis of the amplifying device and the zero beam-loading susceptance means that there will be no detuning due to the presence of the beam. It should be noted that a large number of approxi-

mations have been made in the derivation of this result and that the results of the calculations are only an approximation.

It was shown that the beam-loading admittance can be written as the sum of four terms:

$$\frac{Y}{G_0} = \sum_{(n)}^{\bullet} \frac{Y^{(n)}}{G_0} ,$$

where $Y^{(n)}/G_0$ represents the contribution to the total beam loading due to the n th wave. The four waves, corresponding to the homogeneous solution of Eq. (II.56), propagate as

$$\exp [- jk_1 (1 - \alpha_1 a_1) z] \exp [jw^{(n)} k_{q1} z] .$$

where the $w^{(n)}$ are the roots of Eq. (II.C.9). A numerical example is used to illustrate the distribution of the total beam-loading conductance among the different waves. Consider the case where

$$\nu = 0.95$$

$$k_1 b = 10^{-3}$$

$$n = 20 .$$

The $w^{(n)}$ can be calculated for different values of $|m|^2$:

wave no.	$\|m\|^2 = 16 \times 10^{-4}$	$\|m\|^2 = 0.84$
1	2.1	2.1
2	- 2.0	2.0
3	$j\ 0.03 - 1.6 \times 10^{-5}$	$j\ 0.69 + 4 \times 10^{-4}$
4	$-j\ 0.03 - 1.6 \times 10^{-5}$	$-j\ 0.69 + 4 \times 10^{-4}$

The waves numbered 1 and 2 correspond to what Louisell[7] has called the slow modes, and the numerical values agree with the ones he found.

The components of the beam loading corresponding to these waves for different values of $y = u_0/v_{ph}$ are shown in the following table (where only the real part is tabulated):

		values of $y = u_0/v_{ph}$		
	wave no.	0.95	0.97	1.0
$\|m\|^2 = 16 \times 10^{-4}$	1	2×10^{-6}	3×10^{-6}	5×10^{-6}
	2	0	0	0
	3	277.2	79.06	21.280
	4	- 275.9	- 78.51	- 21.282
$\|m\|^2 = 0.84$	1	7×10^{-4}	1.4×10^{-3}	2×10^{-4}
	2	$- 3 \times 10^{-5}$	$- 5 \times 10^{-6}$	$- 8 \times 10^{-5}$
	3	11.24	3.19	0.831
	4	- 9.85	- 2.149	- 1.54

The beam-loading conductance corresponding to the slow modes (waves 1 and 2) is extremely small; this confirms the assumptions of Louisell, who stated that the pump had very little effect on these waves because their phase velocities are different from the phase velocities of the fast modes (waves 3 and 4). The fast waves are extremely sensitive to the pump power, and their action is the important phenomenon in the parametric pumping. Wave 3 , corresponding to a decaying wave, gives a positive beam-loading conductance and can be said to carry positive power. The fourth wave gives a negative beam-loading conductance. It is mainly the amount of coupling to each of the fast modes which determines the sign of the beam loading. Stronger interaction with wave 4 for $y = 1$ creates the negative conductance $\mathrm{Re}\,(Y/G_0) \simeq - 0.7$ which will be used for parametric amplification. As was stated previously, this wave is obtained by making the sum of the contributions from each wave

$$\mathrm{Re}\left(\frac{Y}{G_0}\ \text{total}\right) = \sum_n \mathrm{Re}\left[\frac{Y^{(n)}}{G_0}\right] \simeq - 0.7$$

CHAPTER IX

TENTATIVE DESIGN OF THE SPACE-CHARGE WAVE PARAMETRIC AMPLIFIER

Parametric pumping creates, under certain conditions, a negative beam-loading conductance in a long-interaction klystron cavity. If this cavity is used with a circulator (Fig. II.22) any signal applied to arm No. 1 is fed into the cavity and any signal coming out of the cavity is directed toward the load (arm No. 2).

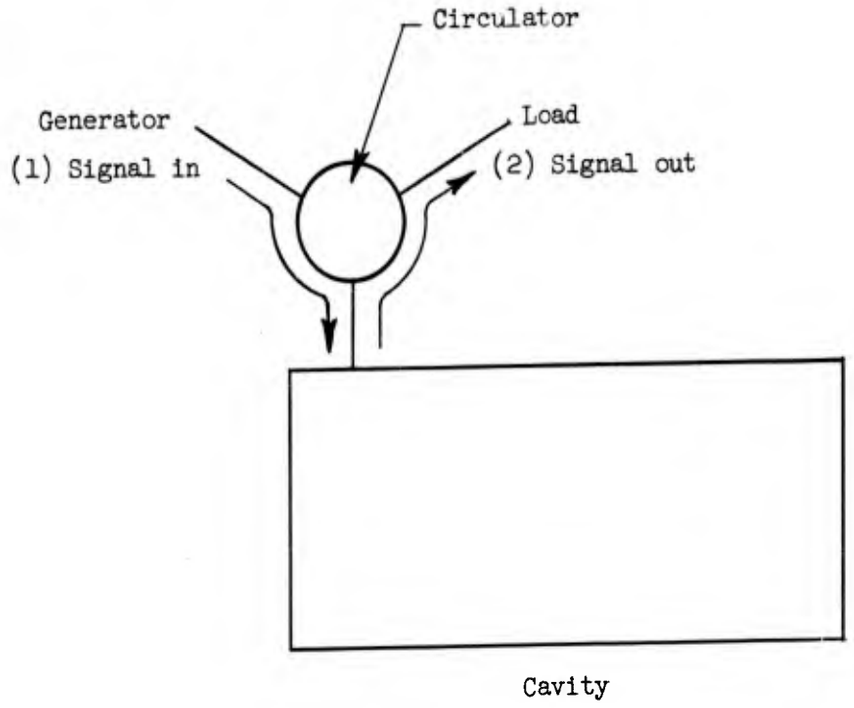

FIG. II.22--Input-output cavity.

An approximate equivalent for the cavity is shown (Fig. II.23a) when the pump power is zero. The generator is represented by a current source i_g with an internal conductance G_g ; G_{sh} is the shunt conductance of the cavity and G_L is the load conductance. The term Y_{BO} is the beam-loading admittance with no pump present; its real part is positive since the cavity does not couple at all with the slow space-charge wave. At resonance, neglecting the detuning effect of the beam-loading susceptance,

the equivalent circuit is shown in Fig. II.23b. The available power in such a circuit is

$$\text{Power available in} = \frac{i_g^2}{4G_g} . \qquad \text{(II.80)}$$

When the pump power is turned on, the equivalent circuit at resonance is shown in Fig. II.23c, neglecting again the beam-loading susceptance. The conductance $-G_B(|m|^2)$ is the negative conductance introduced by the parametric pumping; its value depends on the level of the pump $|m|^2$. The output power is

$$P_{out} = \frac{i_L^2}{G_L} , \qquad \text{(II.81)}$$

where i_L is the current in the load. The gain, defined as

$$\text{gain} = \frac{P_{out}}{P_{\text{available in}}} , \qquad \text{(II.82)}$$

can easily be calculated from Eqs. (II.80) and (II.81):

$$\text{gain} = \frac{4G_L G_g}{[G_g + G_{sh} + G_L - G_B(|m|^2)]^2} \qquad \text{(II.83)}$$

where
- G_L is the load conductance
- G_g is the internal conductance of the generator
- G_{sh} is the shunt conductance of the cavity
- $-G_B(|m|^2)$ is the beam-loading conductance due to the parametric pumping.

The start oscillation condition is obtained when gain is infinite. That is, where

$$|G_B| = (G_B)_{start} = G_g + G_{sh} + G_L ,$$

when $|G_B| < (G_B)_{start}$, amplification occurs, and the small-signal gain depends on the strength of the pump field, as G_B is a function of $|m|^2$.

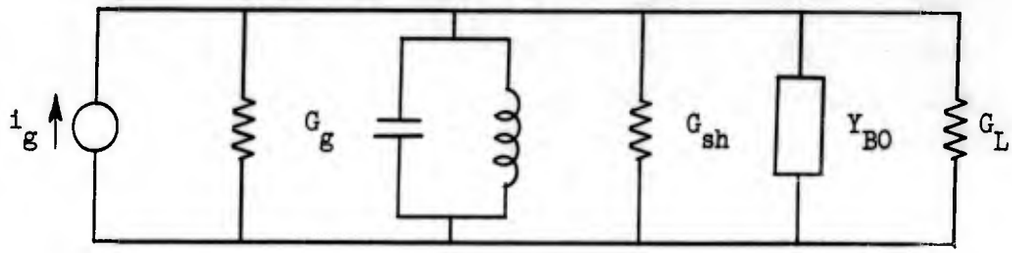

(a)

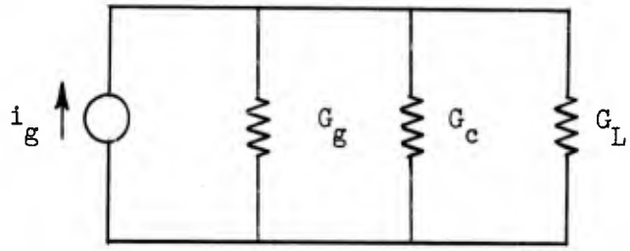

(b)

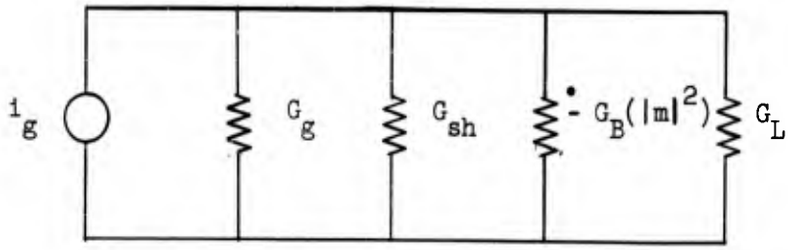

(c)

FIG. II.23--Equivalent circuits of the output cavity.

(a) No Pump Power

(b) No Pump Power at Resonance

(c) Resonance and Pump Power Present

The design of the parametric amplifier is slightly different from the standard design since one cavity can be considered as being, at the same time, the input cavity, the amplifying region and the output cavity.

A schematic of the parametric amplifier is shown in Fig. II.24. The first cavity (I) is used to remove the noise from the fast space-charge wave at the signal frequency. The second cavity (Ia) removes the noise at the idler frequency. When the idler and signal frequencies are not very different, that is, when the idler frequency falls within the bandwidth of the first cavity (I), the second cavity (Ia) can be suppressed. The third cavity (II) impresses on the beam a fast space-charge wave at the pump frequency and this fast wave will react with the signal frequency in the last cavity (III) to create the parametric amplification.

For a numerical example, let the signal frequency be $f_1 = 900$ Mc/s and the ratio ν of the signal to the idler frequency be $\nu = 0.95$.

A. COUPLER (I).

The design of the first coupler which removes the noise at the signal frequency was given in Chapter VII. It was found that:

a (radius of the helix) $= 2 \times 10^{-3}$ m

p (pitch of the helix) $= 1.3 \times 10^{-3}$ m

N (number of turns of the helix) $= 54$

Q_L (loaded Q) $= 10$

The following values were chosen for the perveance of the electron gun K, the beam diameter $2b$, and the beam potential V_0 .

K (perveance) $= 6 \times 10^{-7}$ mks

$2b$ (beam diameter) $= 1.6 \times 10^{-3}$ m

V_0 (beam voltage) $= 1500$ volts.

B. COUPLER (Ia).

As the signal and idler frequencies are very close and since the loaded Q : Q_L of the first cavity is low, there is no need for this

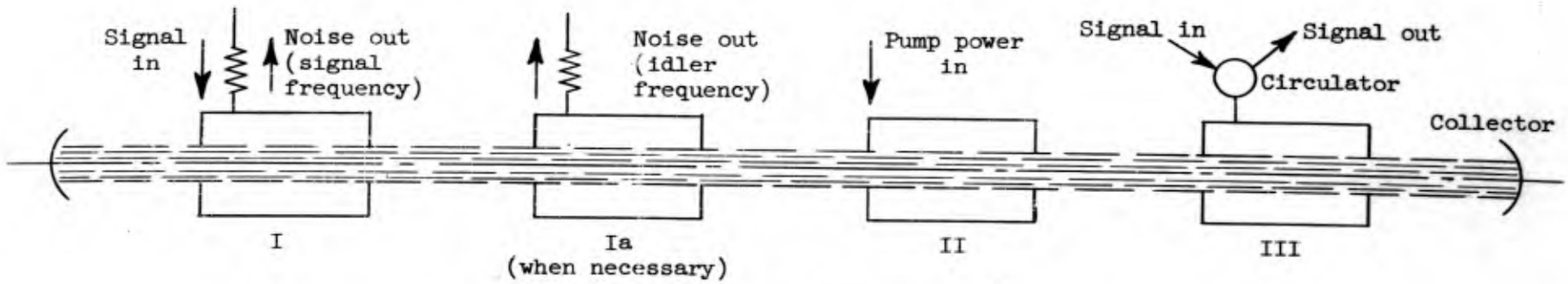

FIG. II.24--Schematic of the parametric amplifier.

coupler. The noise at the signal and at the idler frequency will be extracted by the first cavity.

C. COUPLER (II).

The radius of the helix will be $a = 2 \times 10^{-3}$ m as for the first cavity. For a cavity 2 wavelengths long ($n = 4$), the number of turns will be determined from Eq. (II.20):

$$N = \frac{n}{2(\omega/c)a} = 27 .$$

With a ratio b/a of the beam to the circuit radius of 0.4 (determined in the first coupler), the reduction factor R equals 0.27 . Then from Eq. (II.21), $tg\psi$ equals 0.105 , and the pitch of the helix is $p = 2\pi a\, tg\psi = 1.3$ m/m . There is no restriction on the loaded Q of the cavity, except for the impedance matching between the cavity and the pump generator.

D. INPUT-OUTPUT COUPLER (III).

The following parameters were chosen in the preceding paragraph:

$$y = \frac{u_0}{v_{ph}} = 1 \quad \text{then} \quad \frac{u_0}{c} = \frac{v_{ph}}{c}$$

$$a_1 = 1$$

$$n = 20 .$$

From the definition of $\alpha_3 = \omega_{q3}/\omega_3$ it is found that

$$\alpha_3 = a_1 \left(\frac{n+2}{n} y - 1 \right) = 0.1$$

as $a_1 = 1$

$$\alpha_1 = \alpha_3 = \frac{\omega_{q1}}{\omega_1} = 0.1 .$$

The condition $y = 1$ transforms Eq. (II.21) into

$$\frac{n+2}{2NR\,(a/b)(u_0/c)\sqrt{3.03 \times 10^4 K}} = 1$$

where a/b , u_0/c and K have already been determined. The reduction factor is found to be $R = 0.15$ and, with the same helix radius $a = 2 \times 10^{-3}$m , $N = 266$. The pitch angle is given by

$$p = 2\pi a \, tg\psi = 0.97 \times 10^{-3}\text{m} .$$

Using the relation

$$\frac{\omega_q}{\omega} = R \frac{a}{b} \frac{\sqrt{K \; 3.03 \times 10^4}}{(\omega/u_0)\, a} ,$$

it can be verified that

$$\alpha_1 = 0.1 \simeq \alpha_3 .$$

The table below presents a summary of all the conditions:

	COUPLER I	COUPLER II	COUPLER III
Description	Removes the noise at the signal and idler frequencies.	Impresses the fast wave at the pump frequency.	Input-Output Coupler
Helix Radius	2.10^{-3}m	2.10^{-3}m	2.10^{-3}m
Helix Pitch	1.3×10^{-3}m	1.3×10^{-3}m	0.97×10^{-3}m
Number of Turns	54	27	266
Loaded Q	10		

Signal frequency = 900 Mc/s

Pump. frequency $\simeq$ 1800 Mc/s

K (perveance) = 6×10^{-7}

V_0 (beam voltage) = 1500 volts

Beam diameter = 1.6×10^{-3}m .

CHAPTER X

CONCLUSION

A space-charge wave parametric amplifier was studied in this second part of the work. This amplifier uses long interaction resonant cavities supporting a sinusoidal longitudinal resonant electric field. It was shown that these cavities can be designed to couple only to the fast space-charge wave.

In the same fashion then, an electron beam modulated at the pump frequency creates a varying reactance across a narrow gap in a klystron cavity, leading to a negative conductance across this gap. It was shown that the same effect exists in a long interaction cavity where a negative beam-loading conductance is created by the presence of the parametrically pumped beam.

In the case of a double-gap klystron cavity it was shown that if the electron beam is velocity modulated at the first gap, the presence of parametric pumping creates a negative beam-loading conductance at the second gap for conditions where the beam loading in absence of parametric pumping would be purely reactive. Then the beam-loading admittance was calculated for a long interaction klystron cavity, and it was shown that a negative beam-loading conductance may be created under certain conditions; this led to the design of a parametric amplifier using fast space-charge waves.

It was hoped that in order to avoid interaction with higher order modes, parametric amplification could be obtained under conditions where there are no growing waves in the electron beam. However, the parametric effect is too small to be useful when there are only running waves present. For this reason it may be doubtful that the noise figure obtained with such an amplifier could be much better than the noise figure obtained by Ashkin and others in their parametric amplifiers using fast space-charge waves.

APPENDIX II.A

BANDWIDTH OF THE FAST-WAVE COUPLER.

Since $\epsilon_s = 1 - (v_{ph}/u_0)(1 + \omega_q/\omega)$, the value of $\Delta\epsilon$ is:

$$|\Delta\epsilon| = \left| \Delta \left(\frac{v_{ph}}{u_0} \frac{\omega_q}{\omega} \right) \right| .$$

For the coupler studied in the preceding paragraph, the phase velocity of the circuit is independent of the frequency and the ration u_0/v_{ph} can be approximated by one. Then the values of ϵ_s and of ϵ_f at the frequency $\omega + \Delta\omega$ are

$$\epsilon_s \Big|_{\omega + \Delta\omega} = -\frac{2}{n} + |\Delta\epsilon| = -\frac{2}{n} + \left| \Delta \left(\frac{\omega_q}{\omega} \right) \right|$$

$$\epsilon_f \Big|_{\omega + \Delta\omega} = -\frac{2}{n} + 2\frac{\omega_q}{\omega} + 2\Delta\left(\frac{\omega_q}{\omega} \right) + |\Delta\epsilon| .$$

The ratio

$$\frac{\beta_{0s}}{\beta_{0f}} \Big|_{\omega + \Delta\omega}$$

is calculated from Eq. (II.22), and

$$\left| \frac{\beta_{0s}}{\beta_{0f}} \right| \simeq \frac{n + 2}{n + 2 - 2(\omega_q/\omega)\, n} \frac{n + 1 - (\omega_q/\omega)\, n}{n + 1} \left[\frac{1 - (\omega_q/\omega)\, n}{\sin n\pi\, \omega_q/\omega} \right] \sin \frac{n\pi}{2} |\Delta\epsilon| .$$

This equation is simplified further with the conditions

$$n \geq 4$$

$$n \frac{\omega_q}{\omega} < 1 .$$

The restriction $n\,(\omega_q/\omega) < 1$ implies that ϵ_f is less than 0 , which is a reasonable assumption, as the coupling coefficient decreases

between $\epsilon = 0$ and $\epsilon = -2/n$; thus

$$\left|\frac{\dot{\beta}_{0s}}{\beta_{0f}}\right| \simeq \frac{n}{2} \frac{\pi \left[1 - (\omega_q/\omega)\, n\right]}{\sin \pi \left[1 - (\omega_q/\omega)\, n\right]} \Delta\epsilon \ .$$

A relation used in Chapter VIII will be used to calculate $\Delta\epsilon$. Equation (II.54) gives

$$\frac{\omega_q}{\omega} = \frac{\omega_{q3}}{\omega_3} \frac{\omega_3}{1 - \exp\left[-0.7\,(\omega_3 b/u_0)\right]} \left\{ \frac{1}{\omega} - \frac{\exp\left[-0.7\,(b\omega/u_0)\right]}{\omega} \right\} ,$$

where ω_3 is the pump frequency

b is the beam radius

ω_{q3} is the reduced plasma frequency for the pump.

Since this calculation yields only an order of magnitude, ω_{q3}/ω can be replaced by 0.1 ; then

$$\frac{\Delta}{\Delta\omega}\left(\frac{\omega_q}{\omega}\right)\Delta\omega = 0.1\, \frac{\Delta\omega}{\omega} \left\{ \frac{1}{a_1} + \frac{0.7(b\omega_3/u_0)\exp\left[-0.7\,(b/u_0)\,\omega\right]}{1 - \exp\left[-0.7\,(b/u_0)\,\omega_3\right]} \right\} .$$

For a pump frequency which is about twice the signal frequency and for a value of $(b/u_0)\,\omega$ comparable to the value used in the example of the previous paragraph, the quantity $\Delta\epsilon$ becomes

$$\frac{\Delta}{\Delta\omega}\left(\frac{\omega_q}{\omega}\right)\Delta\omega \ \leq 0.3\, \frac{\Delta\omega}{\omega} .$$

The bandwidth is

$$\frac{\Delta\omega}{\omega} \leq 7\, \frac{\sin \pi \left[1 - (\omega_q/\omega)\, n\right]}{\pi \left[1 - (\omega_q/\omega)\, n\right]}\, \frac{1}{n}\, \frac{\beta_{0s}}{\beta_{0f}} .$$

APPENDIX II.B

DERIVATION OF THE DIFFERENTIAL EQUATIONS.

The values of $u_3(z)$, $\rho_3(z)$, $\rho_2^*(z)$, and $u_1(z)$ are taken from Eqs. (II.51), (II.37) and (II.46) and are substituted in Eq. (II.35). The following equation is obtained after some straightforward algebra:

$$jk_1 I_1(z) \left\{ 1 - \alpha_1^2 \left[1 - \frac{1}{4} |m|^2 (1 - \alpha_3)^2 \right] \right\} + \frac{dI_1(z)}{dz} \left(2 - \frac{1}{2} \alpha_3 |m|^2 \right.$$

$$\left. + \frac{1}{2} |m|^2 \alpha_3^2 \right) + \frac{j}{k_1} \frac{d^2 I_1(z)}{dz^2} \left(-1 + \frac{\alpha_3}{2} |m|^2 - \frac{3}{4} |m|^2 \alpha_3^2 \right) + j \frac{m}{2} I_2^*(z)$$

$$\times \left[k_3 - k_1 + \alpha_3 (k_1 - 3k_3) + 2k_3 \alpha_3^2 \right] \exp \left[- jk_3 (1 - \alpha_3) z \right] + \frac{m}{2k_2}$$

$$\times \frac{dI_2^*(z)}{dz} \left[\begin{array}{l} - 2k_2 + 2\alpha_3 (k_3 + 2k_2) + \alpha_3^2 \left(- 3k_3 - \dfrac{|m|^2}{4} k_3 \right) \\ + \dfrac{1}{2} \alpha_3^3 |m|^2 k_3 - \dfrac{|m|^2}{4} k_3 \alpha_3^4 \end{array} \right]$$

$$\times \exp \left[- jk_3 (1 - \alpha_3) z \right] + j \frac{m}{2k_2} \frac{d^2 I_2^*(z)}{dz^2} \left(- 1 + 3\alpha_3 - \frac{|m|^2}{4} \alpha_3^2 + \frac{|m|^2}{4} \alpha_3^3 \right)$$

$$= \frac{e}{m} \frac{\rho_0}{u_0} \left[1 - \frac{|m|^2}{4} (1 - \alpha_3)^2 \right] E_1(z) \qquad \text{(II.B.1)}$$

Equation (II.B.1) is a mixed differential equation of the variable $I_1(z)$ and $I_2^*(z)$ with nonconstant coefficients. This linear equation with nonconstant coefficients can be transformed into a linear equation with

constant coefficients with the following change of variables:

$$\left.\begin{aligned} I_1(z) &= i_1(z) \exp\left[- jk_1 (1 - \alpha_1 a_1)\, z\right] \\ &= i_1(z) \exp\left[- jk_1 (1 - \alpha_3)\, z\right] \\ I_2^*(z) &= i_2^*(z) \exp\left[+ jk_2 (1 - \alpha_2 a_2)\, z\right] \\ &= i_2^*(z) \exp\left[+ jk_2 (1 - \alpha_3)\, z\right] . \end{aligned}\right\} \qquad \text{(II.B.2)}$$

The relation

$$\omega_3 = \omega_2 + \omega_1 \qquad \text{(II.B.3)}$$

can be written, dividing by u_0

$$k_3 = k_2 + k_1 \qquad \text{(II.B.4)}$$

since all the terms in the right hand side of Eq. (II.B.1), once the change of variable is made, vary like

$$\exp\left[- jk_1 (1 - \alpha_3)\, z\right] ,$$

or

$$\exp\left[+ jk_2 (1 - \alpha_3)\, z\right] \exp\left[- jk_3 (1 - \alpha_3)\, z\right] = \exp\left[- jk_1 (1 - \alpha_3)\, z\right] ,$$

from Eq. (II.B.4).

It is possible to divide both sides of the Eq. (II.B.1) by

$$\exp\left[- jk_1 (1 - \alpha_3)\, z\right]$$

and an equation with constant coefficients is obtained:

$$
\begin{aligned}
&-\frac{j}{k_1}\left(-1+\alpha_3\frac{|m|^2}{2}-\frac{3}{4}\alpha_3^2|m|^2\right)\frac{d^2 i_1(z)}{dz^2}\\
&\quad+2\alpha_3\left(1+\frac{1}{4}|m|^2-\alpha_3|m|^2+\frac{3}{4}|m|^2\alpha_3^2\right)\frac{di_1(z)}{dz}\\
&\quad+jk_1\alpha_3^2\left[1-\frac{1}{a_1^2}\left(1-\frac{|m|^2}{4}\right)+\frac{3}{4}|m|^2-\alpha_3\frac{|m|^2}{2}\right.\\
&\qquad\left.\times\left(3+\frac{1}{a_1^2}\right)+\frac{1}{4}\alpha_3^2|m|^2\left(3+\frac{1}{a_1^2}\right)\right]i_1(z)\\
&\quad+\frac{jm}{2k_2}\left(-1+3\alpha_3-\alpha_3^2\frac{|m|^2}{4}+\alpha_3^3\frac{|m|^2}{4}\right)\frac{d^2 i_2^*(z)}{dz^2}\\
&\quad+\frac{m}{2k_2}\alpha_3(k_1-k_2)\left[2-\alpha_3\left(3+\frac{|m|^2}{4}\right)+\alpha_3^2\frac{|m|^2}{2}-\alpha_3^3\frac{|m|^2}{4}\right]\frac{di_2^*(z)}{dz}\\
&\quad+\frac{jm}{2}k_1\alpha_3^2\left[-3-\frac{|m|^2}{4}+3\alpha_3\left(1+\frac{|m|^2}{4}\right)-\frac{3}{4}\alpha_3^2|m|^2+\alpha_3^3\frac{|m|^2}{4}\right]i_2^*(z)\\
&=\frac{e}{m}\frac{\rho_0}{u_0}\left[1-\frac{|m|^2}{4}(1-\alpha_3)^2\right]\exp\left[+jk_1(1-\alpha_3)z\right]E_1(z)
\end{aligned}
\qquad \text{(II.B.5)}
$$

A similar equation could have been obtained in the same way by starting with the equation of motion at the idler frequency. Due to the symmetry of the problem, as far as idler and signal are concerned, the second equation will be obtained by changing the subscript 1 to 2 and taking

the complex conjugate:

$$
\begin{aligned}
&-\frac{j}{k_2}\left(-1+\alpha_3\frac{|m|^2}{2}-\frac{3}{4}|m|^2\alpha_3{}^2\right)\frac{d^2 i_2{}^*(z)}{dz^2}\\
&\quad+2\alpha_3\left(1+\frac{1}{4}|m|^2-\alpha_3|m|^2+\frac{3}{4}\alpha_3{}^2|m|^2\right)\frac{di_2{}^*(z)}{dz}\\
&\quad-jk_2\alpha_3{}^2\left[1-\frac{1}{a_2{}^2}\left(1-\frac{|m|^2}{4}\right)+\frac{3}{4}|m|^2-\alpha_3\frac{|m|^2}{2}\right.\\
&\qquad\left.\times\left(3+\frac{1}{a_2{}^2}\right)+\frac{1}{4}\alpha_3{}^2|m|^2\left(3+\frac{1}{a_2{}^2}\right)\right]i_2{}^*(z)\\
&\quad-\frac{jm^*}{2k_1}\left(-1+3\alpha_3-\alpha_3{}^2\frac{|m|^2}{4}+\alpha_3{}^3\frac{|m|^2}{4}\right)\frac{d^2 i_1(z)}{dz^2}\\
&\quad+\frac{m^*}{2k_1}\alpha_3(k_2-k_1)\left[2-\alpha_3\left(3+\frac{|m|^2}{4}\right)+\frac{\alpha_3{}^2}{2}|m|^2-\alpha_3{}^3\frac{|m|^2}{4}\right]\frac{di_1(z)}{dz}\\
&\quad-\frac{jm^*}{2}k_2\alpha_3{}^2\left[-3-\frac{|m|^2}{4}+3\alpha_3\left(1+\frac{|m|^2}{4}\right)-\frac{3}{4}\alpha_3{}^2|m|^2+\alpha_3{}^3\frac{|m|^2}{4}\right]i_1(z)\\
&=\frac{e}{m}\frac{\rho_0}{u_0}\left[1-\frac{|m|^2}{4}(1-\alpha_3)^2\right]\exp\left[-jk_2(1-\alpha_3)z\right]E_2{}^*(z)\ .
\end{aligned}
\tag{II.B.6}
$$

These last two equations can be written in the following way:

$$
\left.
\begin{aligned}
L_1 i_1(z)+L_2 i_2{}^*(z)&=f(z)\\
L_3 i_1(z)+L_4 i_2{}^*(z)&=g(z)\ ,
\end{aligned}
\right\}
\tag{II.B.7}
$$

where L_1 , L_2 , L_3 , L_4 , are linear operators of the form

$$\sum_n a_n\frac{d^n}{dz^n}$$

$$n=0,1,2$$

where the a_n are constants. As these operators commute, the mixed second order differential equations can be transformed into two fourth order equations:

$$\left.\begin{aligned}(L_1L_4 - L_2L_3)\, i_1(z) &= -L_2 g(z) + L_4 f(z)\\ (L_1L_4 - L_2L_3)\, i_2^*(z) &= L_1 g(z) - L_3 f(z)\,.\end{aligned}\right\} \qquad \text{(II.B.8)}$$

Carrying out the algebra Eqs. (II.B.5) and (II.B.6) become

$$\frac{1}{k_1k_2}\, P\, \frac{d^4 i_1(z)}{dz^4} + 2j\alpha_3\, \frac{(k_2 - k_1)}{k_1k_2}\, Q\, \frac{d^3 i_1(z)}{dz^3}$$

$$+ \alpha_3^2\, R\, \frac{d^2 i_1(z)}{dz^2} + 2jk_1\alpha_3^3\, S\, \frac{di_1(z)}{dz} + k_1k_2\alpha_3^4\, T\, i_1(z)$$

$$= -\frac{e}{m}\frac{\rho_0}{u_0}\left[1 - \frac{m^2}{4}(1 - \alpha_3^2)\right]\left\{U\, E_1(z) \exp\left[jk_1 (1 - \alpha_3)\, z\right]\right.$$

$$\left. - m\, W\, E_2^*(z) \exp\left[-jk_2 (1 - \alpha_3)\, z\right]\right\} \qquad \text{(II.B.9)}$$

with

$$P = \left[\left(1 - \frac{|m|^2}{2}\alpha_3 + \frac{3}{4}|m|^2\alpha_3^2\right)^2 - \frac{|m|^2}{4}\left(1 - 3\alpha_3 - \frac{|m|^2}{4}\alpha_3^2 + \frac{|m|^2}{4}\alpha_3^3\right)^2\right]$$

$$Q = \left\{\begin{aligned}&\left(-1 + \alpha_3\frac{|m|^2}{2} - \frac{3}{4}|m|^2\alpha_3^2\right)\left(1 + \frac{1}{4}|m|^2 - \alpha_3|m|^2 + \frac{3}{4}|m|^2\alpha_3^2\right)\\ &-\frac{|m|^2}{4}\left(-1 + 3\alpha_3 - \alpha_3^2\frac{|m|^2}{4} + \alpha_3^3\frac{|m|^2}{4}\right)\left[2 - \alpha_3\left(3 + \frac{|m|^2}{4}\right) + \alpha_3^2\frac{|m|^2}{2}\right.\\ &\left.\qquad - \alpha_3^3\frac{|m|^2}{4}\right)\end{aligned}\right\}$$

$$
R = \left\{ \left(-1 + \alpha_3 \frac{|m|^2}{2} - \frac{3}{4}\alpha_3^2 |m|^2 \right) \left\{ \frac{k_2}{k_1} \left[1 - \frac{1}{a_2^2}\left(1 - \frac{|m|^2}{4}\right) + \frac{3}{4}|m|^2 - \frac{|m|^2}{2} \right.\right.\right.
$$

$$
\left.\left.\left. \times \alpha_3 \left(\frac{1}{a_2^2} + 3 \right) + \frac{1}{4}|m|^2 \alpha_3^2 \left(\frac{1}{a_2^2} + 3 \right) \right] \right.\right.
$$

$$
\left.\left. + \frac{k_1}{k_2} \left[1 - \frac{1}{a_1^2}\left(1 - \frac{|m|^2}{4}\right) + \frac{3}{4}|m|^2 - \alpha_3 \frac{|m|^2}{2} \right.\right.\right.
$$

$$
\left.\left.\left. \times \left(\frac{1}{a_1^2} + 3 \right) + \frac{1}{4}|m|^2 \alpha_3^2 \left(\frac{1}{a_1^2} + 3 \right) \right] \right\} \right\}
$$

$$
- \frac{|m|^2}{4} \left\{ 2\left(-1 + 3\alpha_3 - \frac{|m|^2}{4}\alpha_3^2 + \frac{|m|^2}{4}\alpha_3^3 \right) \right.
$$

$$
\left. \times \left[-3 - \frac{|m|^2}{4} + 3\alpha_3 \left(1 + \frac{|m|^2}{4} - \frac{3}{4}\alpha_3^2 |m|^2 \right) + \alpha_3^3 \frac{|m|^2}{4} \right] \right\}
$$

$$
- \frac{(k_1 - k_2)^2}{k_1 k_2} \left[2 - \alpha_3 \left(2 + \frac{|m|^2}{4} \right) - \alpha_3^2 \frac{|m|^2}{4} \right]^2
$$

$$
+ 4\left(1 + \frac{1}{4}|m|^2 - \alpha_3 |m|^2 + \frac{3}{4}\alpha_3^2 |m|^2 \right)^2
$$

$$
S = \left\{ \left(1 + \frac{|m|^2}{4} - \alpha_3 |m|^2 + \frac{3}{4} |m|^2 \alpha_3^2 \right) \right.
$$

$$
\times \left\{ \left[1 - \frac{1}{a_1^2} \left(1 - \frac{|m|^2}{4} \right) + \frac{3}{4} |m|^2 - \frac{|m|^2}{2} \right.\right.
$$

$$
\left.\left. \times \alpha_3 \left(\frac{1}{a_1^2} + 3 \right) + \alpha_3^2 \frac{|m|^2}{4} \left(\frac{1}{a_1^2} + 3 \right) \right] \right.
$$

$$
\left. - \frac{k_2}{k_1} \left[1 - \frac{1}{a_2^2} \left(1 - \frac{|m|^2}{4} \right) + \frac{3}{4} |m|^2 - \frac{|m|^2}{2} \right.\right.
$$

$$
\left.\left. \times \alpha_3 \left(\frac{1}{a_2^2} + 3 \right) + \alpha_3^2 \frac{|m|^2}{4} \left(\frac{1}{a_2^2} + 3 \right) \right] \right\}
$$

$$
+ \frac{|m|^2}{4} \left(1 - \frac{k_2}{k_1} \right) \left[2 - \alpha_3 \left(3 + \frac{|m|^2}{4} \right) + \alpha_3^2 \frac{|m|^2}{2} - \alpha_3^3 \frac{|m|^2}{4} \right]
$$

$$
\left. \times \left[- 3 - \frac{|m|^2}{4} + 3\alpha_3 \left(1 + \frac{|m|^2}{4} \right) - \frac{3}{4} \alpha_3^2 |m|^2 + \alpha_3^3 \frac{|m|^2}{4} \right] \right\}
$$

$$
T = \left\{ \left[1 - \frac{1}{a_1^2} \left(1 - \frac{|m|^2}{4} \right) + \frac{3}{4} |m|^2 - \frac{|m|^2}{2} \alpha_3 \left(3 + \frac{1}{a_1^2} \right) \right] \right.
$$

$$
\left. \times \left[1 - \frac{1}{a_2^2} \left(1 - \frac{|m|^2}{4} \right) + \frac{3}{4} |m|^2 - \frac{|m|^2}{2} \alpha_3 \left(3 + \frac{1}{a_2^2} \right) + \frac{|m|^2}{4} \alpha_3^2 \left(3 + \frac{1}{a_2^2} \right) \right] \right.
$$

$$
\left. - \frac{|m|^2}{4} \left[- 3 - \frac{|m|^2}{4} + 3\alpha_3 \left(1 + \frac{|m|^2}{4} \right) - \frac{3}{4} \alpha_3^2 |m|^2 + \alpha_3^3 \frac{|m|^2}{4} \right] \right\}
$$

$$U = \left\{ \begin{array}{l} -\frac{j}{k_2}\left[-1+\alpha_3\frac{|m|^2}{2}-\frac{3}{4}|m|^2\alpha_3^2\right]\frac{d^2}{dz^2} \\ +2\alpha_3\left[1+\frac{1}{4}|m|^2-\alpha_3|m|^2+\frac{3}{4}\alpha_3^2|m|^2\right]\frac{d}{dz} \\ -jk_2\alpha_3^2\left[\begin{array}{l} 1-\frac{1}{a_2^2}\left(1-\frac{|m|^2}{4}\right)+\frac{3}{4}|m|^2-\alpha_3\frac{|m|^2}{2} \\ \times\left(3+\frac{1}{a_2^2}\right)+\frac{1}{4}\alpha_3^2|m|^2\left(3+\frac{1}{a_2^2}\right) \end{array}\right] \end{array} \right\}$$

$$W = \left\{ \begin{array}{l} \frac{j}{2k_2}\left[-1+3\alpha_3-\alpha_3^2\frac{|m|^2}{4}+\alpha_3^2\frac{|m|^2}{4}\right]\frac{d^2}{dz^2} \\ +\frac{\alpha_3(k_1-k_2)}{2k_2}\left[2-\alpha_3\left(3+\frac{|m|^2}{4}\right)+\alpha_3^2\frac{|m|^2}{2}-\alpha_3^3\frac{|m|^2}{4}\right]\frac{d}{dz} \\ +\frac{jk_1}{2}\alpha_3^2\left[-3-\frac{|m|^2}{4}+3\alpha_3\left(1+\frac{|m|^2}{4}\right)-\frac{3}{4}\alpha_3^2|m|^2+\alpha_3^3\frac{|m|^2}{4}\right] \end{array} \right\}$$

and where in the right hand side the derivative d^n/dz^n operates on

$$E_1(z)\exp\left[jk_1(1-\alpha_3)z\right]$$

and on

$$E_2^*(z)\exp\left[-jk_2(1-\alpha_3)z\right].$$

A similar equation for $i_2^*(z)$ is obtained in the same fashion.

It can be seen that $L_1L_4 - L_2L_3$ does not depend on m or m^* but only on mm^* and that L_1 and L_4 are independent of the pump.

Then, if $g(z) = 0$, (that is, there is no applied external field at the idler frequency), the current at the signal frequency does not depend on the phase of the pump, as was shown by several authors. In a similar

fashion, if there is no external applied field at the signal frequency, the idler is independent of the phase of the pump.

On the other hand, when an external field is applied, a new independent quantity is added, and the waves at the signal frequency arise from two different independent sources, the first being the signal which is externally applied to the beam, the second being the result of the interaction of the applied idler with the pump. These two signals combine to give the total current at the signal frequency, and they will be added in a way which depends on their relative, independent phases, the phase of the current created by interaction of the idler and pump depending on the relative phases of the latter.

At this point, a further assumption will be made; $|m|^2$ and α_3 will be restricted to be smaller than one:

$$\alpha_3 < 1 .$$

The terms of high order in α_3 can be neglected, and both sides of the equation can be divided by $1 - |m|^2/4$. Introducing a new normalizing parameter ν ,

$$\nu = \frac{\omega_1}{\omega_2} = \frac{k_1}{k_2} ,$$

Eq. (II.B.9) then becomes

$$\frac{d^4 i_1(z)}{dz^4} + 2j\,(\alpha_3 k_1)\left(1 - \frac{1}{\nu}\right)\frac{d^3 i_1(z)}{dz^3}$$

$$+ \frac{(k_1\alpha_3)^2}{\nu}\left\{4 - \frac{1}{2}|m|^2 - \left[\left(1 - \frac{1}{a_2^2}\right)\frac{1}{\nu} + \nu\left(1 - \frac{1}{a_1^2}\right)\right]\right\}\frac{d^2 i_1(z)}{dz^2}$$

$$+ 2j\,\frac{(k_1\alpha_3)^3}{\nu}\left\{1 - \frac{|m|^2}{4} - \frac{1}{a_1^2}\left(1 + \frac{|m|^2}{4}\right) - \frac{1}{\nu}\left[1 - \frac{|m|^2}{4} - \frac{1}{a_2^2}\left(1 + \frac{|m|^2}{4}\right)\right]\right\}\frac{di_1(z)}{dz}$$

$$+ \frac{(k_1\alpha_3)^4}{\nu^2}\left[1 - \frac{|m|^2}{2} + \frac{|m|^4}{16} - \left(\frac{1}{a_1^2} + \frac{1}{a_2^2}\right)\left(1 + \frac{3}{4}|m|^2\right) + \frac{1}{a_1^2 a_2^2}\left(1 - \frac{|m|^2}{4}\right)\right] i_1(z)$$

$$= \eta\,\frac{\rho_0}{u_0}\left\{\begin{array}{l} k_1\left\{j\,\dfrac{d^2}{dz^2} + 2\,\dfrac{(\alpha_3 k_1)}{\nu}\left(1 + \dfrac{|m|^2}{4}\right)\dfrac{d}{dz} - j\,\dfrac{(k_1\alpha_3)^2}{\nu^2}\left[1 - \dfrac{1}{a_2^2}\left(1 - \dfrac{|m|^2}{4}\right) + \dfrac{3}{4}|m|^2\right]\right\} \\ \times E_1(z)\exp\left[+ jk_1(1 - \alpha_3)z\right] \\ \\ -\dfrac{mk_1}{2}\left[\begin{array}{l} -j\,\dfrac{d^2}{dz^2} + 2(\alpha_3 k_1)\left(1 - \dfrac{1}{\nu}\right)\dfrac{d}{dz} \\ \\ +j\,\dfrac{(k_1\alpha_3)^2}{\nu}\left(-3 - \dfrac{|m|^2}{4}\right) \end{array}\right] E_2^*(z)\exp\left[-jk_2(1 - \alpha_3)z\right] \end{array}\right.$$

(II.B.10)

APPENDIX II.C

CALCULATION OF THE AMPLITUDES OF THE SPACE-CHARGE WAVES

The boundary conditions at the plane $z = 0$ are

$$i_1(z = 0) = i_1(0) \qquad \text{(II.C.1)} \qquad i_2^*(z = 0) = i_2^*(0) \qquad \text{(II.C.2)}$$

$$V_1(z = 0) = V_1(0) \qquad \text{(II.C.3)} \qquad V_2^*(z = 0) = V_2^*(0) \qquad \text{(II.C.4)}$$

It has been seen that the modified current densities can be expressed as the sum of four terms:

$$i_1(z) = \sum_{(n)} i_1^{(n)}(z) \qquad \text{(II.C.5)}$$

$$(n) = 1,2,3,4$$

at the signal frequency; the next two

$$i_2^*(z) = \sum_{(n)} i_2^{(n)*}(z) \qquad \text{(II.C.6)}$$

$$(n) = 1,2,3,4$$

at the idler frequency.

When $E_1(z)$ and $E_2^*(z)$ are zero, that is, when there is no field in the drift space, Eq. (II.56) becomes

$$\frac{d^4 i_1(z)}{dz^4} + 2j\,(\alpha_3 k_1)\left(1 - \frac{1}{\nu}\right)\frac{d^3 i_1(z)}{dz^3} + \frac{(k_1\alpha_3)^2}{\nu}\left\{4 - \frac{1}{2}|m|^2 - \left[\left(1 - \frac{1}{a_2^2}\right)\frac{1}{\nu} + \nu\left(1 - \frac{1}{a_1^2}\right)\right]\right\}\frac{d^2 i_1(z)}{dz^2} + 2j\,\frac{(k_1\alpha_3)^3}{\nu}\left\{1 - \frac{|m|^2}{4} - \frac{1}{a_1^2}\left(1 + \frac{|m|^2}{4}\right) - \frac{1}{\nu}\left[1 - \frac{|m|^2}{4} - \frac{1}{a_2^2}\left(1 + \frac{|m|^2}{4}\right)\right]\right\}\frac{di_1(z)}{dz} + \frac{(k_1\alpha_3)^4}{\nu^2}\left[1 - \frac{|m|^2}{2} + \frac{|m|^4}{16} - \left(\frac{1}{a_1^2} + \frac{1}{a_2^2}\right)\left(1 + \frac{3}{4}|m|^2\right) + \frac{1}{a_1^2 a_2^2}\left(1 - \frac{|m|^2}{4}\right)\right] i_1(z) = 0 . \qquad \text{(II.C.7)}$$

This equation is linear, has constant coefficients and has no driving term. Its solution is of the form

$$i_1(z) = \sum_{(n)} i_1^{(n)}(z) = \sum_{(n)} i_1^{(n)} \exp\left[j\,(\alpha_3 k_1)\, w^{(n)} z\right] \qquad \text{(II.C.8)}$$

$$(n) = 1,2,3,4$$

where $i_1^{(n)}$ is a complex constant. Substituting back into the differential equation yields

$$(w)^4 + 2\left(1 - \frac{1}{\nu}\right)(w)^3 - \frac{1}{\nu}\left\{4 - \frac{1}{2}|m|^2 - \left[\left(1 - \frac{1}{a_2^2}\right)\frac{1}{\nu} + \nu\left(1 - \frac{1}{a_1^2}\right)\right]\right\}(w)^2$$

$$- 2\nu\left\{1 - \frac{|m|^2}{4} - \frac{1}{a_1^2}\left(1 + \frac{|m|^2}{4}\right) - \frac{1}{\nu}\left[1 - \frac{|m|^2}{4} - \frac{1}{a_2^2}\left(1 + \frac{|m|^2}{4}\right)\right]\right\}(w)$$

$$+ \frac{1}{\nu^2}\left[1 - \frac{|m|^2}{2} + \frac{|m|^4}{16} - \left(\frac{1}{a_1^2} + \frac{1}{a_2^2}\right)\left(1 + \frac{3}{4}|m|^2\right) + \frac{1}{a_1^2 a_2^2}\left(1 - \frac{|m|^2}{4}\right)\right] = 0 . \qquad \text{(II.C.9)}$$

The roots of this quartic determine the $w^{(n)}$.

From the mixed differential equation [Eq. (II.B.5)] it is found that

$$i_2^*(z) = \sum_{(n)} i_2^{(n)*}(z) = \sum_{(n)} i_2^{(n)*} \exp\left[j\,(\alpha_3 k_1)\, w^{(n)} z\right] \qquad \text{(II.C.10)}$$

$$(n) = 1,2,3,4 .$$

The four independent boundary equations provide the four equations necessary to calculate the $i_1^{(n)}$. For this purpose, independent relations between the $i_1^{(n)}$'s , $i_2^{(n)*}$'s , $v_1^{(n)}$'s , and the $v_2^{(n)*}$'s will be derived.

Equation (II.B.5) where $E_1(z) = E_2^*(z) = 0$ provides the relation between the $i_1^{(n)}$'s and the $i_2^{(n)*}$'s . Using Eqs. (II.C.8) and (II.C.10)

Eq. (II.B.5) yields

$$j\,(\alpha_3 k_1)^2 \exp\left[j\,(\alpha_3 k_1)\, w^{(n)} z\right]$$

$$\times \left[- \left[w^{(n)}\right]^2 + 2\left(1 + \frac{|m|^2}{4}\right) w^{(n)} + 1 - \frac{1}{a_1^2}\left(1 - \frac{|m|^2}{4}\right) + \frac{3}{4}|m|^2 \right]$$

$$\times i_1^{(n)} + \frac{m}{2}\left[- \nu \left[w^{(n)}\right]^2 + 2(\nu - 1)\, w^{(n)} - 3 - \frac{|m|^2}{4} \right] i_2^{(n)*} = 0 \qquad \text{(II.C.11)}$$

Thus the result is

$$i_2^{(n)*} = \frac{1}{m} A^{(n)} i_1^{(n)} \qquad \text{(II.C.12)}$$

with

$$A^{(n)} = - 2 \left\{ \left[w^{(n)}\right]^2 + 2\left(1 + \frac{1}{4}|m|^2\right) w^{(n)} + 1 - \frac{1}{a_1^2}\left(1 - \frac{|m|^2}{4}\right) + \frac{3}{4}|m|^2 \right\}$$

$$\times \left\{ \nu \left[w^{(n)}\right]^2 + 2(\nu - 1)\, w^{(n)} - 3 - \frac{|m|^2}{4} \right\}^{-1} \qquad \text{(II.C.13)}$$

$A^{(n)}$ is independent of the phase of the pump. Equation (II.C.2) can now be written

$$\sum_{(n)} A^{(n)} i_1^{(n)} = m i_2^*(0) \qquad \text{(II.C.14)}$$

at the input plane $z = 0$. Two relations between the $i_1^{(n)}$'s have been found. Two others are needed; they will be derived from Eqs. (II.C.3) and (II.C.4) once the velocities can be expressed in function of the currents. The equations of motion at the signal and idler frequencies were

found to be

$$j\omega_1 u_1(z) + u_0 \frac{du_1(z)}{dz} + \frac{1}{2}\frac{d}{dz}\left[u_3(z)u_2^*(z)\right] = \frac{e}{m}\left[\frac{j}{\epsilon_0\omega_1} I_1(z)\right] \qquad \text{(II.C.15)}$$

and

$$j\omega_2 u_2^*(z) + u_0 \frac{du_2^*(z)}{dz} + \frac{1}{2}\frac{d}{dz}\left[u_3^*(z)u_1(z)\right] = -\frac{e}{m}\left[\frac{j}{\epsilon_0\omega_2} I_2^*(z)\right] \qquad \text{(II.C.16)}$$

The quantities $u_1^{(n)}$ and $u_2^{(n)*}$ are defined by

$$\left.\begin{aligned} u_1(z) &= \sum_{(n)} u_1^{(n)}(z) = \sum_{(n)} u_1^{(n)} \exp\left[j\,(\alpha_3 k_1)\, w^{(n)} z\right] \\ u_1^*(z) &= \sum_{(n)} u_2^{(n)*}(z) = \sum_{(n)} u_2^{(n)*} \exp\left[j\,(\alpha_3 k_1)\, w^{(n)} z\right] \\ & \qquad (n) = 1,2,3,4\,. \end{aligned}\right\} \qquad \text{(II.C.17)}$$

Since $u_1^{(n)}(z)$ and $I_1^{(n)}(z)$ vary as does

$$\exp\left[-jk_1(1-\alpha_3)z\right] \exp\left[jk_1\alpha_3 w^{(n)} z\right],$$

and $u_2^{(n)*}(z)$, $I_2^{(n)*}(z)$ vary as does

$$\exp\left[+jk_2(1-\alpha_3)z\right] \exp\left[jk_1\alpha_3 w^{(n)} z\right],$$

therefore Eqs. (II.C.15) and (II.C.16) yield

$$u_1^{(n)}\left[w^{(n)} + 1\right] + \frac{1}{2} m \left\{\left[1 + w^{(n)}\right]\alpha_3 - 1\right\} u_2^{(n)*} = \frac{\alpha_3}{a_1^2}\frac{u_0}{I_0} i_1^{(n)} \qquad \text{(II.C.18)}$$

$$\frac{1}{2} m^* \left\{1 - \alpha_3\left[1 - \nu w^{(n)}\right]\right\} + \left[\nu w^{(n)} - 1\right] u_2^{(n)*} = -\frac{\alpha_3}{m}\frac{u_0}{I_0}\frac{1}{a_2^2} A^{(n)} i_1^{(n)} \qquad \text{(II.C.19)}$$

Then the result is

$$u_1^{(n)} = B^{(n)} \frac{\alpha_3 u_0}{I_0} i_1^{(n)}$$

with (II.C.20)

$$B^{(n)} = \left\{ \frac{1}{a_1^2} [\nu w^{(n)} - 1] + \frac{1}{2} \frac{A^{(n)}}{a_2^2} \left[- 1 + \alpha_3 [1 + w^{(n)}] \right] \right\}$$

$$\times \left\{ - 1 + w^{(n)}(\nu - 1) + \nu [w^{(n)}]^2 - \frac{|m|^2}{4} \left[- 1 + \alpha_3 [2 + w^{(n)}(1 - \nu)] \right] \right\}^{-1}$$

and

$$u_2^{(n)*} = C^{(n)} \frac{\alpha_3 u_0}{m I_0}$$

with (II.C.21)

$$C^{(n)} = \left\{ \frac{A^{(n)}}{a_2^2} [1 + w^{(n)}] + \frac{1}{2} \frac{|m|^2}{a_1^2} \left[1 - \alpha_3 [1 - \nu w^{(n)}] \right] \right\}$$

$$\times \left\{ - 1 + w^{(n)}(\nu - 1) + \nu [w^{(n)}]^2 - \frac{|m|^2}{4} \left[- 1 + \alpha_3 [2 + w^{(n)}(1 - \nu)] \right] \right\}^{-1}$$

As could be predicted, the current density at the signal frequency does not depend on the phase of the pump when there is neither initial current nor initial velocity at the idler frequency. It should be noticed that this statement is true only for the case $\nu \neq 1$, that is, in the non-degenerate case. If the signal and idler frequencies are equal, there is no distinction between signal and idler any more, so that the previous case cannot exist. The amplitudes $i_1^{(n)}$ of the four waves at the signal frequency can now be calculated by solving the system of four linear

equations:

$$\left.\begin{aligned}
&\sum_{(n)} i_1^{(n)} = i_1(0) \\
&\sum_{(n)} A^{(n)} i_1^{(n)} = m i_2^*(0) \\
&\sum_{(n)} B^{(n)} i_1^{(n)} = \frac{I_0}{\alpha_3 u_0} v_1(0) \\
&\sum_{(n)} C^{(n)} i_1^{(n)} = \frac{m I_0}{\alpha_3 u_0} v_2^*(0) \\
&\qquad (n) = 1,2,3,4 \ .
\end{aligned}\right\} \qquad \text{(II.C.22)}$$

APPENDIX II.D

CALCULATION OF THE CURRENT DENSITY AT THE SIGNAL FREQUENCY IN A RESONANT CAVITY SUPPORTING A SINUSOIDAL ELECTRIC FIELD

The Laplace transform of Eq. (II.75) is:

$$i_1(s) = \left\{ \mathcal{L}[f(z)] + s\frac{d^2 i_1(0)}{dz^2} + \frac{d^3 i_1(0)}{dz^3} + 2j\,(k_1\alpha_3)\left(1 - \frac{1}{\nu}\right)\frac{d^2 i_1(0)}{dz^2} \right\}$$

$$\times \left\{ s^4 + 2j\,(\alpha_3 k_1)\left(1 - \frac{1}{\nu}\right)s^3 + \frac{(k_1\alpha_3)^2}{\nu}\left\{ 4 - \frac{1}{2}|m|^2 - \left[\left(1 - \frac{1}{a_2^2}\right)\right.\right.\right.$$

$$\left.\left.\left. \times \nu + \nu\left(1 - \frac{1}{a_1^2}\right)\right]\right\} s^2 + 2j\,\frac{(k_1\alpha_3)^3}{\nu^2}\left\{ 1 - \frac{|m|^2}{4} - \frac{1}{a_1^2}\right.$$

$$\times \left(1 + \frac{|m|^2}{4}\right) - \frac{1}{\nu}\left[1 - \frac{|m|^2}{4} - \frac{1}{a_2^2}\left(1 + \frac{|m|^2}{4}\right)\right]\Bigg\} s + \frac{(k_1\alpha_3)^4}{\nu^2}$$

$$\times \left[1 - \frac{|m|^2}{4} + \frac{|m|^4}{16} - \left(\frac{1}{a_1^2} + \frac{1}{a_2^2}\right)\left(1 + \frac{3}{4}|m|^2\right) + \frac{1}{a_1^2 a_2^2}\left(1 - \frac{|m|^2}{4}\right)\right] \Bigg\}^{-1} \qquad \text{(II.D.1)}$$

where $f(z)$ is the right hand side of Eq. (II.75) and $\mathcal{L}[f(z)]$ is its transform.

The calculation of the terms due to the boundary conditions will be made first. Equations (II.B.5) and (II.B.6) subjected to the boundary conditions become

$$-\frac{j}{k_1}\frac{d^2 i_1(0)}{dz^2} - \frac{jm}{2k_2}\frac{d^2 i_2^*(0)}{dz^2} = \frac{I_0}{2V_0}\left(1 - \frac{|m|^2}{4}\right) \qquad \text{(II.D.2)}$$

$$+\frac{j}{k_2}\frac{d^2 i_2^*(0)}{dz^2} + \frac{jm^*}{2k_1}\frac{d^2 i_1(0)}{dz^2} = 0 \,. \qquad \text{(II.D.3)}$$

From these equations one obtains

$$\frac{d^2 i_1(0)}{dz^2} = jk_1 \frac{I_0}{2} \frac{A\sqrt{2}}{L} \qquad \text{(II.D.4)}$$

$$\frac{d^2 i_2^*(0)}{dz^2} = - j \frac{m^*}{4} k_2 I_0 \frac{A\sqrt{2}}{L} . \qquad \text{(II.D.5)}$$

If Eq. (II.B.5) is differentiated, the value of $d^3(z = 0)/dz^3$ is found to be

$$\frac{d^3 i_1(0)}{dz^3} = - k_1^2 \frac{I_0 A\sqrt{2}}{2L} (1 - 3\alpha_3) . \qquad \text{(II.D.6)}$$

One divided by the denominator of Eq. (II.D.1), subjected to the change of variable

$$s^{(n)} = j\alpha_3 k_1 w^{(n)} \qquad \text{(II.D.7)}$$

can be written

$$\sum_j \frac{M^{(n)}}{(\alpha_3 k_1)^3} \frac{1}{s - s^{(n)}} \qquad \text{(II.D.8)}$$

$$(n) = 1,2,3,4$$

with

$$M^{(n)} = \prod_{(m)} \frac{1}{s^{(n)} - s^{(m)}}$$

$$(m) \neq (n)$$

$$(n) = 1,2,3,4$$

$$(m) = 1,2,3,4 .$$

Equation (II.D.1) then becomes

$$i_1(s) = \sum_{(n)} \frac{M^{(n)}}{(\alpha_3 k_1)^3} \frac{1}{s - s^{(n)}} \left[s \frac{d^2 i_1(0)}{dz^2} + \frac{d^3 i_1(0)}{dz^3} + 2jk_1\alpha_3 \left(1 - \frac{1}{\nu}\right) \frac{d^2 i_1(0)}{dz^2} \right]$$

$$+ \mathcal{L}[f(z)] \sum_{(n)} \frac{M^{(n)}}{(\alpha_3 k_1)^3} \frac{1}{s - s^{(n)}} \qquad \text{(II.D.9)}$$

$$(n) = 1,2,3,4 \ .$$

The inverse Laplace transform of Eq. (II.D.9) must be taken. It is well known that the inverse transform of a product is given by a convolution integral, thus

$$\mathcal{L}^{-1}\left\{ \mathcal{L}[f(z)] \sum_{(n)} \frac{M^{(n)}}{(\alpha_3 k_1)^3} \frac{1}{s - s^{(n)}} \right\} = \frac{1}{(\alpha_3 k_1)^3} \sum_{(n)} M^{(n)}$$

$$\times \int_0^z f(z - x) \exp\left[j (\alpha_3 k_1) w^{(n)} x\right] dx \ .$$

(II.D 10)

If the algebra is carried through, the current density at the signal frequency is found to be

$$I_1(z) = i_1(z) \exp\left[- jk_1 (1 - \alpha_3) z\right]$$

$$= + j \frac{A\sqrt{2}}{2L} \frac{I_0}{k_1} \sum_{(n)} \left\{ + \left\{ \begin{array}{l} G^{(n)} + \left[\exp\left[j \left[\alpha_3 k_1 w^{(n)} - k_1 (1 - \alpha_3) \right] z \right] \right. \\ \left. - \exp\left(+ jk_1 yz\right) \right] \\ + G^{(n)} - \left[\exp\left[j \left[\alpha_3 k_1 w^{(n)} - k_1 (1 - \alpha_3) \right] z \right] \right. \\ \left. - \exp\left(- jk_1 yz\right) \right] \\ + H^{(n)} \exp\left[jk_1 \left(\alpha_3 w^{(n)} - 1 + \alpha_3 \right) z \right] \end{array} \right\} \right.$$

$$(n) = 1,2,3,4$$

(II.D.11)

with

$$y = \frac{n\pi}{k_1 L} = \frac{u_0}{v_{ph}}$$

where v_{ph} is the phase velocity of the circuit and where

$$G^{(n)+} = - j \frac{M^{(n)}}{\alpha_3^3} \frac{\left[- (1/2)(1 + y)^2 + \alpha_3 (1 + y) c - \alpha_3^2 b \right]}{\alpha_3 w^{(n)} - (1 - \alpha_3 + y)} \qquad \text{(II.D.12)}$$

$$G^{(n)-} = - j \frac{M^{(n)}}{\alpha_3^3} \frac{\left[- (1/2)(1 - y)^2 + \alpha_3 (1 - y) c - \alpha_3^2 b \right]}{\alpha_3 w^{(n)} - (1 - \alpha_3 - y)} \qquad \text{(II.D.13)}$$

$$b = \frac{1}{2} + \frac{1}{\nu} + \frac{1}{2\nu^2} - \frac{1}{2a_2^2 \nu^2} + \frac{|m|^2}{4} \left(\frac{1}{\nu} + \frac{1}{2a_2^2 \nu^2} + \frac{3}{2\nu^2} \right)$$

$$c = 1 + \frac{1}{\nu} + \frac{|m|^2}{4\nu}$$

$$H^{(n)} = + j \frac{M^{(n)}}{\alpha_3^3} \left[\alpha_3 w^{(n)} + 1 - \alpha_3 - \frac{2\nu_3}{\nu} \right]$$

(term due to the boundary conditions) .

Then finally, the result is

$$I_1(z) = j \frac{A\sqrt{2}}{2L} \frac{I_0}{k_1} \sum_{(n)} K^{(n)} \exp \left\{ j \left[\alpha_3 k_1 w^{(n)} - k_1 (1 - \alpha_3) \right] z \right\}$$

$$- G^{(n)+} \exp (+ jyk_1 z) - G^{(n)-} \exp (- jyk_1 z)$$

where

$$K^{(n)} = G^{(n)+} + G^{(n)-} + H^{(n)} .$$

LIST OF REFERENCES

1. H. A. Haus and F.H.N. Robinson, "The Minimum Noise Figure of Microwave-Beam Amplifiers," Proc. I.R.E. 43, 981-991 (August 1955).

2. W.R. Beam, "Determination of the Sign of Power Flow in Electron-Beam Waves," Proc. I.R.E. 48, 1170 (June 1960)

3. P. A. Sturrock, "In What Sense Do Slow Waves Carry Negative Energy?" M.L. No. 712, Microwave Laboratory, W. W. Hansen Laboratories of Physics, Stanford University, Stanford, California (April 1960).

4. P. A. Sturrock, "Parametric Refrigeration: A Mechanism for Removal of Noise from the Slow Wave of an Electron Beam," M.L. No. 656, Microwave Laboratory, W. W. Hansen Laboratories of Physics, Stanford University, Stanford, California (October 1959).

5. T. J. Bridges, "An Electron-Beam Parametric Amplifier," Proc. I.R.E. 46, 494-495 (February 1958).

6. W. H. Louisell and C. F. Quate, "Parametric Amplification of Space-Charge Waves," Proc. I.R.E. 46, 707-716 (April 1958).

7. W. H. Louisell, "A Three-Frequency Electron-Beam Parametric Amplifier and Frequency Converter," J. of Electr. and Contr. First Series 6, 1-25 (January 1959).

8. G. Wade and H. Heffner, "Gain, Bandwidth and Noise in Cavity Type Parametric Amplifiers Using An Electron Beam," T.R. No. 54, Electron Devices Laboratory, Stanford Electronics Laboratory, Stanford University, Stanford, California (March 1959).

9. A. Ashkin, "Parametric Amplification of Space-Charge Waves," J. Appl. Phys. 29, 1646-1651 (December 1958).

10. A. Ashkin, Part Three, I.R.E. Wescon Convention Record, 13-22 (1958).

11. R. Adler, "Parametric Amplification of the Fast Electron Wave," Proc. I.R.E. 46, 1300-1301 (June 1958).

12. R. Adler, G. Herbeck, G. Wade, "A Low-Noise Electron-Beam Parametric Amplifier," Proc. I.R.E. 46, 1756-1757 (October 1958).

13. R. Adler, G. Herbeck, G. Wade, "The Quadrupole Amplifier: A Low-Noise Parametric Device," Proc. I.R.E. 47, 1713-1723 (October 1959).

14. R. H. Pantell, "Electrostatic Electron-Beam Couplers," I.R.E. Trans. on Electron Devices (PGED) ED-8, 35-43 (January 1961).

15. T. Wessel-Berg, "General Theory of Klystrons With Arbitrary Extended Interaction Field," M.L. No. 376, Microwave Laboratory, W. W. Hansen Laboratories of Physics, Stanford University, Stanford, California (March 1957).

16. D. A. Watkins, Topics in Electromagnetic Theory, (John Wiley and Sons, Inc., New York, 1958).

17. W. J. Cunningham, Introduction to Nonlinear Analysis, (McGraw-Hill Book Company, New York, 1958).

18. A. Ashkin, W. H. Louisell, C. F. Quate, "Fast-Wave Couplers For Longitudinal-Beam Parametric Amplifiers," J. of Elect. and Contr. 7, (July 1959).

19. J. R. Pierce, Traveling-Wave Tubes, (Van Nostrand, Princeton, 1950).

Contract AF 19(604)-1930

LIST A

Code	Organization	No. of Copies
AF 5	AFMTC (AFMTC Technical Library - MU-135) Patrick Air Force Base, Florida	1
AF 18	AUL Maxwell Air Force Base, Alabama	1
AF 43	WADD (WCLJA-2) Aeronautical Systems Center (AMC) Wright-Patterson Air Force Base, Ohio	1
AF 124	RADC (RCOIL-2) Griffiss Air Force Base, New York	1
AF 139	Air Force Missile Development Center (MDGRT) Holloman Air Force Base, New Mexico	1
AF 244	AFRD Attention: AFOSR Library Washington 25, D. C.	1
AF 318	WADD (ARL, Technical Library) Building 450 Wright-Patterson Air Force Base, Ohio	1
AF 319	ARDC (RDRS) Andrews Air Force Base Washington 25, D. C.	1
AR 5	U. S. Army Signal Engineering Laboratories Technical Documents Center Evans Signal Laboratory Belmar, New Jersey	1
Ar 9	Chief of Research and Development Department of the Army Washington 25, D. C. Attention: Scientific Information Branch	1
Ar 67	Army Rocket and Guided Missile Agency Redstone Arsenal, Alabama Attention: ORDXR-OTL, Technical Library	1
G 2	ASTIA Arlington Hall Station Arlington 12, Virginia	10

Code	Organization	No. of Copies
G 68	National Aeronautics and Space Agency 1520 H Street, N. W. Washington 25, D. C. Attention: Library	1
G 109	Director Langley Research Center National Aeronautics and Space Administration Langley Field, Virginia	1
M 6	ARCRL, Office of Aerospace Research (CRRELT) L. G. Hanscom Field Bedford, Massachusetts	10
N 1	Director, Avionics Division (AV) Bureau of Aeronautics Department of the Navy Washington 25, D. C.	1
N 29	Director (Code 2027) U. S. Naval Research Laboratory Washington 25, D. C.	1
I 292	Director, USAF Project RAND via: Air Force Liaison Office The Rand Corporation 1700 Main Street Santa Monica, California	1
AF 127	Boston Sub Office Patent Prosecution Branch (Hq. AMC) Murphy General Hospital Building 133 424 Trapelo Road Waltham 54, Massachusetts	1
Ar 107	U. S. Army Aviation Human Research Unit U. S. Continental Army Command P. O. Box 438 Fort Rucker, Alabama Attention: Maj. Arne H. Eliasson	1
G 6	Office of Technical Services Department of Commerce Washington 25, D. C. Attention: Technical Reports Section	2
G 8	Library Boulder Laboratories National Bureau of Standards Boulder, Colorado	1

Code	Organization	No. of Copies
M 63	Institute of the Aeronautical Sciences 2 East 64th Street New York 21, New York Attention: Librarian	1
U 32	Massachusetts Institute of Technology Research Laboratory of Electronics Building 26, Room 327 Cambridge 39, Massachusetts Attention: John H. Hewitt	1

LIST I

AF 247	WADD (WCLKTR) Wright-Patterson Air Force Base, Ohio	1
Ar 103	Commanding Officer U. S. Army Signal Research and Development Lab. Fort Monmouth, New Jersey Attention: SIGFM/EL-PRG	1
G 112	Oak Ridge National Laboratory P. O. Box X Oak Ridge, Tennessee Attention: Central Research Laboratory	1
I 774	Lenkurt Electric Company, Inc. 1105 Country Road San Carlos, California Attention: D. Mawdsley, Mail Stop 85	1
I 775	Radio Research Laboratories Kokubunji, P. O. Tokyo, Japan	1
I 925	Hughes Aircraft Company P. O. Box 278 Newport Beach, California Attention: Miss Eileen D. Andjulis Assistant Librarian	1
I 943	General Telephone and Electronics Laboratories, Inc. Microwave Physics Laboratory 4020 Fabian Way Palo Alto, California Attention: Librarian	1

Code	Organization	No. of Copies
I 944	Bomac Laboratories, Inc. Salem Road Beverly, Massachusetts Attention: Mr. Arthur McCoubrey, Manager Research and Development	1
U 238	University of Southern California University Park Los Angeles 7, California Attention: Z. A. Kaprielian Associate Professor of Electrical Engineering	1
U 290	Dr. A. L. Cullen Department of Electrical Engineering University of Sheffield Sheffield 1, England	1
U 358	University of Arizona Tucson 25, Arizona Attention: Professor Donald C. Stinson Electrical Engineering Department	1
U 359	The University of British Columbia Department of Electrical Engineering Vancouver 8 B.C., Canada Attention: G. B. Walker Microwave Laboratory	1
U 391	University of Illinois Electrical Engineering Research Laboratory Urbana, Illinois Attention: Professor P. D. Coleman Ultramicrowave Group	1
AF 329	Hq. ARDC (RDR-62) Reference 4619-Ca Andrews Air Force Base Washington 25, D. C.	2

LIST A-P

G 70	Advisory Group on Electron Tubes 346 Broadway, 8th Floor New York 13, New York Attention: Secretary, Working Group on Semiconductor Devices	2

Code	Organization	No. of Copies
N 160	U. S. Naval Research Laboratory Washington 25, D. C. Attention: Mr. F. J. Liberatore, Code 7420 Radiation Division	1
I 13	Bell Telephone Laboratories, Inc. Whippany Laboratory Whippany, New Jersey Attention: Technical Information Library	2
I 53	Hughes Aircraft Company Florence Avenue and Teale Street Culver City, California Attention: Documents Section Research and Development Library	1
I 96	Sandia Corporation Sandia Base P. O. Box 5800 Albuquerque, New Mexico Attention: Mrs. B. R. Allen, Librarian	1
I 237	General Electric Company Microwave Laboratory 601 South California Avenue Palo Alto, California Attention: Librarian	1
I 260	Sylvania Electric Products Inc. Electronic Defense Laboratory P. O. Box 205 Mountain View, California Attention: Library	1
I 266	International Tele and Tele Corp. Federal Telecommunication Laboratories 500 Washington Avenue Nutley 10, New Jersey Attention: Technical Library	1
I 297	Sperry Gyroscope Company Division of Sperry Rand Corporation Great Neck, New York Attention: Mrs. Florence W. Turnbull, Engineering Librarian	1
I 305	General Electric Company Power Tube Department Electronics Components Division Building 269, Room 205 One River Road Schenectady 5, New York	1

Code	Organization	No. of Copies
I 306	General Telephone and Electronics Laboratories, Inc. Bayside, New York Attention: Mr. D. Lazare, Manager Technical Services	1
I 309	Litton Industries, Inc. 960 Industrial Road San Carlos, California Attention: Document Custodian Engineering Department	1
I 310	Varian Associates 611 Hansen Way Palo Alto, California Attention: Mr. Norman P. Hiestand	1
I 312	Space Technology Laboratories, Inc. Attention: Mrs. Margaret C. Whitnah Chief, Information Services P. O. Box 95001 Los Angeles 45, California	1
I 366	Radio Corporation of America Defense Electronic Products Camden, New Jersey Attention: Mr. S. Schach, Building 10-5 Standards Engineering, Section 577	1
I 367	Stanford Research Institute Document Center Menlo Park, California Attention: Acquisitions	1
I 370	General Telephone and Electronics Laboratories, Inc. Bayside, New York Attention: Dr. T. G. Polanyi Head Thermionics Branch	1
I 382	RCA Laboratories David Sarnoff Research Center Princeton, New Jersey Attention: Dr. Harwick Johnson	1
I 384	Bell Telephone Laboratories Murray Hill Laboratory Murray Hill, New Jersey Attention: Dr. J. R. Pierce	2

Code	Organization	No. of Copies
I 432	Varian Associates 611 Hansen Way Palo Alto, California Attention: Mr. W. J. Dodds	1
I 435	General Electric Company P. O. Box 1088 Schenectady, New York Attention: Mr. E. D. McArthur Research Laboratories	1
I 450	Bell Telephone Laboratories, Inc. Murray Hill, New Jersey Electron Tube Development Department Attention: Mr. J. A. Hornbeck	1
I 547	The Rand Corporation 1700 Main Street Santa Monica, California Attention: Technical Librarian	1
I 562	Philips Laboratories A Division of North American Philips Co., Inc. Irvington-on-Hudson, New York Attention: Gilbert Kelton Security Officer	1
I 577	Raytheon Manufacturing Company 520 Winter Street Waltham, Massachusetts Attention: Mr. O. T. Fundingsland	1
I 594	Research Technology Associates Jones Road Waltham, Massachusetts Attention: J. Babakian	1
I 595	Gianninni Research Santa Ana, California Attention: J. K. Hagele Technical Librarian	1
I 666	Rama-Wooldridge A Division of Thompson Ramo-Wooldridge, Inc. 8433 Fallbrook Avenue Canoga Park, California Attention: Technical Information Services	1

Code	Organization	No. of Copies
I 756	Varian Associates 611 Hansen Way Palo Alto, California Attention: Mr. C. W. McClelland Technical Publications Manager	1
I 759	Stanford Research Institute Menlo Park, California Attention: Mr. C. J. Cook	1
I 760	General Atomic Division of General Dynamics Corporation P. O. Box 608 San Diego, California Attention: Mr. M. Rosenbluth	1
I 761	Linfield Research Institute McMinnville, Oregon Attention: Dr. W. P. Dyke, Director	1
I 762	Columbia Radiation Laboratory 538 West 120th Street New York 27, New York	
I 763	Sperry Gyroscope Company Engineering Library Mail Station C-39 Great Neck, Long Island, New York	1
I 764	Watkins-Johnson Company 3333 Hillview Avenue Palo Alto, California Attention: Dr. H. R. Johnson	1
I 765	Westinghouse Electric Corporation Friendship International Airport Box 746 Baltimore 3, Maryland Attention: G. Ross Kilgore, Manager Applied Research Department Baltimore Laboratory	1
I 766	Services Electronic Research Laboratories Baldock, Herts, England Attention: Dr. Boot	1
I 767	Standard Telephone Laboratories Harlow, Essex, England Attention: Dr. E. A. Ash	1

Code	Organization	No. of Copies
I 768	Eitel-McCullough, Inc. 798 San Mateo Avenue San Bruno, California Attention: Librarian	1
I 769	Hewlett-Packard Company 275 Page Mill Road Palo Alto, California	1
I 770	Hughes Aircraft Company Research and Development Laboratories Culver City, California Attention: L. M. Field	1
I 771	Advanced Kinetics Inc. P. O. Box 1803 Newport Beach, California Attention: Dr. R. Waniek	1
I 772	RCA Laboratories Princeton, New Jersey Attention: Harwell Johnson	1
U 2	California Institute of Technology Jet Propulsion Laboratory Pasadena 4, California Attention: Documents Library	1
U 21	The Johns Hopkins University Radiation Laboratory 1315 St. Paul Street Baltimore 2, Maryland Attention: Librarian	1
U 22	The Johns Hopkins University Department of Physics Homewood Campus Baltimore 18, Maryland Attention: Dr. Donald E. Kerr	1
U 26	Massachusetts Institute of Technology Lincoln Laboratory P. O. Box 73 Lexington 73, Massachusetts Attention: Mary A. Granese, Librarian	1
U 40	New York University Department of Physics College of Arts and Science Washington Square, New York 3, New York Attention: Professor J. H. Rohrbaugh	1

Code	Organization	No. of Copies
U 42	Ohio State University Research Foundation 1314 Kinnear Road Columbus 8, Ohio Attention: Professor E. M. Boone Department of Electrical Engineering	1
U 59	Library Georgia Technology Research Institute Engineering Experiment Station 722 Cherry Street, N. W. Atlanta, Georgia Attention: Mrs. J. H. Crosland, Librarian	1
U 79	University of Michigan Engineering Research Institute Radiation Laboratory Attention: Professor K. M. Siegel 912 N. Main Street Ann Arbor, Michigan	1
U 100	University of California Electronics Research Laboratory 332 Cory Hall Berkeley 4, California Attention: J. R. Whinnery	1
U 102	Harvard University Technical Reports Collection Gordon McKay Library 303A Pierce Hall Oxford Street Cambridge 38, Massachusetts Attention: Librarian	1
U 107	University of California 390 Cory Hall Berkeley 4, California Attention: Dr. Charles Susskind	1
U 150	University of Washington Department of Electrical Engineering Seattle 5, Washington Attention: Mr. A. E. Harrison	1
U 168	George Washington University Electronics Research Projects - Building V Washington 6, D. C. Attention: Dr. N. T. Grisamore	1

Code	Organization	No. of Copies
U 169	Electronics Research Laboratory Illinois Institute of Technology 3301 S. Dearborn Street Chicago 16, Illinois Attention: Dr. George I. Cohn	1
U 209	New York University College of Engineering 346 Broadway New York, New York Attention: Mr. L. S. Schwartz, Research Division	1
U 228	University of Kansas Electrical Engineering Department Lawrence, Kansas Attention: Dr. H. Unz	1
U 237	Polytechnic Institute of Brooklyn Microwave Research Institute 55 Johnson Street Brooklyn, New York Attention: Dr. N. Marcuvitz	1
U 240	Illinois Institute of Technology Technology Center Department of Electrical Engineering Chicago 16, Illinois Attention: Paul C. Yuen Electronics Research Laboratory	1
U 284	Dr. J. T. Senise Instituto Tecnológico de Aeronáutica São José dos Campos São Paulo, Brazil	1
U 288	Polytechnic Institute of Brooklyn Microwave Research Institute 55 Johnson Street Brooklyn 1, New York	1
U 292	University of Maryland College Park, Maryland Attention: Dr. J. M. Burgers	1
U 294	University of Illinois Electrical Engineering Research Laboratory Urbana, Illinois Attention: Dr. A. A. Dougal	1

Code	Organization	No. of Copies
U 308	Brandeis University Waltham, Massachusetts Attention: Dr. E. P. Gross	1
U 320	California Institute of Technology 1201 East California Street Pasadena, California Attention: Professor R. W. Gould	1
U 321	University of California Radiation Laboratory Livermore, California Attention: N. Christofilos	1
U 322	University of California Radiation Laboratory Livermore, California Attention: S. A. Colgate	1
U 323	University of California Radiation Laboratory Livermore, California Attention: R. F. Post	1
U 324	Princeton University Princeton, New Jersey Attention: L. Spitzer Project Matterhorn	1
U 325	Massachusetts Institute of Technology 77 Massachusetts Avenue Cambridge, Massachusetts Attention: W. P. Allis	1
U 326	University of California Electrical Engineering Department Berkeley 4, California Attention: Professor J. R. Singer	1
U 327	University of California Radiation Laboratory Berkeley, California Attention: Dr. R. K. Wakerling Information Division Building 50, Room 128	1
U 328	University of Chicago Institute of Air Weapons Research Museum of Science and Industry Chicago 37, Illinois Attention: Mrs. Norma Miller Technical Librarian	;

Code	Organization	No. of Copies
U 329	University of Florida Department of Electrical Engineering Gainesville, Florida Attention: Professor W. E. Lear	1
U 330	University of Illinois Control Systems Laboratories Urbana, Illinois Attention: Professor Daniel Alpert	1
U 331	University of Illinois Department of Electrical Engineering Urbana, Illinois Attention: Professor L. Goldstein	1
U 332	University of Illinois Department of Physics Urbana, Illinois Attention: Dr. John Bardeen	1
U 333	Johns Hopkins University Radiation Laboratory 1315 St. Paul Street Baltimore 2, Maryland Attention: J. M. Minkowski	1
U 334	Iowa State University Physics Department Iowa City, Iowa Attention: Professor Frank MacDonald	1
U 335	University of Colorado Department of Electrical Engineering Boulder, Colorado Attention: Professor W. G. Worcester	1
U 337	McMurray College Department of Physics Abilene, Texas Attention: Dr. Virgil E. Bottom	1
U 338	University of Michigan 3506 East Engineering Building Ann Arbor, Michigan Attention: Electron Tube Laboratory	1
U 339	University of Minnesota Institute of Technology Department of Electrical Engineering Minneapolis, Minnesota Attention: Professor A. van der Ziel	1

Code	Organization	No. of Copies
U 340	Ohio University College of Applied Science Athens, Ohio Attention: D. B. Green	1
U 341	Oregon State College Department of Electrical Engineering Corvallis, Oregon Attention: H. J. Oorthuys	1
U 342	Princeton University Department of Electrical Engineering Princeton, New Jersey	1
U 343	Purdue University Research Library Lafayette, Indiana Attention: Electrical Engineering Department	1
U 344	Rensselaer Polytechnic Institute Office of the Librarian Troy, New York	1
U 345	Scientific Attaché Swedish Embassy 2249 R Street, N. W. Washington 8, D. C.	1
U 346	Rutgers University Physics Department Newark 2, New Jersey Attention: Dr. Charles Pine	1
U 347	University of Texas Military Physics Research Laboratory Box 8036 University Station Austin, Texas	1
U 348	University of Utah Electrical Engineering Department Salt Lake City, Utah Attention: Richard W. Grow	1
U 349	Yale University Sloane Physics Laboratory New Haven, Connecticut	1
U 350	University of Puerto Rico College of Agriculture and Mechanical Arts Mayaguez, Puerto Rico Attention: Dr. Braulio Dueno	1

Code	Organization	No. of Copies
U 351	The Royal Institute of Technology Stockholm 70, Sweden Attention: Dr. B. Agdur	1
U 352	Drexel Institute of Technology Department of Electrical Engineering Philadelphia 4, Pennsylvania Attention: F. B. Haynes	1
U 353	Forsvarets Forskningsinstitutt Avdeling for Radar Bergen, Norway Attention: Tore Wessel-Berg	1
U 354	Massachusetts Institute of Technology Research Laboratory of Electronics Cambridge 39, Massachusetts Attention: L. D. Smullin	1
U 355	Massachusetts Institute of Technology Research Laboratory of Electronics Cambridge 39, Massachusetts Attention: S. C. Brown	1
U 356	University of Chicago Midway Laboratories 6220 S. Drexel Avenue Chicago, Illinois Attention: P. J. Dickerman	1
	Hq. AFCRL Office of Aerospace Research (CRRC) L. G. Hanscom Field Bedford, Massachusetts	4
U 107	University of Michigan Electronic Defense Group Engineering Research Institute Ann Arbor, Michigan Attention: J. A. Boyd, Supervisor.	1

UNCLASSIFIED